

Rational Synthesis of Normal, Abnormal and Anionic NHC-Gallium Alkyl complexes: Structural, Stability and Isomerization Insights

Marina Uzelac,^a Alberto Hernán-Gómez,^a David R. Armstrong,^a Alan R. Kennedy^a and Eva Hevia^a

^aWestCHEM, Department of Pure and Applied Chemistry, University of Strathclyde, 295 Cathedral Street, Glasgow, G1 1XL, UK

eva.hevia@strath.ac.uk

Contents

Experimental Details.....	2
Thermal isomerisation experiments.....	8
Kinetic measurements	16
DFT calculations.....	19
NMR spectra of products	37

Experimental Details

General

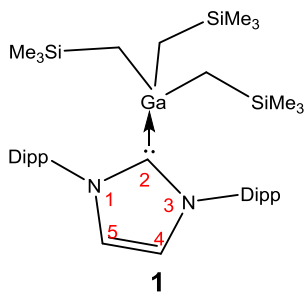
All reactions were carried out using standard Schlenk and glove box techniques under an inert atmosphere of argon. Solvents (THF, hexane and toluene) were dried by heating to reflux over sodium benzophenone ketyl and distilled under nitrogen prior to use. NMR spectra were recorded on a Bruker DPX 400 MHz spectrometer, operating at 400.13 MHz for ¹H, and 100.62 MHz for ¹³C{¹H}. Elemental analyses were obtained using a Perkin Elmer 2400 elemental analyser. Li(CH₂SiMe₃) in the form of a 1.0 M solution in pentane and anhydrous GaCl₃ were purchased from Sigma Aldrich Chemicals and Alfa Aesar respectively, and used as received. [Ga(CH₂SiMe₃)₃]¹, IPr,² IPr-d₂,³ IMes,⁴ iBu,⁵ [Mg(CH₂SiMe₃)₂],⁶ [Zn(CH₂SiMe₃)₂],⁷ [Mg(CH₂SiMe₃)₂·IPr]⁸ and GaCl₃·IPr⁹ were prepared according to literature methods.

X-Ray Crystallography

Crystallographic data were measured at 123(2) K on Oxford Diffraction Gemini S or Xcalibur E instruments with graphite-monochromated Mo ($\lambda=0.71073\text{ \AA}$) or Cu (1.54180 \AA) radiation. All structures were solved and refined to convergence on F^2 using all unique reflections and programs from the SHELX family.¹⁰ Final models included constrained and restrained models for disorder for three monosilyl groups bound to Ga (structures **2** and **4**); for isopropyl and SiMe₃ groups (structure **1**); for an isopropyl group (structure **6**); and for two THF ligands (structure **3**). Of these structures, the quality of that for compound **4** is the only one to be seriously compromised by disorder. Selected crystallographic data are presented in Table S1 and full details in cif format can be obtained free of charge from the Cambridge Crystallographic Data Centre via www.ccdc.cam.ac.uk/data_request/cif.

Synthesis of [IPrGa(CH₂SiMe₃)₃] (**1**)

Equimolar amounts of Ga(CH₂SiMe₃)₃ (0.36 g, 1 mmol) and bis(2,6-diisopropylphenyl)imidazol-2-ylidene (IPr) (0.39 g, 1 mmol) were suspended in hexane (10 ml) and stirred for one hour at room temperature. The resulting yellow suspension was gently heated until all of the visible solid had dissolved. Slow cooling of the resulting solution afforded a crop of colourless crystals (0.54 g, 75%). Anal. Calcd for C₃₉H₆₉N₂Si₃Ga: C, 65.06; H, 9.66; N, 3.89. Found: C, 65.00; H, 10.08; N, 3.94.



¹H NMR (298 K, C₆D₆) δ (ppm) -0.95 (6H, s, CH₂SiMe₃), 0.18 (27H, s, Si(CH₃)₃), 0.94 (12H, d, CH(CH₃)₂), 1.39 (12H, d, CH(CH₃)₂), 2.71 (4H, sept, CH(CH₃)₂), 6.40 (2H, s, imidazole backbone CH), 7.11 (4H, d, m-CH), 7.26 (2H, t, p-CH).

¹³C{¹H} NMR (298 K, C₆D₆) 0.4 (CH₂SiMe₃), 3.6 (Si(CH₃)₃), 23.0 (CH(CH₃)₂), 26.0 (CH(CH₃)₂), 29.0 (CH(CH₃)₂), 124.3 (m-CH), 124.4 (imidazole backbone CH), 130.7 (p-CH), 136.3 (i-C), 145.8 (o-C), 186.6 (C:).

¹ L. M. Dennis, W. Patnode, *J. Am. Chem. Soc.* **1932**, 54, 182.

² L. Hintermann, *Beilstein Journal of Organic Chemistry* **2007**, 3, 1.

³ R. M. Stolley, H. A. Duong, D.R. Thomas, J. Louie, *J. Am. Chem. Soc.* **2012**, 134, 15154.

⁴ A. J. Arduengo, R. Krafczyk, R. Schmutzler, H. A. Craig, J. R. Goerlich, W. J. Marshall, M. Unterzag, *Tetrahedron* **1999**, 55, 14523.

⁵ E. C. Hurst, K. Wilson, I. J. Fairlamb, V. Chechik, *New J. Chem.* **2009**, 33, 1837.

⁶ R. A. Andersen, G. Wilkinson, *J. Chem. Soc., Dalton Trans.* **1977**, 809.

⁷ M. Westerhausen, B. Rademacher, W. Poll, *Journal of Organometallic Chemistry* **1991**, 421, 175

⁸ A. R. Kennedy, J. Klett, R. E. Mulvey, S. D. Robertson, *Eur. J. Inorg. Chem.* **2011**, 4675.

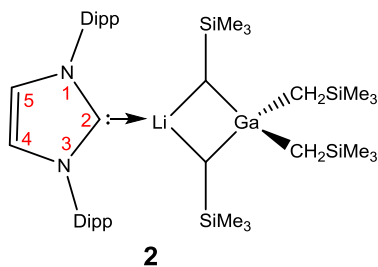
⁹ N. Marion, E. C. Escudero-Adan, J. Benet-Buchholz, E. D. Stevens, L. Festerbank, M. Malacria, S. P. Nolan, *Organometallics* **2007**, 26, 3256.

¹⁰ G. M. Sheldrick, *Acta Crystallogr.*, **2008**, A64, 112.

¹H NMR (298 K, *d*₈-THF) δ(ppm) -1.13 (6H, br s, CH₂SiMe₃), -0.20 (27H, s, Si(CH₃)₃), 1.14 (12H, d, CH(CH₃)₂), 1.36 (12H, br s, CH(CH₃)₂), 2.76 (4H, sept, CH(CH₃)₂), 7.32-7.48 (8H, mult, imidazole backbone CH + ArCH). ¹³C{¹H} NMR (298 K, *d*₈-THF) 0.7 (CH₂SiMe₃), 3.4 (Si(CH₃)₃), 23.6 (CH(CH₃)₂), 25.9 (CH(CH₃)₂), 29.5 (CH(CH₃)₂), 124.7 (*m*-CH), 126.0 (imidazole backbone CH), 130.9 (*p*-CH), 137.5 (*i*-C), 146.7(*o*-C). Carbene C could not be detected.

Synthesis of [IPrLiGa(CH₂SiMe₃)₄] (2)

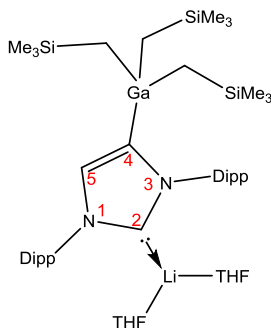
Li(CH₂SiMe₃) (1M in pentane, 1 mL, 1 mmol) was added to a solution of GaR₃ (0.33 g, 1 mmol in 10 mL hexane) and stirred for 1h at room temperature. To this suspension of [LiGaR₄]_∞, 1 equivalent of IPr (0.39 g, 1 mmol) was added and the resulting orange suspension was stirred for another hour at room temperature. To the resulting orange suspension toluene was added dropwise with gentle heating until all of the visible solid has dissolved. Slow cooling of the resulting solution afforded X-ray quality crystals. The mixture was then concentrated and kept at -26 °C for a couple of days to yield a crop of colourless crystals (0.39 g, 48%). Anal. Calcd for C₄₃H₈₀N₂Si₄LiGa: C, 63.36; H, 10.02; N, 3.44. Found: C, 63.01; H, 10.37; N, 3.54.



¹H NMR (298 K, C₆D₆) δ(ppm) -0.96, -0.91 (8H, s, CH₂SiMe₃), 0.21 (36H, s, Si(CH₃)₃), 0.97 (12H, d, CH(CH₃)₂), 1.32 (12H, d, CH(CH₃)₂), 2.65 (4H, sept, CH(CH₃)₂), 6.34 (2H, s, imidazole backbone CH), 7.08 (4H, d, *m*-CH), 7.22 (2H, t, *p*-CH). ⁷Li NMR (298 K, C₆D₆, reference LiCl in D₂O at 0.00 ppm): δ 0.80. Because of poor solubility ¹³C spectrum was not obtained. By switching to the donor solvent *d*₈-THF it was evident from ¹H and ⁷Li that the co-complex was broken and the free IPr and LiGaR₄ were identified.

Synthesis of (THF)₂Li[:C{[N(2,6-*i*-Pr₂C₆H₃)]₂CHCGa(CH₂SiMe₃)₃}] (3)

Li(CH₂SiMe₃) (1 mL, 1M in pentane, 1 mmol) was added *via* syringe to a suspension of IPr (0.39 g, 1 mmol) in hexane (10 mL) at room temperature to form a white suspension. After stirring overnight, a hexane solution of Ga(CH₂SiMe₃)₃ (0.33 g, 1 mmol in 5 mL hexane) was added *via* cannula and stirred for 3h at room temperature. The reaction mixture was then concentrated to approximately 5 mL and 1 mL of THF was added to afford a colourless solution. Overnight storage of the solution at -30 °C provided a batch of colourless crystals (0.44 g, 56 %). Anal. Calcd for C₄₇H₈₄N₂Si₃LiO₂Ga: C, 64.88; H, 9.73; N, 3.22. Found: C, 65.00; H, 10.08; N, 3.65.

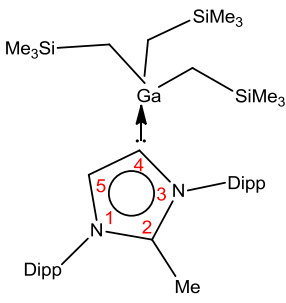
**3**

¹H NMR (298 K, *d*₈-THF) δ(ppm) -1.18 (6H, s, CH₂SiMe₃), -0.17 (27H, s, Si(CH₃)₃), 1.07-1.11 (12H, mult, CH(CH₃)₂), 1.18 (6H, d, CH(CH₃)₂), 1.29 (6H, d, CH(CH₃)₂), 3.0 (4H, mult, CH(CH₃)₂), 6.64 (1H, s, imidazole backbone CH), 7.16-7.34 (6H, mult, *m*-CH + *p*-CH). ¹³C{¹H} NMR (298 K, *d*₈-THF) 0.1 (CH₂SiMe₃), 3.6 (Si(CH₃)₃), 23.2 (CH(CH₃)₂), 24.8 (CH(CH₃)₂), 25.2 (CH(CH₃)₂), 26.7 (CH(CH₃)₂), 28.4 (CH(CH₃)₂), 28.6 (CH(CH₃)₂), 123.4 (*p*-CH), 124.0(*p*-CH), 127.8 (*m*-CH), 128.7 (*m*-CH), 129.2 (imidazole backbone CH), 140.1 (*i*-C), 143.6 (*i*-C), 147.1 (*o*-C), 147.3 (*o*-C), 155.0 (C-Ga), 201.5 (C:). ⁷Li NMR (298 K, *d*₈-THF, reference LiCl in D₂O at 0.00 ppm): δ 0.12.

¹H NMR (298 K, C₆D₆) δ(ppm) -0.60 (6H, s, CH₂SiMe₃), 0.40 (27H, s, Si(CH₃)₃), 1.01 (12H, mult, CH(CH₃)₂), 1.06 (8H, mult, THF), 1.27 (6H, d, CH(CH₃)₂), 1.58 (6H, d, CH(CH₃)₂), 2.56 (8H, mult, THF), 3.00 (2H, sept, CH(CH₃)₂), 3.21 (2H, sept, CH(CH₃)₂), 6.99 (1H, s, imidazole backbone CH), 7.0-7.2 (mult, ArCH overlapping with C₆D₆).

Synthesis of [CH₃C{[N(2,6-*i*Pr₂C₆H₃)]₂CHCGa(CH₂SiMe₃)₃}] (4)

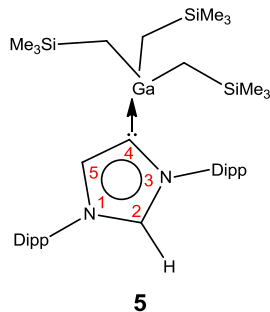
A toluene solution of **3** (0.43 g, 0.5 mmol in 15 mL of toluene) was cooled down to -80 °C and stirred for 20 min. To this slurry, a toluene solution of MeOTf (0.08 g, 0.5 mmol in 3 mL of toluene) was added dropwise and stirred for an hour. The mixture was filtered through Celite to remove LiOTf and washed with more toluene (5 mL). The solvent was exchanged *in vacuo* to hexane (5 mL) to which 2 mL of fresh toluene were added. Obtained suspension was gently heated until a yellow solution was obtained which upon slow cooling afforded X-ray quality crystals. This mixture was then kept overnight at -30 °C to yield a crop of colourless crystals (0.25 g, 68%). Anal. Calcd for C₄₀H₇₁N₂Si₃Ga: C, 65.28; H, 10.00; N, 3.81. Found: C, 65.04; H, 9.91; N, 4.08.

**4**

¹H NMR (298 K, *d*₈-THF) δ(ppm) -1.09 (6H, s, CH₂SiMe₃), -0.13 (27H, s, Si(CH₃)₃), 1.09 (6H, d, CH(CH₃)₂), 1.20 (6H, d, CH(CH₃)₂), 1.36 (6H, d, CH(CH₃)₂), 2.04 (3H, s, CH₃), 2.51 (2H, sept, CH(CH₃)₂), 2.72 (2H, sept, CH(CH₃)₂), 7.13 (1H, s, imidazole backbone), 7.34-7.48 (mult, 6H, Ar-CH). ¹³C{¹H} NMR (298 K, *d*₈-THF) 0.5 (CH₂SiMe₃), 3.5 (Si(CH₃)₃), 12.2 (CH₃), 24.0 (CH(CH₃)₂), 24.4 (CH(CH₃)₂), 24.9 (CH(CH₃)₂), 25.4 (CH(CH₃)₂), 28.9 (CH(CH₃)₂), 29.3 (CH(CH₃)₂), 125.3(*m*-CH), 125.8 (*m*-CH), 130.0 (*p*-CH), 131.7 (imidazole backbone CH), 132.1 (*p*-CH), 132.1(*i*-C), 135.1 (*i*-C), 145.0 (NCMeN), 146.3 (*o*-C), 146.5 (*o*-C), 161.2 (C-Ga).

Synthesis of [*a*IPrGa(CH₂SiMe₃)₃] (**5**)

To a THF solution of **3** (0.43 g, 0.5 mmol in 10 mL of THF) IMesHCl (0.17 g, 0.5 mmol) was added from solid addition tube and stirred for 6h at room temperature. The mixture was filtered through Celite and washed with more THF (2 x 5 mL). Clear filtrate was concentrated to *ca.* 5 mL in volume to which 2 mL of hexane was added and stored at -30 °C to afford colourless crystals of title compound (0.22 g, 61%). Anal. Calcd for C₃₉H₆₉N₂Si₃Ga: C, 65.06; H, 9.66; N, 3.89. Found: C, 65.42; H, 9.76; N, 4.19.

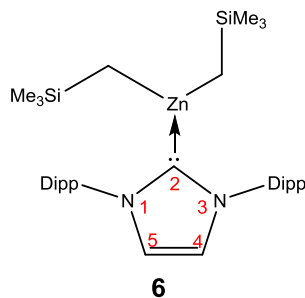


¹H NMR (298 K, C₆D₆) δ(ppm) -0.67 (6H, s, CH₂SiMe₃), 0.29 (27H, s, Si(CH₃)₃), 0.85 (6H, d, CH(CH₃)₂), 0.91 (6H, d, CH(CH₃)₂), 1.07 (6H, d, CH(CH₃)₂), 1.41 (6H, d, CH(CH₃)₂), 2.37 (2H, sept, CH(CH₃)₂), 2.73 (2H, sept, CH(CH₃)₂), 6.93 (2H, d, m-CH), 6.94 (1H, s, imidazole backbone CH), 6.97 (1H, s, C2-H), 7.08 (2H, d, m-CH), 7.11-7.23 (2H, two triplets, p-CH).

¹H NMR (298 K, d₈-THF) δ(ppm) -1.07 (6H, s, CH₂SiMe₃), -0.13 (27H, s, Si(CH₃)₃), 1.10 (6H, d, CH(CH₃)₂), 1.18 (6H, d, CH(CH₃)₂), 1.27 (6H, d, CH(CH₃)₂), 1.38 (6H, d, CH(CH₃)₂), 2.59 (2H, sept, CH(CH₃)₂), 2.77 (2H, sept, CH(CH₃)₂), 7.19 (1H, s, imidazole backbone CH), 7.35-7.41 (4H, two doublets, m-CH), 7.48-7.58 (2H, two triplets, p-CH), 9.00 (1H, s, C2-H). ¹³C{¹H} NMR (298 K, d₈-THF) -0.1 (CH₂SiMe₃), 3.4 (Si(CH₃)₃), 22.9 (CH(CH₃)₂), 24.6(CH(CH₃)₂), 24.9 (CH(CH₃)₂), 26.7 (CH(CH₃)₂), 29.1 (CH(CH₃)₂), 29.3 (CH(CH₃)₂), 124.6 (m-CH), 125.2 (m-CH), 131.1 (p-CH), 131.2 (imidazole backbone CH), 131.8 (p-CH), 132.1(i-C), 135.6(i-C), 139.2 (NCHN), 146.5 (o-C), 146.7 (o-C), 162.8 (C-Ga).

Synthesis of [IPrZn(CH₂SiMe₃)₂] (**6**)

Zn(CH₂SiMe₃)₂ (0.92 mL, 0.54 M in hexane, 0.5 mmol) was added *via* syringe to a suspension of IPr (0.19 g, 0.5 mmol) in hexane (10 mL) at room temperature to form a white suspension and stirred for 15 min at room temperature. The reaction mixture was then gently heated until all of the visible solid had dissolved. Slow cooling of the resulting solution afforded X-ray quality crystals (0.22 g, 70%). Anal. Calcd for C₃₅H₅₈N₂Si₂Zn: C, 66.90; H, 9.30; N, 4.46. Found: C, 66.67; H, 9.46; N, 4.81.

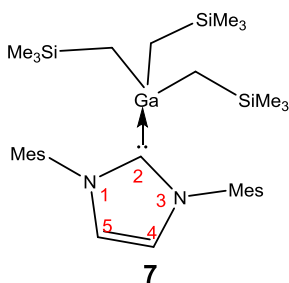


¹H NMR (298 K, C₆D₆) δ(ppm) -0.99 (4H, s, CH₂SiMe₃), 0.10 (18H, s, Si(CH₃)₃), 1.00 (12H, d, CH(CH₃)₂), 1.34 (12H, d, CH(CH₃)₂), 2.82 (4H, sept, CH(CH₃)₂), 6.44 (2H, s, imidazole backbone CH), 7.11 (4H, d, m-CH), 7.23 (2H, t, p-CH).

$^{13}\text{C}\{\text{H}\}$ NMR (298 K, C_6D_6). -0.8 (CH_2SiMe_3), 3.9 ($\text{Si}(\text{CH}_3)_3$), 23.4 ($\text{CH}(\text{CH}_3)_2$), 25.3 ($\text{CH}(\text{CH}_3)_2$), 28.7 ($\text{CH}(\text{CH}_3)_2$), 123.3 ($m\text{-CH}$), 124.5 (*imidazole backbone CH*), 130.5 (*p*-CH), 135.6 (*i-C*), 145.6 (*o-C*), 192.2 (*C*:).

Synthesis of [IMesGa(CH_2SiMe_3)₃] (7)

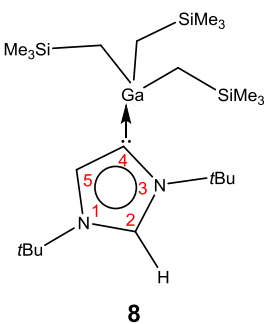
Equimolar amounts of $\text{Ga}(\text{CH}_2\text{SiMe}_3)_3$ (0.36 g, 1 mmol) and bis(1,3,5-trimethylphenyl)imidazol-2-ylidene (IMes) (0.30 g, 1 mmol) were mixed in hexane (10 ml) and stirred for one hour at room temperature. The resulting orange solution was concentrated to the half of its volume and placed at -27 °C to yield a crop of orange crystals (0.22 g, 34%). Anal. Calcd for $\text{C}_{33}\text{H}_{57}\text{N}_2\text{Si}_3\text{Ga}$: C, 62.34; H, 9.04; N, 4.41. Found: C, 62.45; H, 9.52; N, 4.77.



^1H NMR (298 K, C_6D_6) δ (ppm) -0.91 (6H, s, CH_2SiMe_3), 0.22 (27H, s, $\text{Si}(\text{CH}_3)_3$), 1.99 (12H, s, CH_3), 2.16 (6H, s, CH_3), 5.92 (2H, s, imidazole backbone CH), 6.77 (4H, d, $m\text{-CH}$). $^{13}\text{C}\{\text{H}\}$ NMR (298 K, C_6D_6). -0.6 (CH_2SiMe_3), 3.5 ($\text{Si}(\text{CH}_3)_3$), 18.2 (CH_3), 21.1 (CH_3), 122.9 ($m\text{-CH}$), 129.6 (imidazole backbone CH), 135.3 (*p*-CH), 135.9 (*i-C*), 139.6 (*o-C*), 182.2 (*C*:).

Synthesis of [*a*IBuGa(CH_2SiMe_3)₃] (8)

Equimolar amounts of $\text{Ga}(\text{CH}_2\text{SiMe}_3)_3$ (0.17 g, 0.5 mmol) and bis(*tert*-butyl)imidazol-2-ylidene (IBu) (0.09 g, 0.5 mmol) were suspended in hexane (10 ml) and stirred for one hour at room temperature. The resulting white suspension was gently heated until all of the visible solid had dissolved. Slow cooling of the resulting solution afforded a crop of colourless crystals (0.11 g, 43%).



^1H NMR (298 K, C_6D_6) δ (ppm) -0.23 (6H, s, CH_2SiMe_3), 0.33 (27H, s, $\text{Si}(\text{CH}_3)_3$), 0.87 (9H, s, $\text{C}(\text{CH}_3)_3$), 1.33 (9H, s, $\text{C}(\text{CH}_3)_3$), 7.09 (1H, s, imidazole backbone CH), 7.21 (1H, s, C2-H). $^{13}\text{C}\{\text{H}\}$ NMR (298 K, C_6D_6). 2.0 (CH_2SiMe_3), 3.6 ($\text{Si}(\text{CH}_3)_3$), 29.3($\text{C}(\text{CH}_3)_3$), 30.4($\text{C}(\text{CH}_3)_3$), 56.5 ($\text{C}(\text{CH}_3)_3$), 59.1 ($\text{C}(\text{CH}_3)_3$), 126.6 (imidazole backbone CH), 126.9 (NCHN), 160.1 (C-Ga).

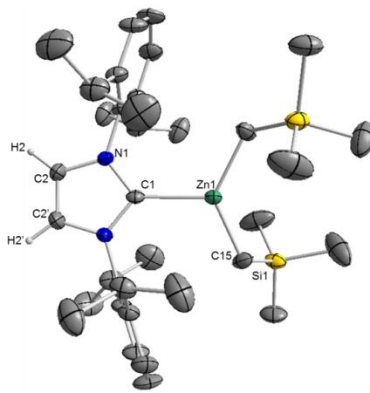


Figure S1: Molecular structure of **6** with 50% probability displacement ellipsoids. All hydrogen atoms except those on imidazole ring and minor disorder in isopropyl groups are omitted for clarity. Selected geometrical parameters (distances in Å and angles in deg): Zn(1)-C(1) 2.141(3), Zn(1)-C(15) 2.008(2), N(1)-C(1) 1.359(2), N(1)-C(2) 1.379(3), C(2)-C(2') 1.343(3), C(15)-Zn(1)-C(15') 129.54(17), C(15)-Zn(1)-C(1) 115.23(9), C(1)-N(1)-C(2) 111.86(18), N(1)-C(1)-N(1') 103.2(3), N(1)-C(1)-Zn(1) 128.42(13) C(2')-C(2)-N(1) 106.56(11).

Table S1. Selected crystallographic and refinement parameters.

Compound	1	2	3	4	5·THF	6
Empirical formula	C ₃₉ H ₆₉ GaN ₂ Si ₃	C ₄₃ H ₈₀ GaLi N ₂ Si ₄	C ₄₇ H ₈₄ GaLiN ₂ O ₂ Si ₃	C ₄₀ H ₇₁ GaN ₂ Si ₃	C ₄₃ H ₇₇ GaN ₂ Si ₃ O	C ₃₅ H ₅₈ N ₂ Si ₂ Zn
Formula weight	719.95	814.11	870.09	733.97	792.05	628.38
Crystal system	triclinic	monoclinic	monoclinic	monoclinic	Triclinic	monoclinic
Space group	P -1	P 2 ₁ /m	P 2 ₁ /n	P 2 ₁ /c	P -1	C 2/c
χ (Å)	1.54180	1.54178	0.71073	1.5418	1.5418	0.71073
a (Å)	10.5026(5)	11.519(3)	11.5267(5)	21.8907(5)	11.3181(5)	10.6838(3)
b (Å)	11.3327(7)	20.858(2)	18.7832(8)	11.0318(2)	13.8704(7)	19.4876(5)
c (Å)	19.4036(9)	11.942(3)	24.6800(10)	20.6366(4)	17.8645(6)	18.4437(4)
α (°)	85.025(4)	90	90	90	69.483(4)	90
β (°)	85.154(4)	117.73(4)	90.988(4)	117.951(3)	71.891(3)	102.692(2)
γ (°)	71.124(5)	90	90	90	67.251(4)	90
V (Å ³)	2173.1(2)	2539.7(13)	5342.6(4)	4402.27(19)	2371.9(2)	3746.18(17)
Z	2	2	4	4	2	4
μ (mm ⁻¹)	1.840	1.838	0.616	1.825	1.734	0.743
20max (°)	140.19	146.30	59.37	146.24	146.42	58.00
Measured reflections	23467	10178	33505	41051	26816	14303
Unique reflections	8155	5035	13836	8683	9334	4828
Observed reflections	7542	3752	9993	7710	8334	3553
R _{int}	0.0237	0.0550	0.0405	0.1203	0.0304	0.0396
R [on F, obs refln only]	0.0327	0.0579	0.0531	0.0887	0.0351	0.0489
wR [on F ² , all data]	0.0879	0.1567	0.1200	0.2603	0.0945	0.1112
GoF	1.026	1.061	1.066	1.064	1.015	1.034
Largest diff peak/hole (e Å ⁻³)	0.329; -0.295	0.582; -0.749	0.666; -0.690	1.503; -2.003	0.472; -0.255	0.583; -0.461

Thermal isomerisation experiments

1. Study on the model system $\text{GaR}_3\cdot\text{IPr}$

Isolated compound **1** was used as a model system to study the influence of the solvent and additives. A 0.25 M solutions of pure crystalline compound **1** in deuterated solvent (C_6D_6 or $d_8\text{-THF}$) were prepared and sealed in Young's tap NMR tubes. Sealed tube was heated at 100 °C for a specific time followed by recording of ^1H NMR spectra (at room temperature) on a Bruker DPX 400 MHz spectrometer, operating at 400.13 MHz. Yields were calculated *versus* ferrocene which was used as an internal standard. We followed the isomerisation of pure **1** into **5** in C_6D_6 (Fig S2), $d_8\text{-THF}$ (Fig S3) and then in the presence of excess of IPr (Fig S4) and gallium reagent (Fig S5).

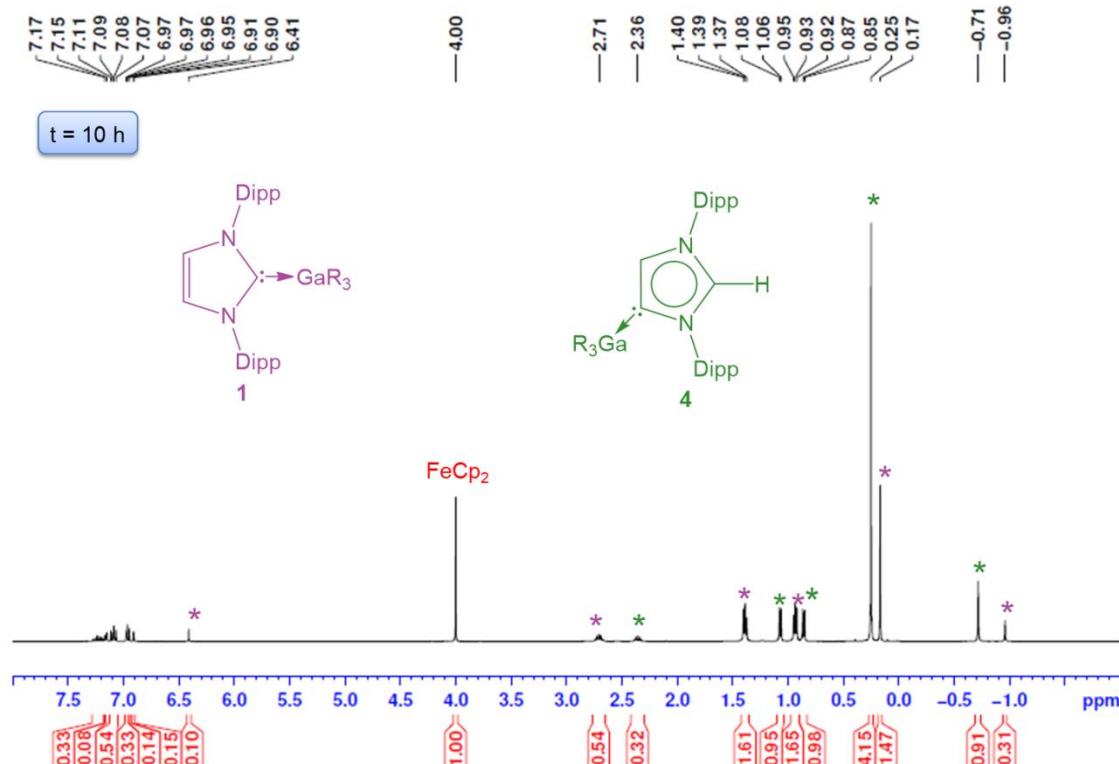


Figure S2: ^1H NMR of mixture of **1** and **5** (77%) in C_6D_6 solution obtained after 10 hours of heating of **1** at 100 °C.

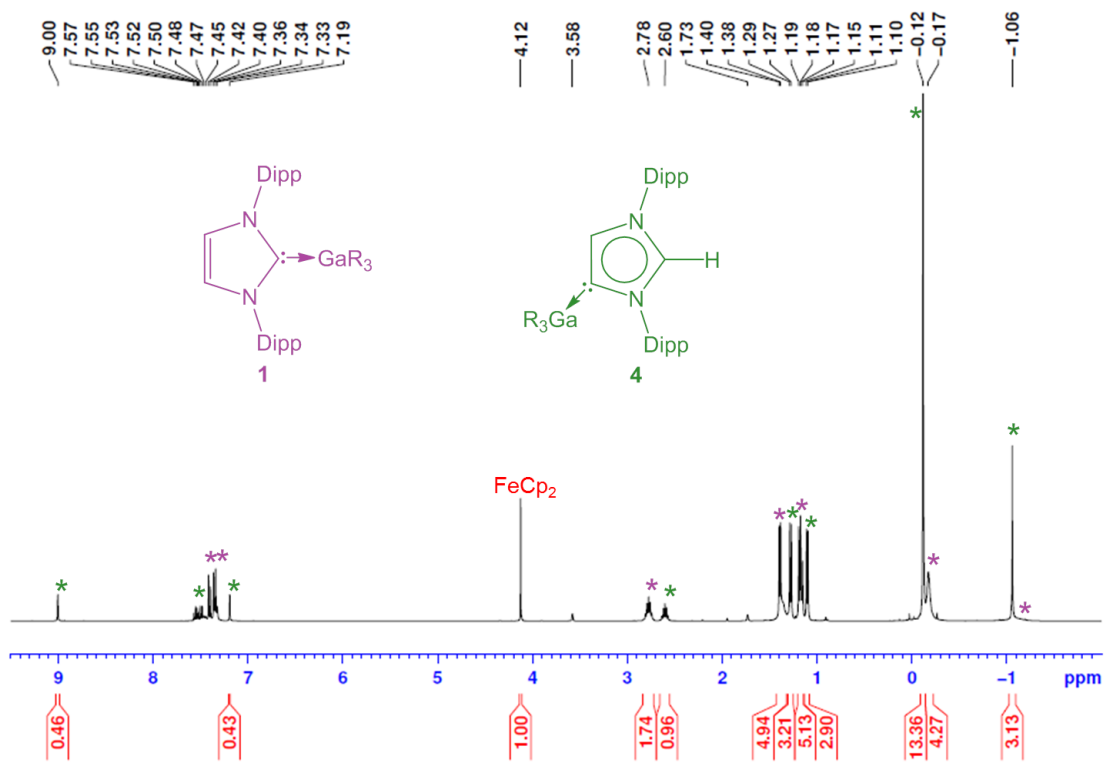


Figure S3: ^1H NMR of mixture of **1** and **5** (75%) in d_8 -THF solution obtained after 1 hour of heating of **1** at 100 °C.

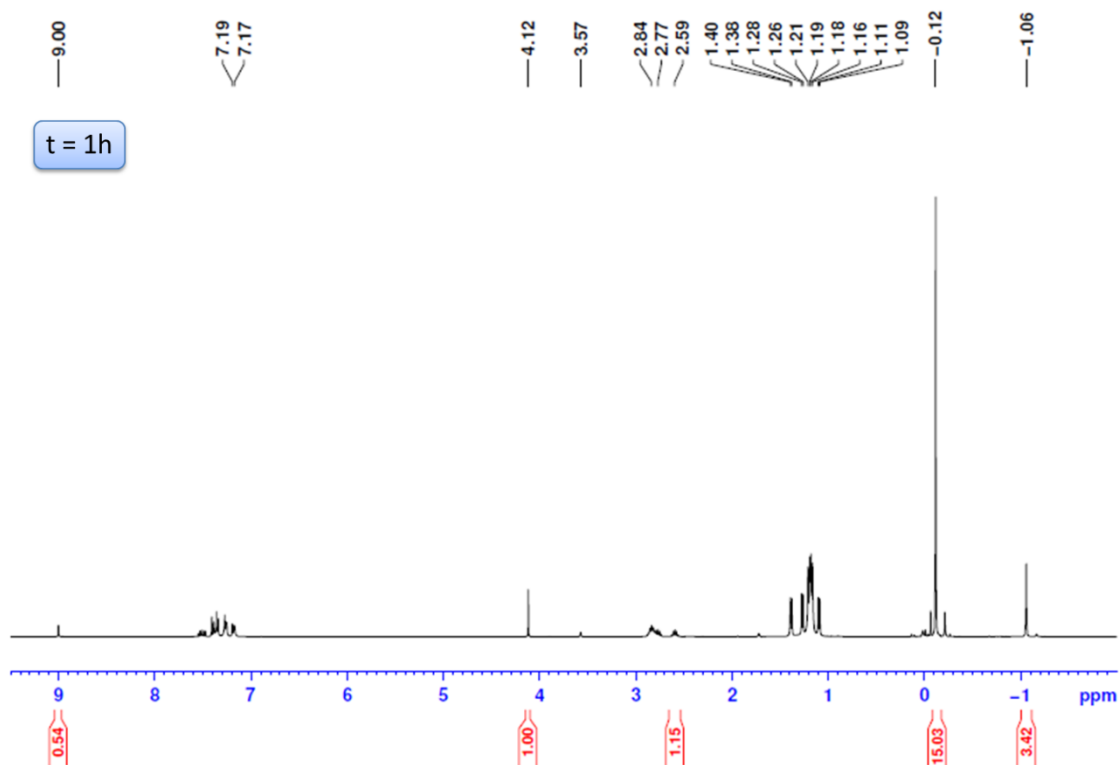


Figure S4: ^1H NMR of mixture of **1** and **5** (98% yield) in d_8 -THF solution obtained after 1 hour of heating of **1** with 2 equivalents of IPr at 100 °C.

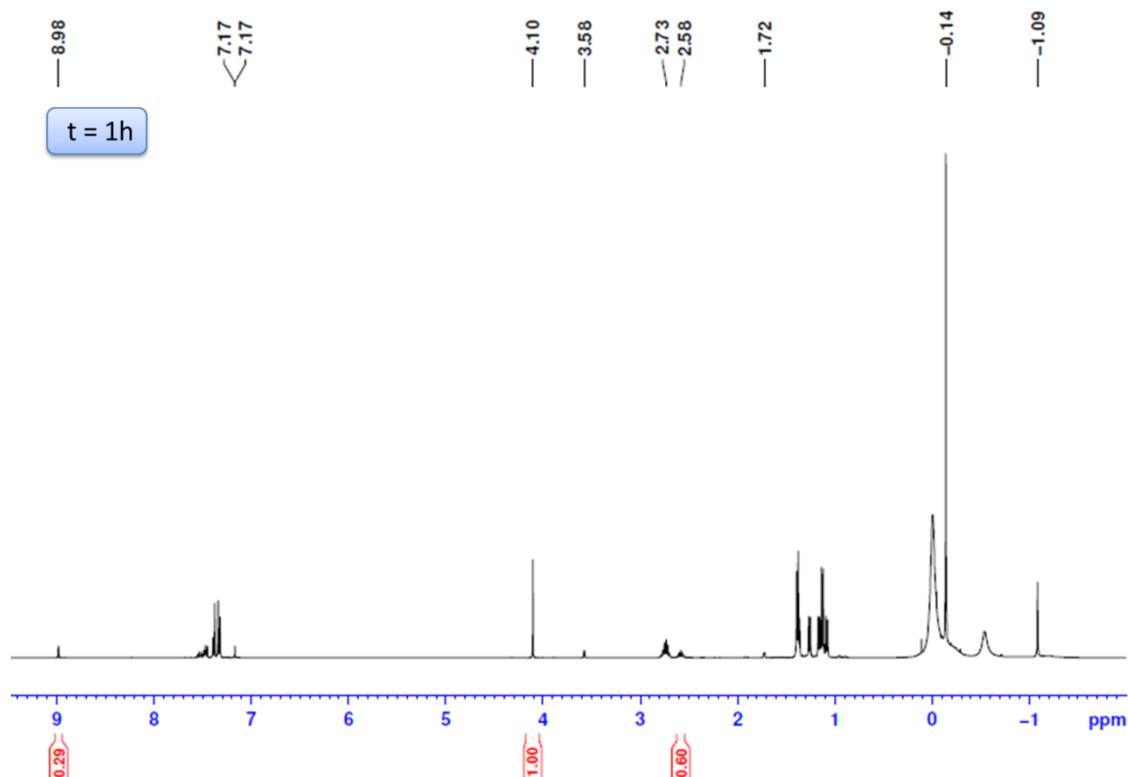


Figure S5: ^1H NMR of mixture of **1** and **5** (47% yield) in d_8 -THF solution obtained after 1 hour of heating of **1** with 2 equivalents of GaR_3 at 100 °C.

2. Extension to other related systems

Samples for the thermal isomerisation experiments were prepared and sealed in Young's tap NMR tubes as described in previous section. In this section we studied other related metal reagents with IPr carbene: MgR_2 (Fig S6-S7), ZnR_2 (Fig S8-S9), GaCl_3 (Fig S10) and other carbenes with GaR_3 : IMes (Fig S11) and IBu (Fig S12-S14).

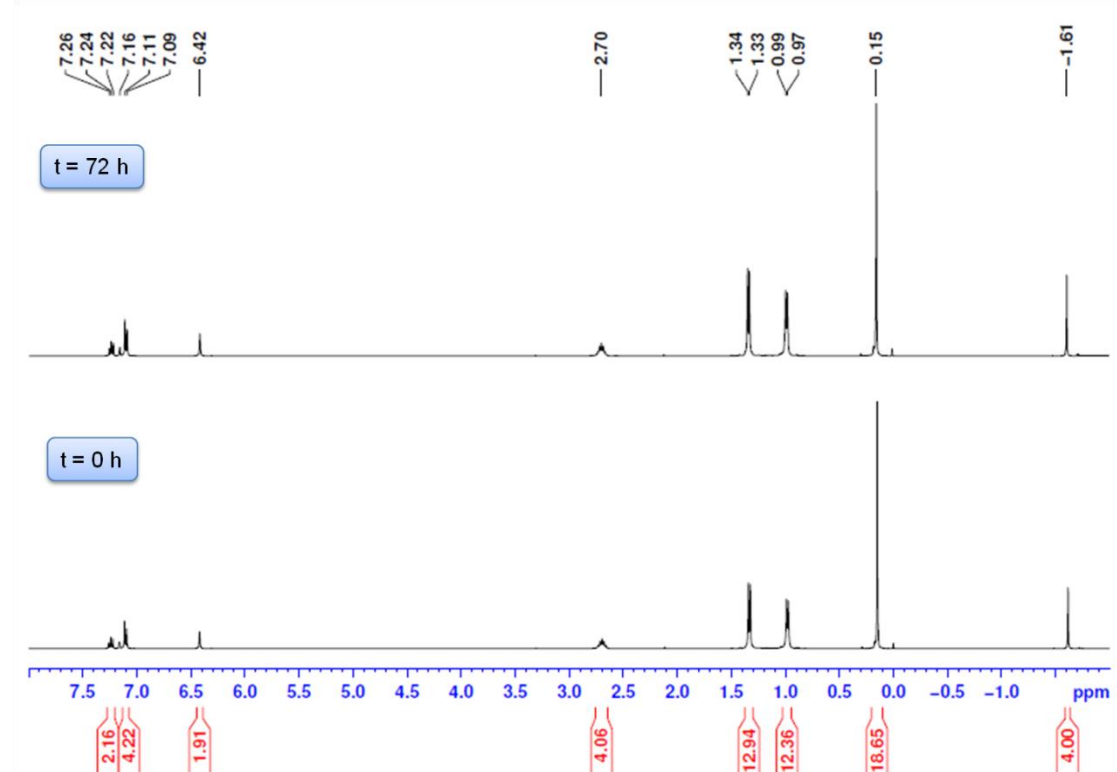


Figure S6: ^1H NMR of $[\text{Mg}(\text{CH}_2\text{SiMe}_3)_2 \cdot \text{IPr}]$ in C_6D_6 solution before (bottom) and after 72 hours of heating at 100°C (top).

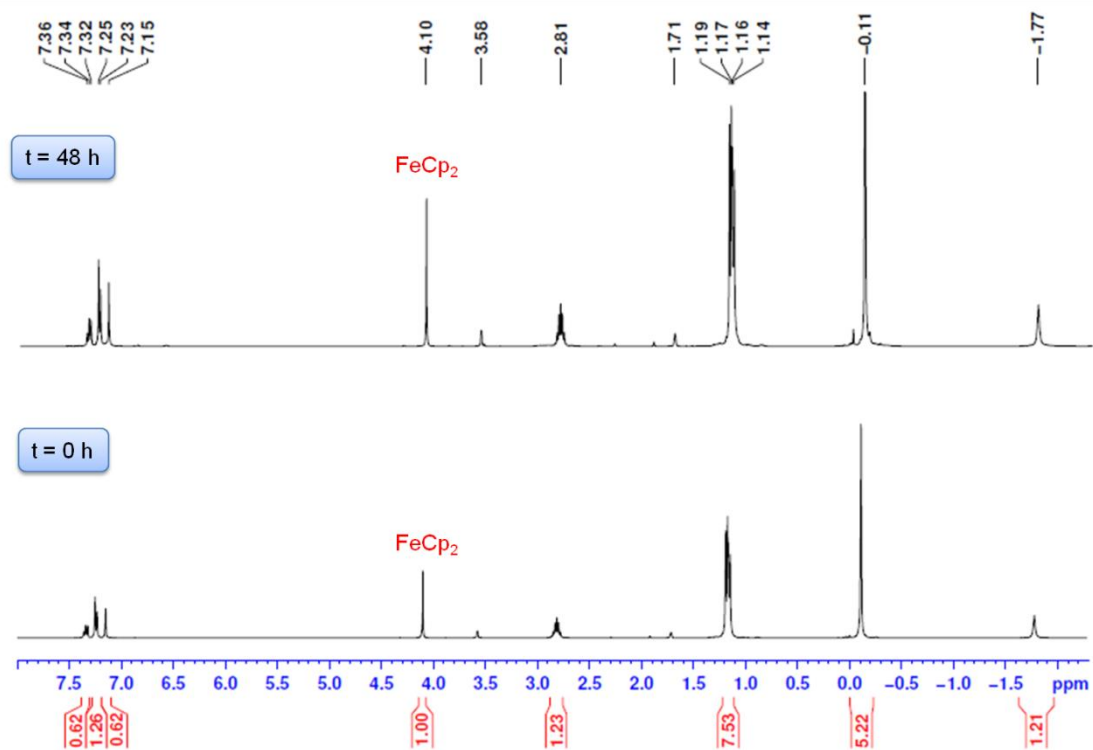


Figure S7: ¹H NMR of [Mg(CH₂SiMe₃)₂·IPr] in *d*₈-THF solution before (bottom) and after 48 hours of heating at 100 °C (top).

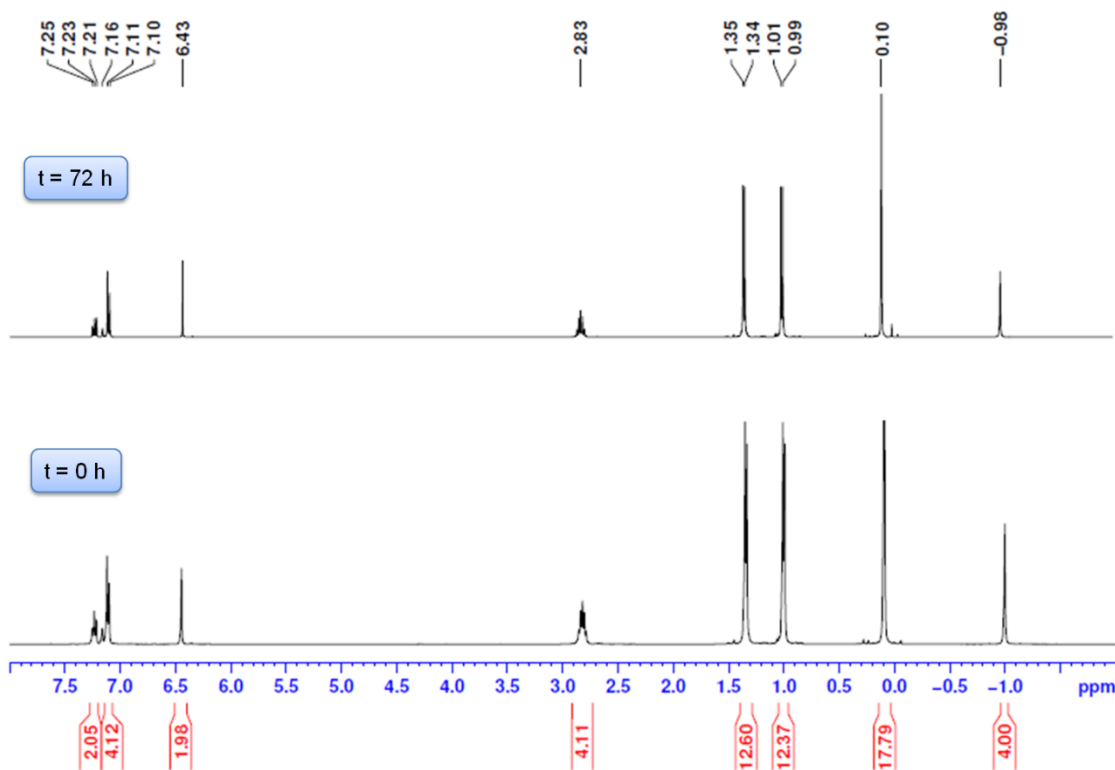


Figure S8: ¹H NMR of **6** in C₆D₆ solution before (bottom) and after 72 hours of heating at 100 °C (top).

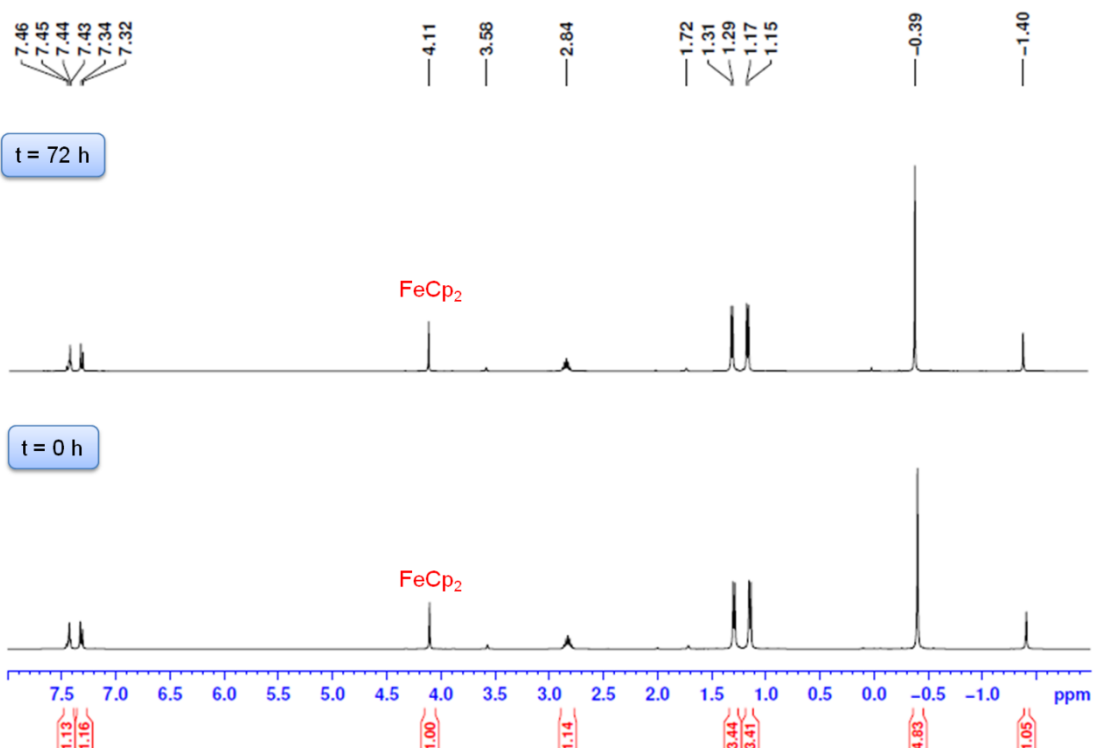


Figure S9: ¹H NMR of **6** in *d*₈-THF solution before (bottom) and after 72 hours of heating at 100 °C (top).

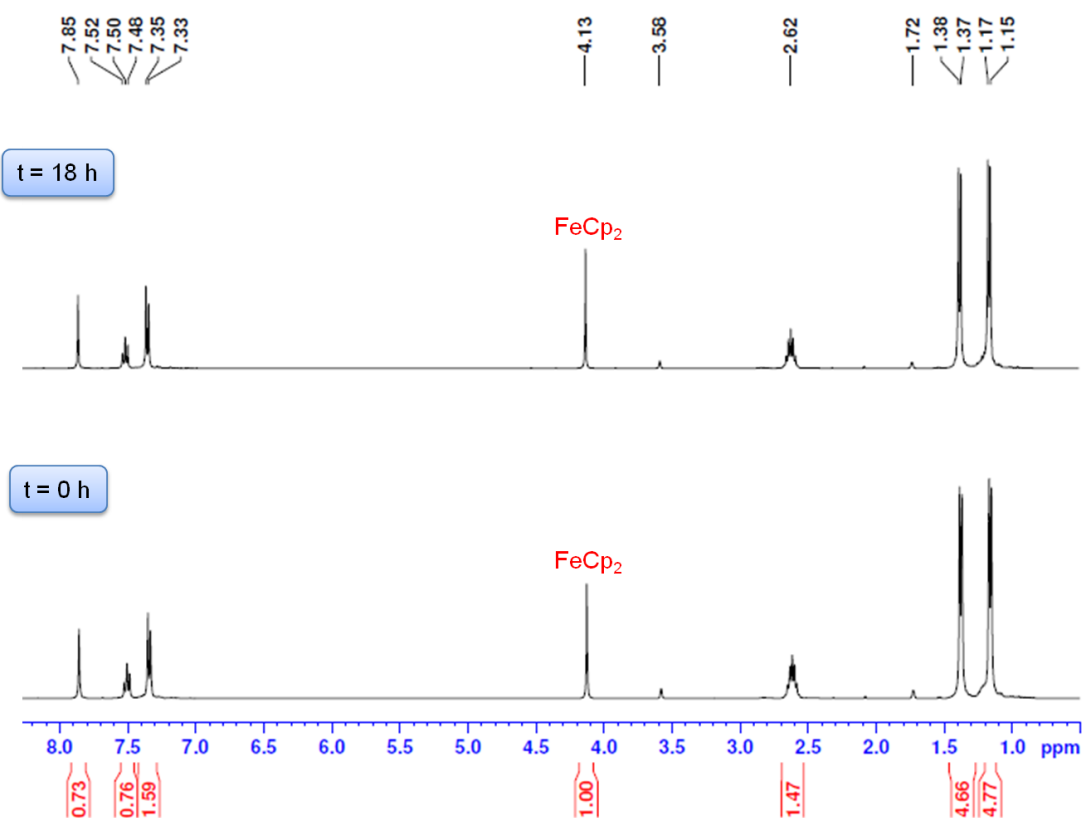


Figure S10: ¹H NMR of [GaCl₃·IPr] in *d*₈-THF solution before (bottom) and after 18 hour of heating at 100 °C (top).

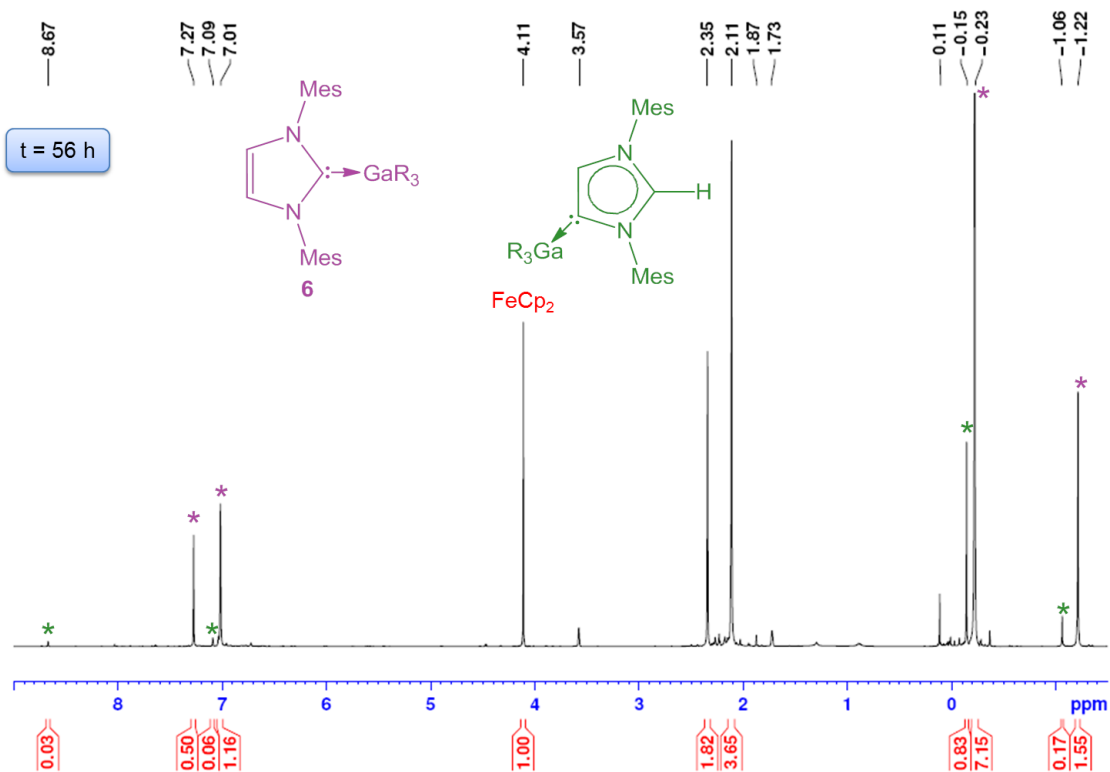


Figure S11: ^1H NMR of mixture of **7** and its abnormal isomer (8 %) in d_8 -THF solution obtained after 56 h of heating at 100 $^\circ\text{C}$.

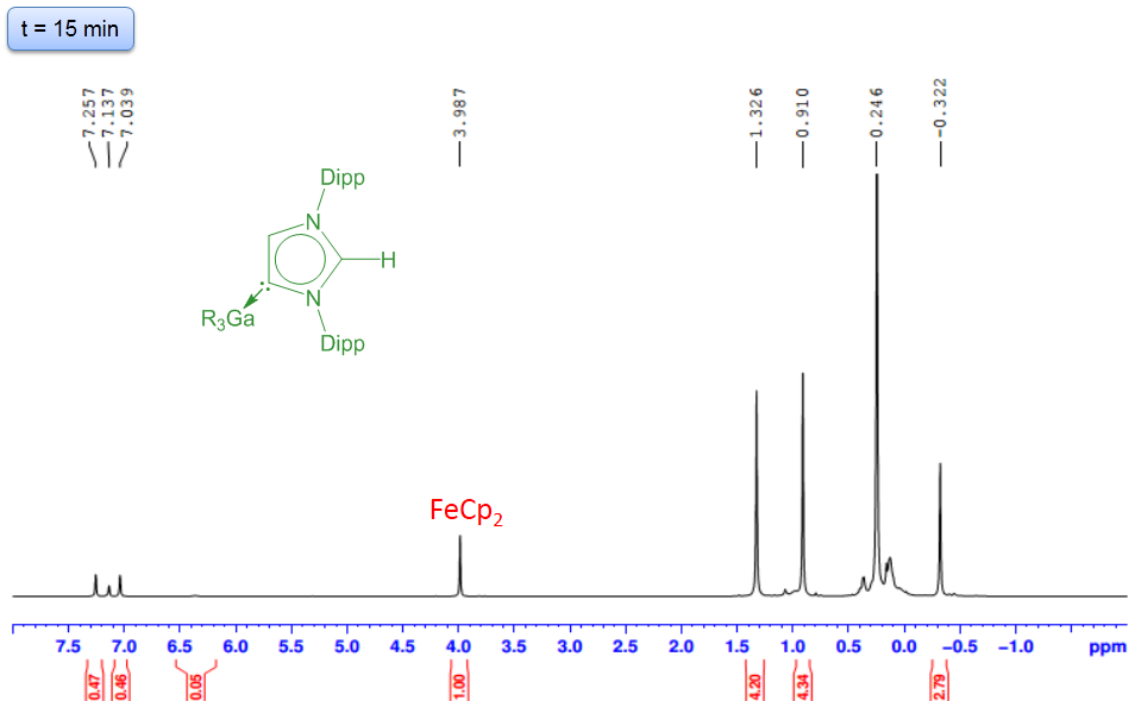


Figure S12: ^1H NMR spectrum of abnormal **8** (94% yield) generated by mixture of free IBu and $\text{Ga}(\text{CH}_2\text{SiMe}_3)_3$ in C_6D_6 after 15 min at room temperature.

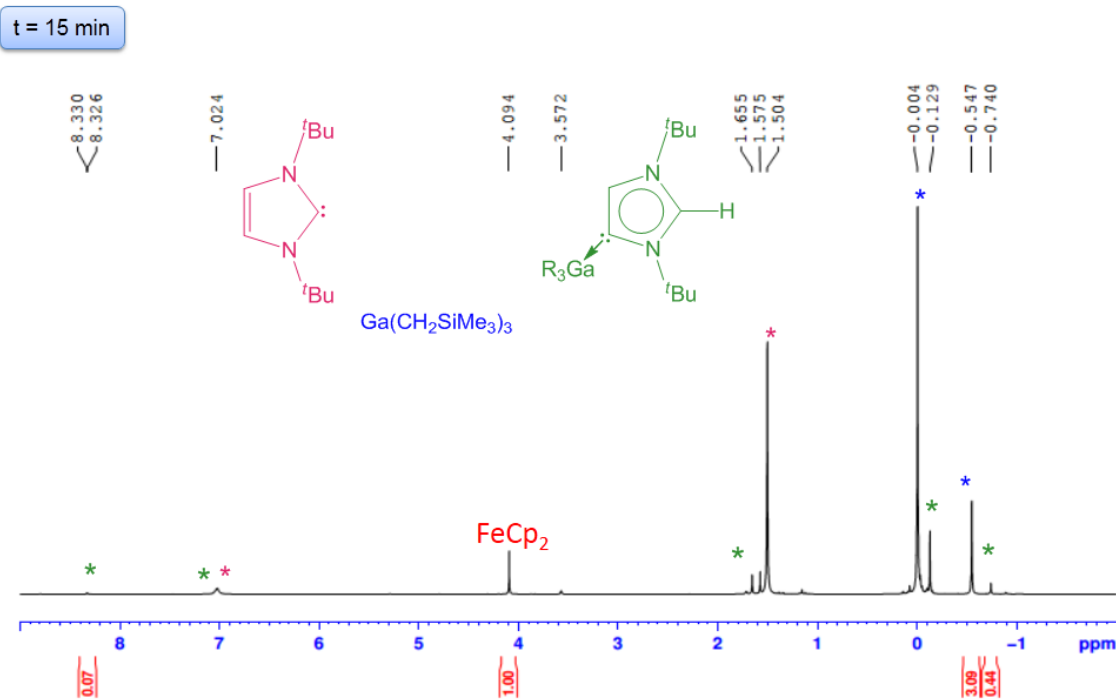


Figure S13: ^1H NMR spectrum of mixture of free IBu, $\text{Ga}(\text{CH}_2\text{SiMe}_3)_3$ and **8** (11% yield) in $d_8\text{-THF}$ after 15 min at room temperature.

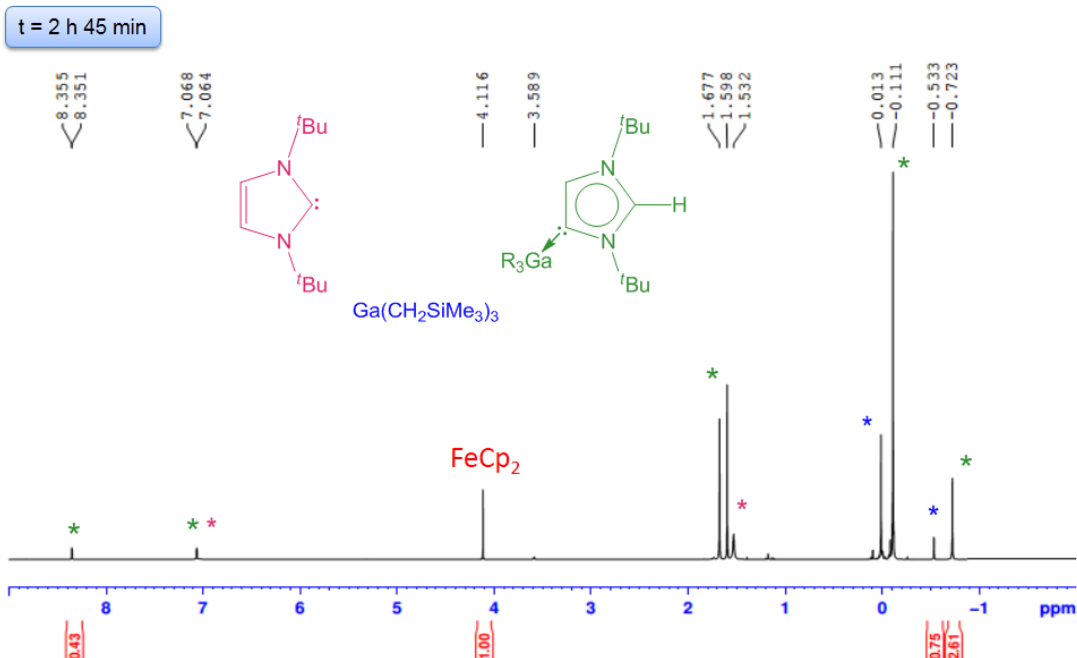


Figure S14: ^1H NMR spectrum of mixture of free IBu, $\text{Ga}(\text{CH}_2\text{SiMe}_3)_3$ and **8** (69% yield) in $d_8\text{-THF}$ after 2 h 45 min at room temperature.

Kinetic measurements

1. Kinetic isotopic effect

65 mg of pure crystalline compound **1** was dissolved in 0.4 mL of *d*₈-THF in the glovebox. The reaction mixture was transferred into a sealed Youngs tap NMR tube. The reaction was heated at 100 °C and regularly monitored by ¹H NMR spectroscopy to determine yields which were calculated by integrating the iPr-methine protons of the product (**5**) versus the ferrocene standard. For kinetic isotopic experiment another sample was prepared in exactly the same fashion but with deuterium atoms incorporated in the starting material (**1^D**).

The data were plotted as molar concentration of the product *versus* time yielding straight lines, which were fitted by conventional linear regression (*r*² > 0.96) and *k* values were obtained from the corresponding slopes.

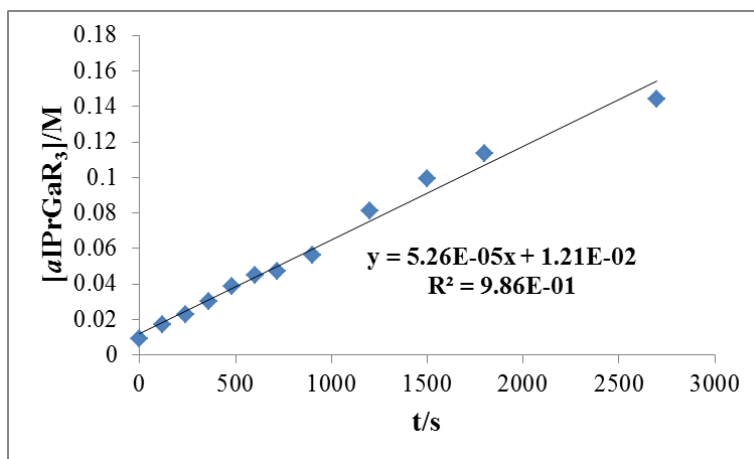


Figure S15: Kinetic analysis performed on the 0.22 M solution of **1** at 100 °C.

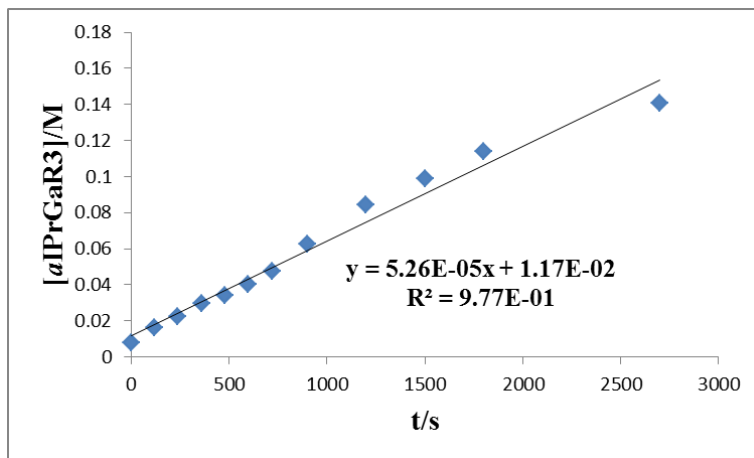


Figure S16: Kinetic analysis performed on the 0.22 M solution of **1^D** at 100 °C.

The ratio of observed constants for **1** and **1^D** revealed no kinetic isotopic effect.

$$\frac{k_H}{k_D} = \frac{5.26 \times 10^{-5}}{5.26 \times 10^{-5}} = 1(\pm 0.05)$$

2. Initial rates

Isomerization of **1** into **5** in *d*₈-THF at 323K was monitored using in situ NMR spectroscopy by following the appearance of the resonance assigned to the new C_{carbene}-H bond (9ppm). The percentage of conversion was restricted to 5–7 % in order to calculate the initial rate (*r*₀) of the reaction. The data were plotted as molar concentration of the product *versus* time yielding

straight lines, which were fitted by conventional linear regression ($r^2 > 0.96$) and r_o values were obtained from the corresponding slopes. A sample plot is shown in Figure S18.

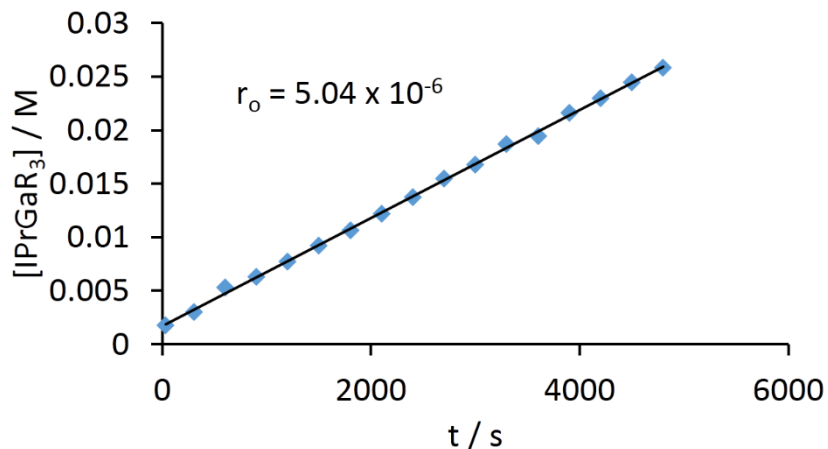


Figure S17: Initial rate over 4800 s (0.42 M [IPrGaR₃])

Reaction orders were determined by plotting initial rate *versus* the respective concentrations.

To investigate the effect of [IPrGaR₃] (**1**) on the reaction rate four experiment were carried out varying the concentration of **1**. Similarly, the effect of IPr and GaR₃ was studied through four and three experiment sets, respectively, varying the concentration of only one component of adduct (**1**) while keeping constant the concentration of the other component. The studied concentration ranges were: [IPrGaR₃] = 0.17 – 0.42 M; [IPr] = 0.29 – 0.55 M; [GaR₃] = 0.32 – 0.74 M.

Table S2: Initial rates for isomerization of **1** into **5** in *d*₈-THF at 323 K and at given initial concentrations of **1**, IPr and GaR₃.

Entry	[IPrGaR ₃] (M)	[IPr] (M)	[GaR ₃] (M)	$r_o \times 10^6$ (Ms ⁻¹)
1	0.17			1.95 ± 0.08
2	0.29			3.26 ± 0.08
3	0.37			4.81 ± 0.03
4	0.42			5.04 ± 0.04
5	0.29	0.07		4.67 ± 0.05
6	0.29	0.15		5.71 ± 0.15
7	0.29	0.26		6.40 ± 0.09
8	0.32		0.16	3.39 ± 0.04
9	0.32		0.31	2.30 ± 0.02
10	0.32		0.42	2.06 ± 0.04

a) Order in [IPrGaR₃]

Entries 1-4 in Table S2.

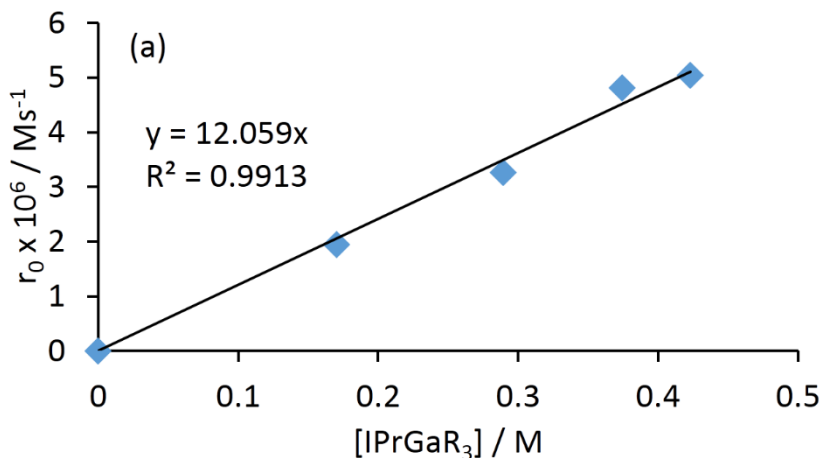


Figure S18. Plot observed Initial rate *vs* [IPrGaR₃]

b) Order in IPr

Entries 2, 5-7 in Table S2.

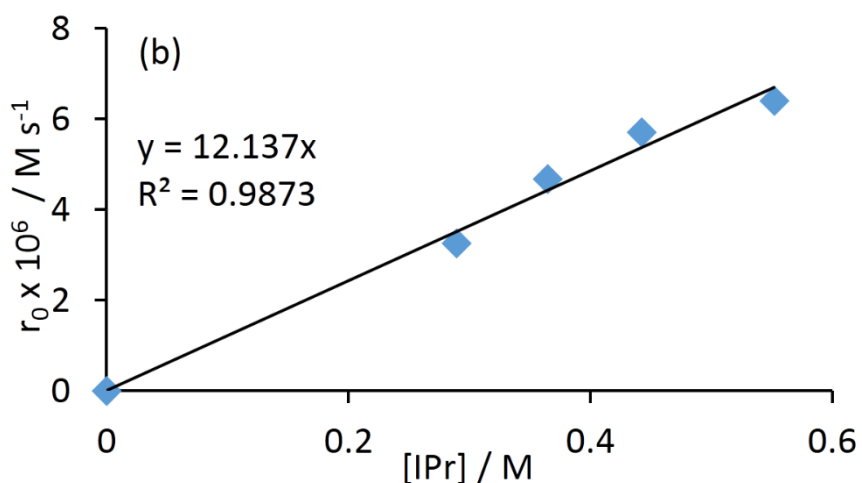
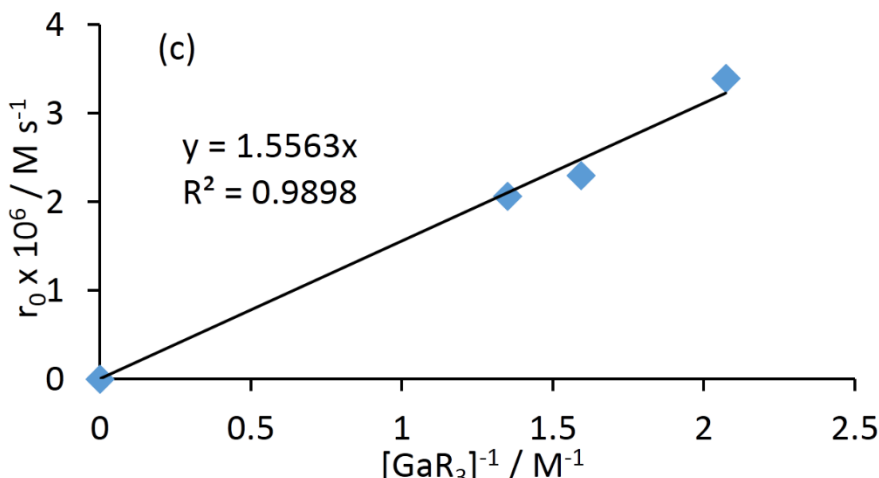


Figure S19. Plot observed Initial rate *vs* [IPr]

c) Order in GaR₃

Entries 8-10 in Table S2.

Figure S20 Plot observed Initial rate vs $[GaR_3]^{-1}$

DFT calculations

Density Functional Theory (DFT) calculations¹¹ were performed using the Gaussian computational package G03.¹² In this series of calculations the geometries of the molecules and ions were optimised by employing the B3LYP density functionals^{13,14} and the 6-311G** basis set.^{15,16} The charge distributions were obtained from a Natural Bond Orbital analysis.¹⁷

Table S3 Comparison of calculated and experimentally found structural parameters for compounds **1** and **5**.

	IPr-GaR ₃ (1)		<i>a</i> IPr-GaR ₃ (5)	
Ga-C_{NHC} (Å)	calculated	experimental	calculated	experimental
	2.333	2.1960(16)	2.146	2.0759(16)
Ga-C_R (Å)	2.038	2.0120(17)	2.045	2.0071(17)
	2.045	2.0164(16)	2.051	2.0257(16)
N-C-N (°)	2.036	2.0034(15)	2.051	2.0262(17)
	102.9	102.80(13)	108.6	107.51(14)

Table S4 Energy differences for complexes **I_R** and **II_R** and **III_R** and **IV_R** (R = Dipp, Mes, *t*Bu), respectively.

R	$\Delta E(\text{II}_R - \text{I}_R)$	$\Delta E(\text{IV}_R - \text{III}_R)$
Dipp	16.1	-1.5

¹¹ W. Kohn, A. D. Becke, R. G. Parr, *J. Phys. Chem.* **1996**, 100, 12974.

¹² Gaussian 03, Revision B.0.5, M. J. Frisch, G. W. Trucks, H. B. Schlegel, G. E. Scuseria, M. A. Robb, J. R. Cheeseman, J. A. Montgomery, Jr., T. Vreven, K. N. Kudin, J. C. Burant, J. M. Millam, S. S. Iyengar, J. Tomasi, V. Barone, B. Mennucci, M. Cossi, G. Scalmani, N. Rega, G. A. Petersson, H. Nakatsuji, M. Hada, M. Ehara, K. Toyota, R. Fukuda, J. Hasegawa, M. Ishida, T. Nakajima, Y. Honda, O. Kitao, H. Nakai, M. Klene, X. Li, J. E. Knox, H. P. Hratchian, J. B. Cross, C. Adamo, J. Jaramillo, R. Gomperts, R. E. Stratmann, O. Yazayev, A. J. Austin, R. Cammi, C. Pomelli, J. W. Ochterski, P. Y. Ayala, K. Morokuma, G. A. Voth, P. Salvador, J. J. Dannenberg, V. G. Zakrzewski, S. Dapprich, A. D. Daniels, M. C. Strain, O. Farkas, D. K. Malick, A. D. Rabuck, K. Raghavachari, J. B. Foresman, J. V. Ortiz, Q. Cui, A. G. Baboul, S. Clifford, J. Cioslowski, B. B. Stefanov, G. Liu, A. Liashenko, P. Piskorz, I. Komaromi, R. L. Martin, D. J. Fox, T. Keith, M. A. Al-Laham, C. Y. Peng, A. Nanayakkara, M. Challacombe, P. M. W. Gill, B. Johnson, W. Chen, M. W. Wong, C. Gonzalez, and J. A. Pople, Gaussian, Inc., Pittsburgh PA, 2003.

¹³ A.D. Becke, *Phys. Rev. A* **1988**, 38, 3098.

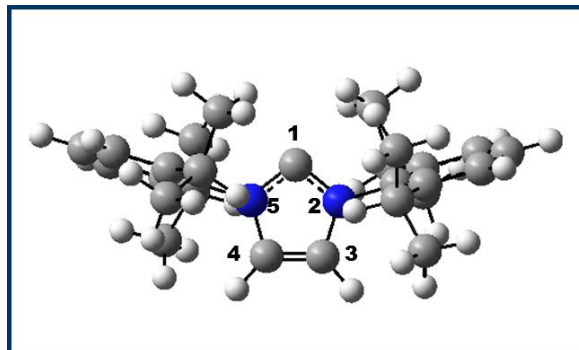
¹⁴ C.T. Lee, W.T. Yang and R.G.Parr, *Phys. Rev. B* **1998**, 37, 785.

¹⁵ A. D. McLean and G. S. Chandler, *J. Chem. Phys.* **1980**, 72, 5639.

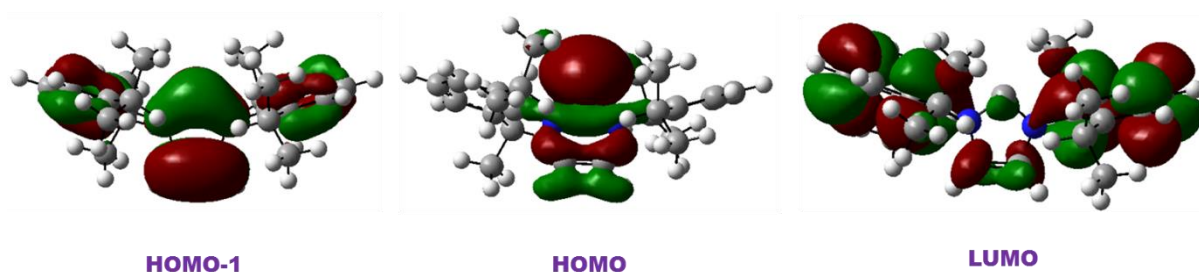
¹⁶ R. Krishnan, J. S. Binkley, R. Seeger and J. A. Pople, *J. Chem. Phys.* **1980**, 72, 650.

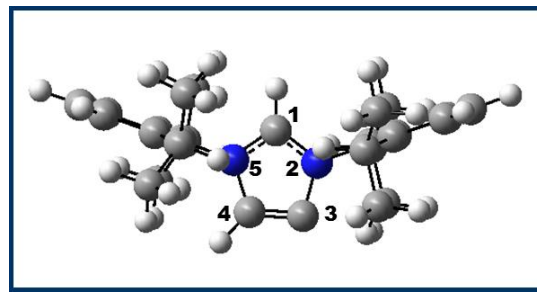
¹⁷ NBO Version 3.1, E. D. Glendening, A. E. Reed, J. E. Carpenter, and F. Weinhold.

Mes	16.8	+2.1
'Bu	17.2	n/a

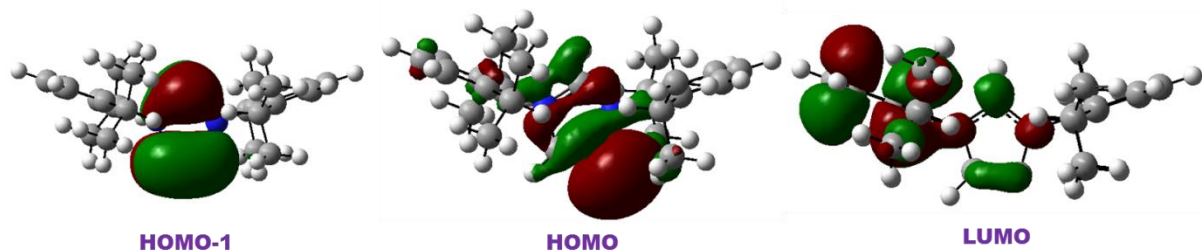
1. Optimized geometry of normal IPr (**I_{IPr}**)**Table S5** optimized geometry of **I_{IPr}**.

Principal bond lengths (Å)	Principal bond angles(°)	Principal Bond Indices
C ₁ -N ₂	112.9	C ₁ -N ₂
N ₂ -C ₃	106.2	N ₂ -C ₃
C ₃ -C ₄	106.2	C ₃ -C ₄
C ₄ -N ₅	112.9	C ₄ -N ₅
N ₅ -C ₁	101.8	N ₅ -C ₁
N ₂ -C ₆	123.8	N ₂ -C ₆
N ₅ -C ₇	123.8	N ₅ -C ₇
	123.2	
	123.2	

**Figure S21:** Representation of molecular orbitals HOMO-1, HOMO and LUMO of **I_{IPr}**.2. Optimized geometry of abnormal IPr (**II_{IPr}**).

**Table S6.** Optimized geometry of **IIIPr**.

Principal bond lengths (Å)	Principal bond angles(°)	Principal Bond Indices
C ₁ -N ₂	C ₁ -N ₂ -C ₃	C ₁ -N ₂
N ₂ -C ₃	N ₂ -C ₃ -C ₄	N ₂ -C ₃
C ₃ -C ₄	C ₃ -C ₄ -N ₅	C ₃ -C ₄
C ₄ -N ₅	C ₄ -N ₅ -C ₁	C ₄ -N ₅
N ₅ -C ₁	N ₅ -C ₁ -N ₂	N ₅ -C ₁
N ₂ -C ₆	C ₁ -N ₂ -C ₆	N ₂ -C ₆
N ₅ -C ₇	C ₁ -N ₅ -C ₇	N ₅ -C ₇
	C ₃ -N ₂ -C ₆	
	C ₄ -N ₅ -C ₇	

**Figure S22:** Representation of molecular orbitals HOMO-1, HOMO and LUMO of **IIIPr**

3. Optimized geometry of GaR₃

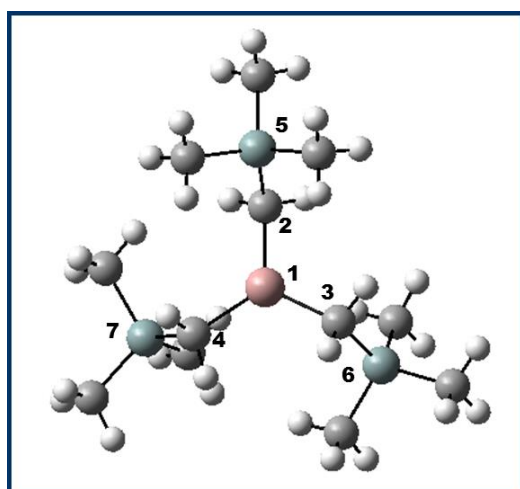
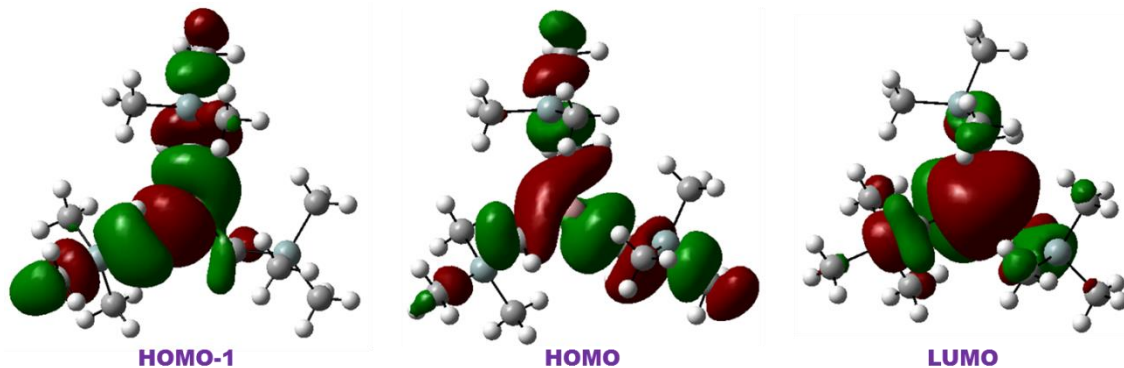
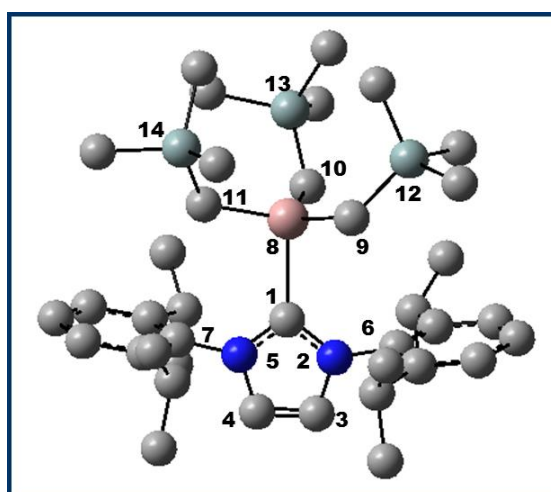


Table S7. Optimized geometry of GaR₃.

Principal bond lengths (Å)		Principal bond angles(°)		Principal Bond Indices	
Ga ₁ -C ₂	1.991	Ga ₁ -C ₂ -Si ₅	117.6	Ga ₁ -C ₂	0.64
Ga ₁ -C ₃	1.996	Ga ₁ -C ₃ -Si ₆	119.8	Ga ₁ -C ₃	0.63
Ga ₁ -C ₄	1.993	Ga ₁ -C ₄ -Si ₇	118.4	Ga ₁ -C ₄	0.64
C ₂ -Si ₅	1.888	C ₂ -Ga ₁ -C ₃	122.1	C ₂ -Si ₅	0.80
C ₃ -Si ₆	1.887	C ₃ -Ga ₁ -C ₄	119.2	C ₃ -Si ₆	0.81
C ₄ -Si ₇	1.888	C ₄ -Ga ₁ -C ₂	118.7	C ₄ -Si ₇	0.81
Si ₅ -C _{Me}	1.893; 1.893; 1.894	C ₂ -Si ₅ -C _{Me}	110.4; 110.0; 110.3	Si ₅ -C _{Me}	0.82; 0.82; 0.82
Si ₆ -C _{Me}	1.895; 1.892; 1.893	C ₃ -Si ₆ -C _{Me}	110.0; 110.3; 109.9	Si ₆ -C _{Me}	0.82; 0.82; 0.82
Si ₇ -C _{Me}	1.894; 1.893; 1.893	C ₄ -Si ₇ -C _{Me}	110.1; 110.0; 110.4	Si ₇ -C _{Me}	0.82; 0.82; 0.82

**Figure S23:** Representation of molecular orbitals HOMO-1, HOMO and LUMO of GaR₃.

4. Optimized geometry of normal IPr·GaR₃ complex (**III_{IPr}**)

**Table S8.** Optimized geometry of **III_{IPr}**.

Principal bond lengths (Å)	Principal bond angles(°)	Principal bond indices
----------------------------	--------------------------	------------------------

C_1-N_2	1.374	$C_1-N_2-C_3$	111.8	C_1-N_2	1.26
N_2-C_3	1.390	$N_2-C_3-C_4$	106.8	N_2-C_3	1.11
C_3-C_4	1.347	$C_3-C_4-N_5$	106.7	C_3-C_4	1.66
C_4-N_5	1.390	$C_4-N_5-C_1$	111.9	C_4-N_5	1.10
N_5-C_1	1.372	$N_5-C_1-N_2$	102.9	N_5-C_1	1.26
N_2-C_6	1.453	$C_1-N_2-C_6$	129.1	N_2-C_6	0.92
N_5-C_7	1.451	$C_1-N_5-C_7$	128.5	N_5-C_7	0.92
C_9-Si_{12}	1.878	$C_3-N_2-C_6$	119.0	C_9-Si_{12}	0.82
$C_{10}-Si_{13}$	1.883	$C_4-N_5-C_7$	119.5	$C_{10}-Si_{13}$	0.82
$C_{11}-Si_{14}$	1.879	$N_2-C_1-Ga_8$	128.5	$C_{11}-Si_{14}$	0.83
C_1-Ga_8	2.333	$N_5-C_1-Ga_8$	128.4	C_1-Ga_8	0.45
Ga_8-C_9	2.038	$C_1-Ga_8-C_9$	102.8	Ga_8-C_9	0.62
Ga_8-C_{10}	2.045	$C_1-Ga_8-C_{10}$	97.8	Ga_8-C_{10}	0.61
Ga_8-C_{11}	2.036	$C_1-Ga_8-C_{11}$	104.5	Ga_8-C_{11}	0.62
$Si_{12}-C_{Me}$	1.903; 1.896; 1.894	$Ga_8-C_9-C_{12}$	127.5	$Si_{12}-C_{Me}$	0.81; 0.82; 0.80
$Si_{13}-C_{Me}$	1.897; 1.902; 1.893	$Ga_8-C_{10}-Si_{13}$	126.5	$Si_{13}-C_{Me}$	0.81; 0.82; 0.81
$Si_{14}-C_{Me}$	1.898; 1.903; 1.894	$Ga_8-C_{11}-Si_{14}$	125.4	$Si_{14}-C_{Me}$	0.82; 0.81; 0.81
		$C_9-Si_{12}-C_{Me}$	113.8; 109.4; 111.4		
		$C_{10}-Si_{13}-C_{Me}$	109.0; 113.5; 113.0		
		$C_{11}-Si_{14}-C_{Me}$	109.2; 114.1; 111.6		

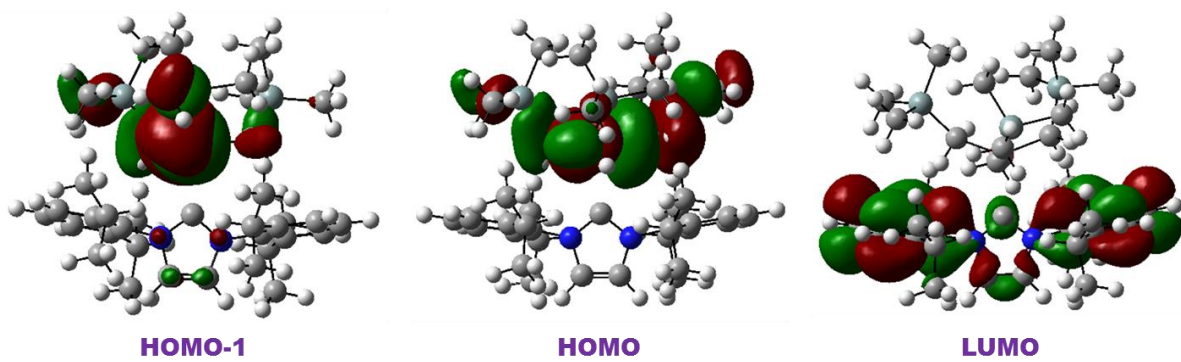
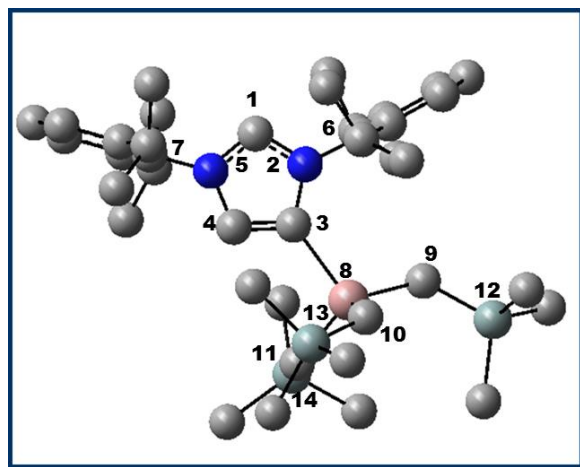
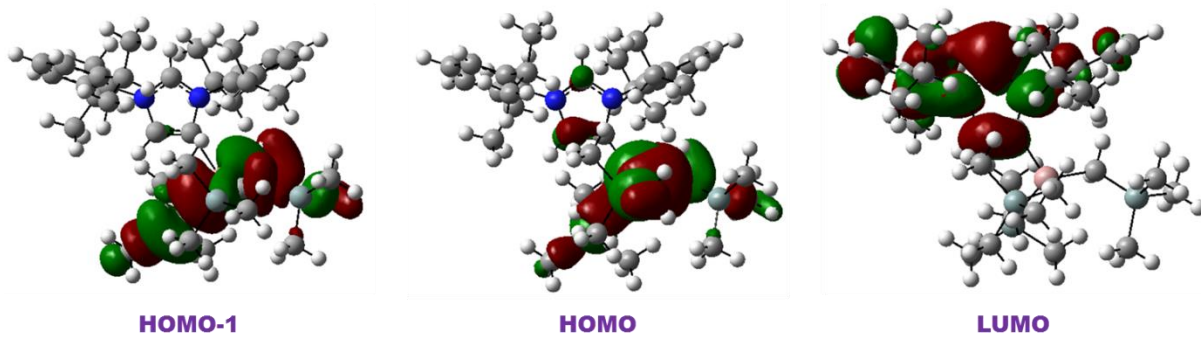
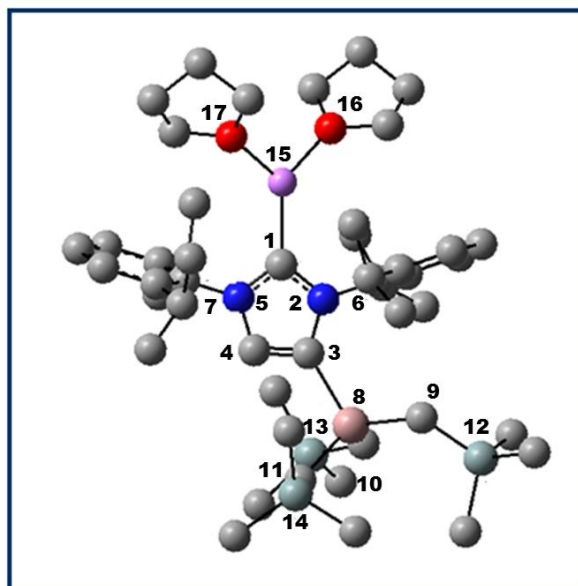


Figure S24 Representation of molecular orbitals HOMO-1, HOMO and LUMO of **III_{IPr}**.

5. Optimized geometry of abnormal IPr·GaR₃ complex (**IV_{IPr}**)

**Table S9** Optimized geometry of **IV_{IPr}**.

Principal bond lengths (Å)	Principal bond angles(°)	Principal bond indices
C ₁ -N ₂	110.8	C ₁ -N ₂ 1.29
N ₂ -C ₃	102.9	N ₂ -C ₃ 1.11
C ₃ -C ₄	110.3	C ₃ -C ₄ 1.61
C ₄ -N ₅	107.3	C ₄ -N ₅ 1.10
N ₅ -C ₁	108.6	N ₅ -C ₁ 1.30
N ₂ -C ₆	121.3	N ₂ -C ₆ 0.91
N ₅ -C ₇	125.3	N ₅ -C ₇ 0.92
Si ₁₂ -C _{Me}	127.9	Si ₁₂ -C _{Me} 0.81; 0.81; 0.80
Si ₁₃ -C _{Me}	127.4	Si ₁₃ -C _{Me} 0.81; 0.82; 0.80
Si ₁₄ -C _{Me}	132.9	Si ₁₄ -C _{Me} 0.82; 0.81; 0.80
C ₃ -Ga ₈	124.2	C ₃ -Ga ₈ 0.53
Ga ₈ -C ₉	107.3	Ga ₈ -C ₉ 0.64
Ga ₈ -C ₁₀	107.9	Ga ₈ -C ₁₀ 0.63
Ga ₈ -C ₁₁	102.0	Ga ₈ -C ₁₁ 0.63
C ₉ -Si ₁₂	120.5	C ₉ -Si ₁₂ 0.83
C ₁₀ -Si ₁₃	125.5	C ₁₀ -Si ₁₃ 0.84
C ₁₁ -Si ₁₄	122.9	C ₁₁ -Si ₁₄ 0.84
	C ₉ -Si ₁₂ -C _{Me} 113.0; 110.6; 110.5	
	C ₁₀ -Si ₁₃ -C _{Me} 110.7; 111.8; 112.6	
	C ₁₁ -Si ₁₄ -C _{Me} 112.4; 110.9; 111.7	

**Figure S25** Representation of molecular orbitals HOMO-1, HOMO and LUMO of **IV_{IPr}**.6. Optimized geometry of $(\text{THF})_2\text{Li}[:\text{C}\{[\text{N}(2,6-\text{iPr}_2\text{C}_6\text{H}_3)]_2\text{CHCGa}(\text{CH}_2\text{SiMe}_3)_3\}]$ (**V_{IPr}**)**Table S10** Optimized geometry of **V_{IPr}**.

Principal bond lengths (Å)	Principal bond angles (°)	Principal bond indices
C ₁ -N ₂	1.372	C ₁ -N ₂
N ₂ -C ₃	1.420	N ₂ -C ₃
C ₃ -C ₄	1.365	C ₃ -C ₄
C ₄ -N ₅	1.400	C ₄ -N ₅
N ₅ -C ₁	1.362	N ₅ -C ₁
N ₂ -C ₆	1.444	N ₂ -C ₆
N ₅ -C ₇	1.440	N ₅ -C ₇
Si ₁₂ -C _{Me}	1.905; 1.897; 1.899	Si ₁₂ -C _{Me}
Si ₁₃ -C _{Me}	1.905; 1.902; 1.897	Si ₁₃ -C _{Me}
Si ₁₄ -C _{Me}	1.901; 1.905; 1.897	Si ₁₄ -C _{Me}
C ₁ -N ₂ -C ₃	114.4	1.25
N ₂ -C ₃ -C ₄	102.3	1.07
C ₃ -C ₄ -N ₅	109.5	1.65
C ₄ -N ₅ -C ₁	111.2	1.06
N ₅ -C ₁ -N ₂	102.7	1.26
C ₁ -N ₂ -C ₆	121.1	0.94
C ₁ -N ₅ -C ₇	125.0	0.92
C ₃ -N ₂ -C ₆	124.5	0.81; 0.81; 0.80
C ₄ -N ₅ -C ₇	123.8	0.81; 0.80; 0.80
N ₂ -C ₃ -Ga ₈	134.3	0.81; 0.80; 0.80

$C_3\text{-Ga}_8$	2.054	$C_4\text{-C}_3\text{-Ga}_8$	123.4	$C_3\text{-Ga}_8$	0.56
$Ga_8\text{-C}_9$	2.044	$C_3\text{-Ga}_8\text{-C}_9$	109.0	$Ga_8\text{-C}_9$	0.63
$Ga_8\text{-C}_{10}$	2.061	$C_3\text{-Ga}_8\text{-C}_{10}$	109.9	$Ga_8\text{-C}_{10}$	0.62
$Ga_8\text{-C}_{11}$	2.058	$C_3\text{-Ga}_8\text{-C}_{11}$	103.8	$Ga_8\text{-C}_{11}$	0.63
$C_9\text{-Si}_{12}$	1.873	$Ga_8\text{-C}_9\text{-Si}_{12}$	121.5	$C_9\text{-Si}_{12}$	0.84
$C_{10}\text{-Si}_{13}$	1.867	$Ga_8\text{-C}_{10}\text{-Si}_{13}$	125.7	$C_{10}\text{-Si}_{13}$	0.85
$C_{11}\text{-Si}_{14}$	1.868	$Ga_8\text{-C}_{11}\text{-Si}_{14}$	123.8	$C_{11}\text{-Si}_{14}$	0.85
$C_1\text{-Li}_{15}$	2.120	$C_9\text{-Si}_{12}\text{-C}_{\text{Me}}$	113.3; 110.6; 111.2	$C_1\text{-Li}_{15}$	0.08
$Li_{15}\text{-O}_{16}$	1.953	$C_{10}\text{-Si}_{13}\text{-C}_{\text{Me}}$	110.9; 113.1; 111.6	$Li_{15}\text{-O}_{16}$	0.02
$Li_{15}\text{-O}_{17}$	1.961	$C_{11}\text{-Si}_{14}\text{-C}_{\text{Me}}$	112.6; 112.1; 111.1	$Li_{15}\text{-O}_{17}$	0.02
		$N_2\text{-C}_1\text{-Li}_{15}$	129.0		
		$N_5\text{-C}_1\text{-Li}_{15}$	128.3		
		$C_1\text{-Li}_{15}\text{-O}_{16}$	130.9		
		$C_1\text{-Li}_{15}\text{-O}_{17}$	129.1		
		$O_{16}\text{-Li}_{15}\text{-O}_{17}$	99.9		

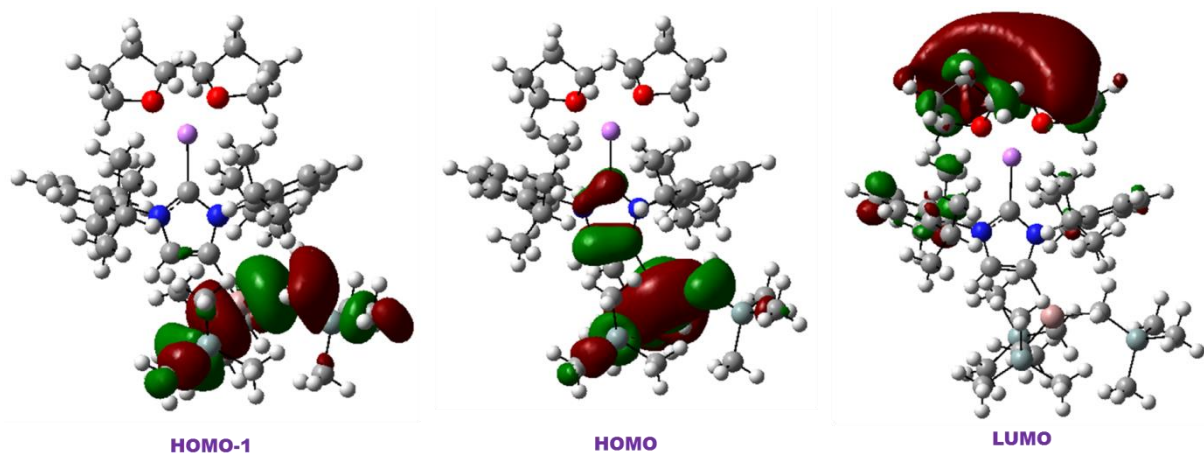
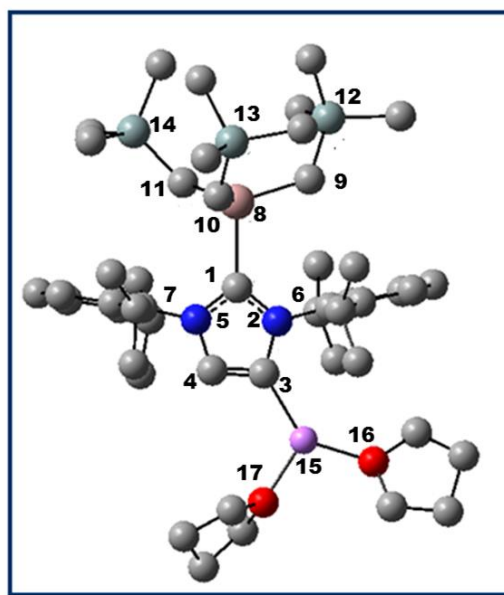


Figure S26 Representation of molecular orbitals HOMO-1, HOMO and LUMO of V_{IPr} .

7. Optimized geometry of $\text{Ga}(\text{CH}_2\text{SiMe}_3)_3[:\text{C}\{[\text{N}(2,6\text{-}^i\text{Pr}_2\text{C}_6\text{H}_3)]_2\text{CHC}(\text{THF})_2\text{Li}\}] (\text{VI}_{\text{IPr}})$

**Table S11** Optimized geometry of VIIPr.

Principal bond lengths (Å)	Principal bond angles (°)	Principal bond indices
C ₁ -N ₂	1.374	C ₁ -N ₂ -C ₃ 115.3
N ₂ -C ₃	1.421	N ₂ -C ₃ -C ₄ 101.2
C ₃ -C ₄	1.364	C ₃ -C ₄ -N ₅ 110.7
C ₄ -N ₅	1.402	C ₄ -N ₅ -C ₁ 110.4
N ₅ -C ₁	1.368	N ₅ -C ₁ -N ₂ 102.4
N ₂ -C ₆	1.441	C ₁ -N ₂ -C ₆ 125.5
N ₅ -C ₇	1.447	C ₁ -N ₅ -C ₇ 129.7
Si ₁₂ -C _{Me}	1.895; 1.905; 1.896	C ₃ -N ₂ -C ₆ 119.0
Si ₁₃ -C _{Me}	1.905; 1.899; 1.895	C ₄ -N ₅ -C ₇ 119.6
Si ₁₄ -C _{Me}	1.898; 1.895; 1.905	N ₂ -C ₁ -Ga ₈ 129.9
C ₁ -Ga ₈	2.272	N ₅ -C ₁ -Ga ₈ 127.3
Ga ₈ -C ₉	2.046	C ₁ -Ga ₈ -C ₉ 105.6
Ga ₈ -C ₁₀	2.054	C ₁ -Ga ₈ -C ₁₀ 99.1
Ga ₈ -C ₁₁	2.046	C ₁ -Ga ₈ -C ₁₁ 101.1
C ₉ -Si ₁₂	1.876	Ga ₈ -C ₉ -Si ₁₂ 126.4
C ₁₀ -Si ₁₃	1.879	Ga ₈ -C ₁₀ -Si ₁₃ 128.1
C ₁₁ -Si ₁₄	1.875	Ga ₈ -C ₁₁ -Si ₁₄ 128.1
C ₃ -Li ₁₅	2.047	C ₉ -Si ₁₂ -C _{Me} 109.3; 112.2; 114.3
Li ₁₅ -O ₁₆	1.966	C ₁₀ -Si ₁₃ -C _{Me} 113.3; 114.0; 109.3
Li ₁₅ -O ₁₇	1.928	C ₁₁ -Si ₁₄ -C _{Me} 114.0; 109.6; 111.6
		C ₄ -C ₃ -Li ₁₅ 123.8

$\text{N}_2\text{-C}_3\text{-Li}_{15}$	135.0
$\text{C}_3\text{-Li}_{15}\text{-O}_{16}$	116.5
$\text{C}_3\text{-Li}_{15}\text{-O}_{17}$	137.8
$\text{O}_{16}\text{-Li}_{15}\text{-O}_{17}$	105.4

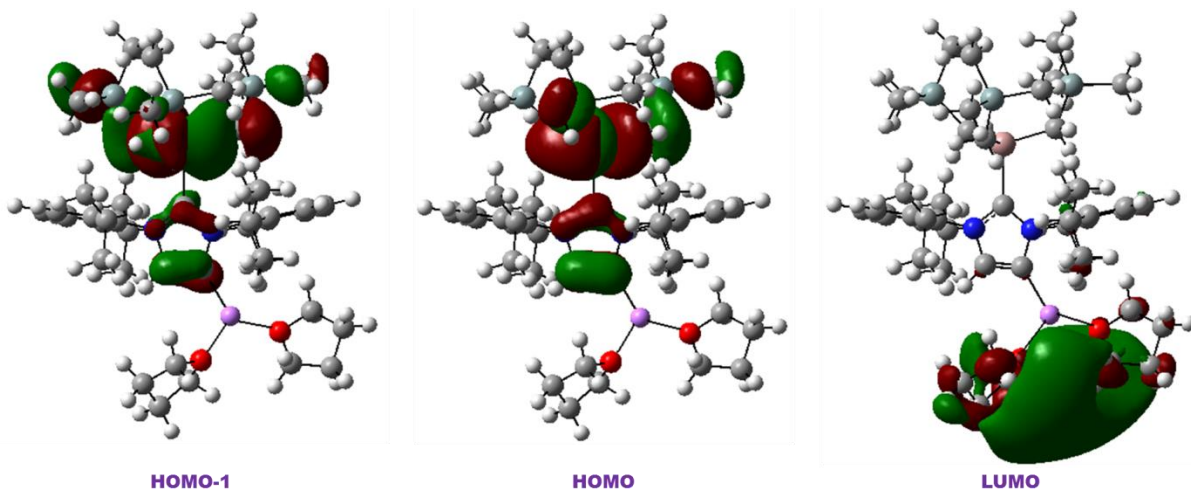


Figure S27 Representation of molecular orbitals HOMO-1, HOMO and LUMO of **VI_{IPr}**.

8. Optimized geometry of normal IMes (**I_{IMes}**)

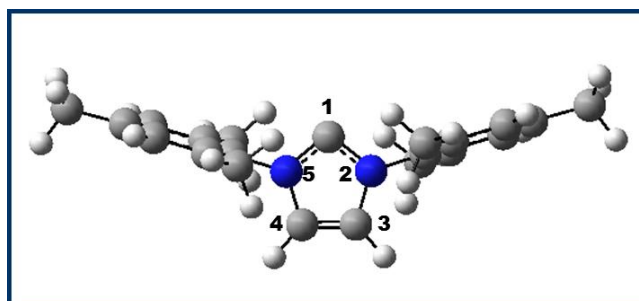


Table S12 Optimized geometry of **I_{IMes}**.

Principal bond lengths (Å)		Principal bond angles(°)		Principal Bond Indices	
$\text{C}_1\text{-N}_2$	1.371	$\text{C}_1\text{-N}_2\text{-C}_3$	113.0	$\text{C}_1\text{-N}_2$	1.24
$\text{N}_2\text{-C}_3$	1.397	$\text{N}_2\text{-C}_3\text{-C}_4$	106.1	$\text{N}_2\text{-C}_3$	1.09
$\text{C}_3\text{-C}_4$	1.351	$\text{C}_3\text{-C}_4\text{-N}_5$	106.1	$\text{C}_3\text{-C}_4$	1.67
$\text{C}_4\text{-N}_5$	1.397	$\text{C}_4\text{-N}_5\text{-C}_1$	113.0	$\text{C}_4\text{-N}_5$	1.09
$\text{N}_5\text{-C}_1$	1.371	$\text{N}_5\text{-C}_1\text{-N}_2$	101.8	$\text{N}_5\text{-C}_1$	1.24
$\text{N}_2\text{-C}_6$	1.439	$\text{C}_1\text{-N}_2\text{-C}_6$	123.6	$\text{N}_2\text{-C}_6$	0.94
$\text{N}_5\text{-C}_7$	1.439	$\text{C}_1\text{-N}_5\text{-C}_7$	123.6	$\text{N}_5\text{-C}_7$	0.94
		$\text{C}_3\text{-N}_2\text{-C}_6$	123.4		
		$\text{C}_4\text{-N}_5\text{-C}_7$	123.4		

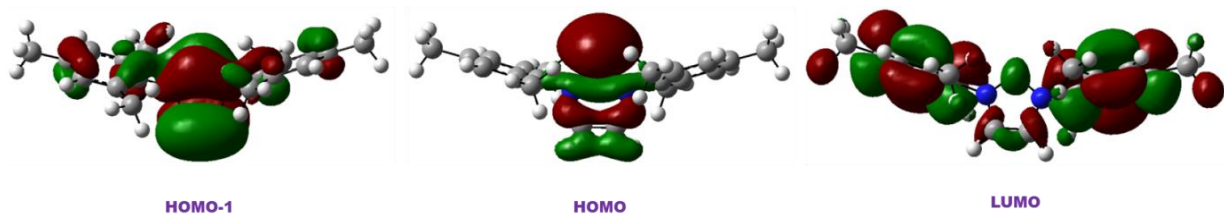


Figure S28 Representation of molecular orbitals HOMO-1, HOMO and LUMO of **I_{IMes}**.

9. Optimized geometry of abnormal IMes (**II_{IMes}**)

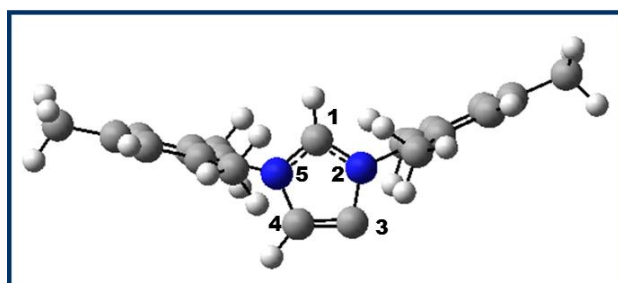


Table S13 Optimized geometry of **II_{IMes}**.

Principal bond lengths (Å)		Principal bond angles(°)		Principal Bond Indices	
C ₁ -N ₂	1.346	C ₁ -N ₂ -C ₃	113.3	C ₁ -N ₂	1.26
N ₂ -C ₃	1.417	N ₂ -C ₃ -C ₄	100.7	N ₂ -C ₃	1.09
C ₃ -C ₄	1.381	C ₃ -C ₄ -N ₅	111.5	C ₃ -C ₄	1.62
C ₄ -N ₅	1.409	C ₄ -N ₅ -C ₁	107.1	C ₄ -N ₅	1.06
N ₅ -C ₁	1.336	N ₅ -C ₁ -N ₂	107.4	N ₅ -C ₁	1.29
N ₂ -C ₆	1.441	C ₁ -N ₂ -C ₆	122.8	N ₂ -C ₆	0.93
N ₅ -C ₇	1.439	C ₁ -N ₅ -C ₇	125.7	N ₅ -C ₇	0.93
		C ₃ -N ₂ -C ₆	123.9		
		C ₄ -N ₅ -C ₇	127.1		

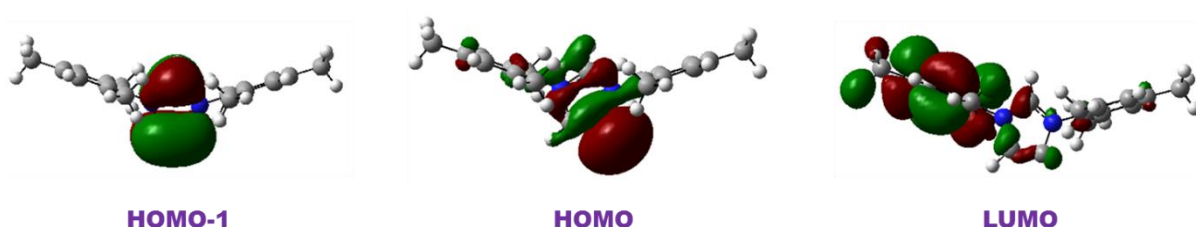
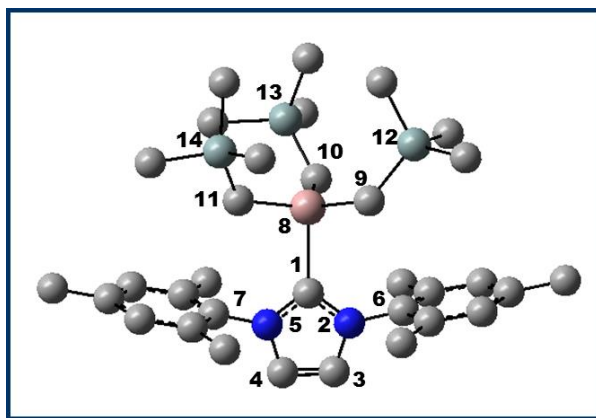
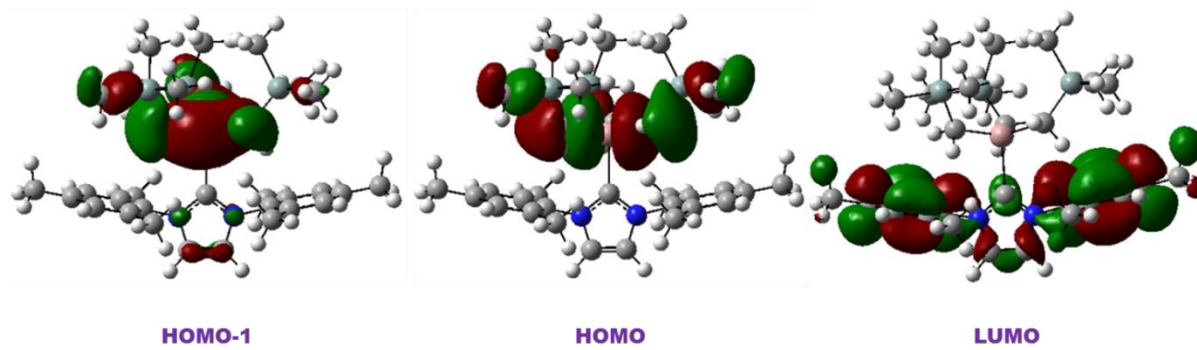
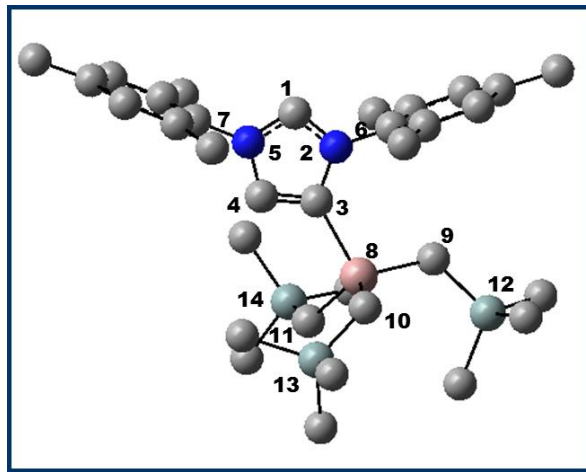


Figure S29 Representation of molecular orbitals HOMO-1, HOMO and LUMO of **II_{IMes}**.

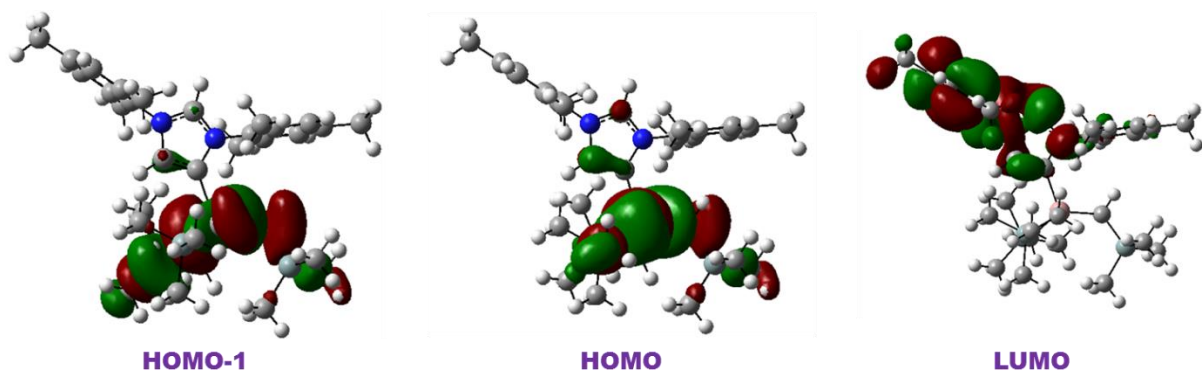
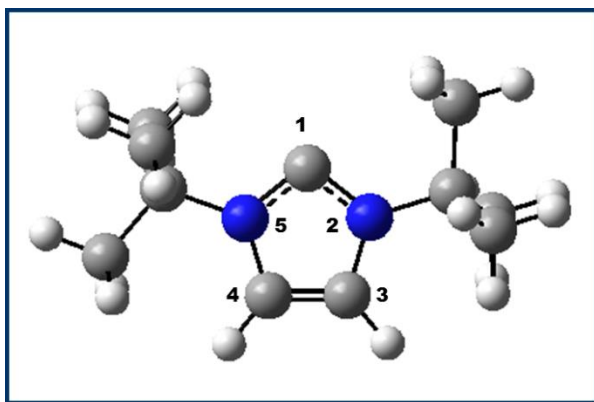
10. Optimized geometry of normal IMes·GaR₃ complex (**III**_{IMes})**Table S14** Optimized geometry of normal **III**_{IMes}.

Principal bond lengths (Å)		Principal bond angles(°)		Principal Bond indices	
C ₁ -N ₂	1.369	C ₁ -N ₂ -C ₃	111.8	C ₁ -N ₂	1.27
N ₂ -C ₃	1.391	N ₂ -C ₃ -C ₄	106.6	N ₂ -C ₃	1.10
C ₃ -C ₄	1.348	C ₃ -C ₄ -N ₅	106.6	C ₃ -C ₄	1.66
C ₄ -N ₅	1.391	C ₄ -N ₅ -C ₁	111.8	C ₄ -N ₅	1.10
N ₅ -C ₁	1.369	N ₅ -C ₁ -N ₂	103.1	N ₅ -C ₁	1.27
N ₂ -C ₆	1.447	C ₁ -N ₂ -C ₆	128.0	N ₂ -C ₆	0.92
N ₅ -C ₇	1.447	C ₁ -N ₅ -C ₇	128.0	N ₅ -C ₇	0.92
Si ₁₂ -C _{Me}	1.903; 1.897; 1.894	C ₃ -N ₂ -C ₆	120.1	Si ₁₂ -C _{Me}	0.81; 0.82; 0.80
Si ₁₃ -C _{Me}	1.903; 1.892; 1.896	C ₄ -N ₅ -C ₇	120.1	Si ₁₃ -C _{Me}	0.81; 0.82; 0.81
Si ₁₄ -C _{Me}	1.896; 1.894; 1.903	N ₂ -C ₁ -Ga ₈	128.3	Si ₁₄ -C _{Me}	0.82; 0.81; 0.80
C ₁ -Ga ₈	2.300	N ₅ -C ₁ -Ga ₈	128.2	C ₁ -Ga ₈	0.47
Ga ₈ -C ₉	2.038	C ₁ -Ga ₈ -C ₉	103.2	Ga ₈ -C ₉	0.63
Ga ₈ -C ₁₀	2.050	C ₁ -Ga ₈ -C ₁₀	96.8	Ga ₈ -C ₁₀	0.61
Ga ₈ -C ₁₁	2.035	C ₁ -Ga ₈ -C ₁₁	101.6	Ga ₈ -C ₁₁	0.63
C ₉ -Si ₁₂	1.877	Ga ₈ -C ₉ -Si ₁₂	125.6	C ₉ -Si ₁₂	0.83
C ₁₀ -Si ₁₃	1.879	Ga ₈ -C ₁₀ -Si ₁₃	126.5	C ₁₀ -Si ₁₃	0.82
C ₁₁ -Si ₁₄	1.877	Ga ₈ -C ₁₁ -Si ₁₄	126.7	C ₁₁ -Si ₁₄	0.83
		C ₉ -Si ₁₂ -C _{Me}	109.2; 111.5; 113.8		
		C ₁₀ -Si ₁₃ -C _{Me}	111.7; 113.0; 109.2		
		C ₁₁ -Si ₁₄ -C _{Me}	111.3; 114.4; 108.8		

**Figure S30** Representation of molecular orbitals HOMO-1, HOMO and LUMO of **III_{IMes}**.11. Optimized geometry of abnormal IMes·GaR₃ complex (**IV_{IMes}**)**Table S15** Optimized geometry of abnormal **IV_{IMes}**.

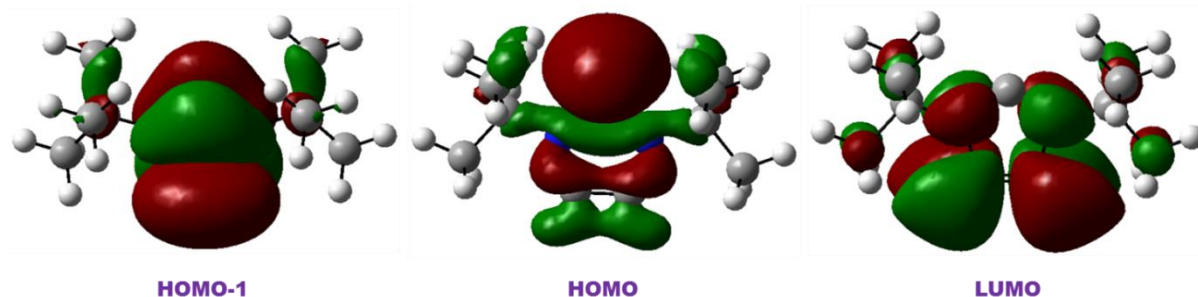
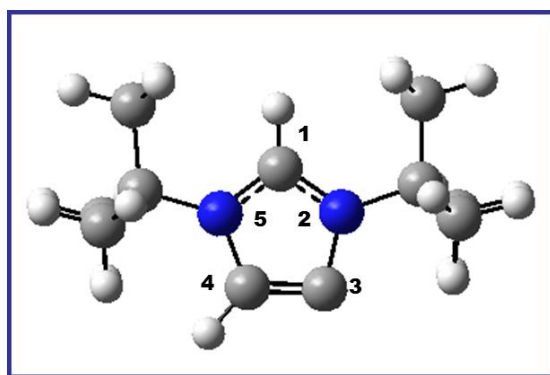
Principal bond lengths (Å)	Principal bond angles(°)	Principal Bond indices
C ₁ -N ₂	111.0	C ₁ -N ₂ 1.29
N ₂ -C ₃	103.0	N ₂ -C ₃ 1.11
C ₃ -C ₄	110.1	C ₃ -C ₄ 1.61
C ₄ -N ₅	107.5	C ₄ -N ₅ 1.10
N ₅ -C ₁	108.4	N ₅ -C ₁ 1.30
N ₂ -C ₆	121.7	N ₂ -C ₆ 0.92
N ₅ -C ₇	125.5	N ₅ -C ₇ 0.92
Si ₁₂ -C _{Me}	127.3	Si ₁₂ -C _{Me} 0.81; 0.81; 0.81
Si ₁₃ -C _{Me}	127.0	Si ₁₄ -C _{Me} 0.82; 0.80; 0.80
Si ₁₄ -C _{Me}	131.6	Si ₁₄ -C _{Me} 0.81; 0.81; 0.80
C ₃ -Ga ₈	125.1	C ₃ -Ga ₈ 0.53
Ga ₈ -C ₉	108.5	Ga ₈ -C ₉ 0.65
Ga ₈ -C ₁₀	101.5	Ga ₈ -C ₁₀ 0.63

$\text{Ga}_8\text{-C}_{11}$	2.050	$\text{C}_3\text{-Ga}_8\text{-C}_{11}$	105.4	$\text{Ga}_8\text{-C}_{11}$	0.64
$\text{C}_9\text{-Si}_{12}$	1.875	$\text{Ga}_8\text{-C}_9\text{-Si}_{12}$	120.0	$\text{C}_9\text{-Si}_{12}$	0.83
$\text{C}_{10}\text{-Si}_{13}$	1.870	$\text{Ga}_8\text{-C}_{10}\text{-Si}_{13}$	123.3	$\text{C}_{10}\text{-Si}_{13}$	0.84
$\text{C}_{11}\text{-Si}_{14}$	1.870	$\text{Ga}_8\text{-C}_{11}\text{-Si}_{14}$	125.1	$\text{C}_{11}\text{-Si}_{14}$	0.84
		$\text{C}_9\text{-Si}_{12}\text{-C}_{\text{Me}}$	110.6; 110.6; 113.2		
		$\text{C}_{10}\text{-Si}_{13}\text{-C}_{\text{Me}}$	110.7; 111.9; 112.4		
		$\text{C}_{11}\text{-Si}_{14}\text{-C}_{\text{Me}}$	110.7; 111.6; 113.0		

**Figure S31** Representation of molecular orbitals HOMO-1, HOMO and LUMO of IV_{IMes} .12. Optimized geometry of normal $\text{I}^{\prime}\text{Bu}$ (I_{tBu})**Table S16** Optimized geometry of I_{tBu} .

Principal bond lengths (Å)		Principal bond angles (°)		Principal bond indices	
$\text{C}_1\text{-N}_2$	1.364	$\text{C}_1\text{-N}_2\text{-C}_3$	112.0	$\text{C}_1\text{-N}_2$	1.26
$\text{N}_2\text{-C}_3$	1.393	$\text{N}_2\text{-C}_3\text{-C}_4$	106.4	$\text{N}_2\text{-C}_3$	1.11
$\text{C}_3\text{-C}_4$	1.354	$\text{C}_3\text{-C}_4\text{-N}_5$	106.4	$\text{C}_3\text{-C}_4$	1.65
$\text{C}_4\text{-N}_5$	1.393	$\text{C}_4\text{-N}_5\text{-C}_1$	112.0	$\text{C}_4\text{-N}_5$	1.11
$\text{N}_5\text{-C}_1$	1.364	$\text{N}_5\text{-C}_1\text{-N}_2$	103.2	$\text{N}_5\text{-C}_1$	1.26

$\text{N}_2\text{-C}_6$	1.494	$\text{C}_1\text{-N}_2\text{-C}_6$	121.4	$\text{N}_2\text{-C}_6$	0.89
$\text{N}_5\text{-C}_7$	1.494	$\text{C}_1\text{-N}_5\text{-C}_7$	121.4	$\text{N}_5\text{-C}_7$	0.89
		$\text{C}_3\text{-N}_2\text{-C}_6$	126.5	$\text{C}_6\text{-C}_{\text{Me}}$	1.00; 0.99; 0.99
		$\text{C}_4\text{-N}_5\text{-C}_7$	126.5	$\text{C}_7\text{-C}_{\text{Me}^{'}}$	1.00; 0.99; 0.99

**Figure S32** Representation of molecular orbitals HOMO-1, HOMO and LUMO of I_{tBu} .13. Optimized geometry of abnormal I_{tBu} (II_{tBu})**Table S17** Optimized geometry of abnormal II_{tBu} .

Principal bond lengths (Å)		Principal bond angles(°)		Principal bond indices	
$\text{C}_1\text{-N}_2$	1.344	$\text{C}_1\text{-N}_2\text{-C}_3$	112.8	$\text{C}_1\text{-N}_2$	1.28
$\text{N}_2\text{-C}_3$	1.411	$\text{N}_2\text{-C}_3\text{-C}_4$	101.0	$\text{N}_2\text{-C}_3$	1.10
$\text{C}_3\text{-C}_4$	1.378	$\text{C}_3\text{-C}_4\text{-N}_5$	111.7	$\text{C}_3\text{-C}_4$	1.62
$\text{C}_4\text{-N}_5$	1.404	$\text{C}_4\text{-N}_5\text{-C}_1$	106.5	$\text{C}_4\text{-N}_5$	1.08
$\text{N}_5\text{-C}_1$	1.339	$\text{N}_5\text{-C}_1\text{-N}_2$	107.9	$\text{N}_5\text{-C}_1$	1.29
$\text{N}_2\text{-C}_6$	1.494	$\text{C}_1\text{-N}_2\text{-C}_6$	125.5	$\text{N}_2\text{-C}_6$	0.89
$\text{N}_5\text{-C}_7$	1.490	$\text{C}_1\text{-N}_5\text{-C}_7$	127.2	$\text{N}_5\text{-C}_7$	0.89
		$\text{C}_3\text{-N}_2\text{-C}_6$	121.7	$\text{C}_6\text{-C}_{\text{Me}}$	1.00; 0.99; 0.99
		$\text{C}_4\text{-N}_5\text{-C}_7$	126.3	$\text{C}_7\text{-C}_{\text{Me}^{'}}$	1.00; 0.99; 0.99

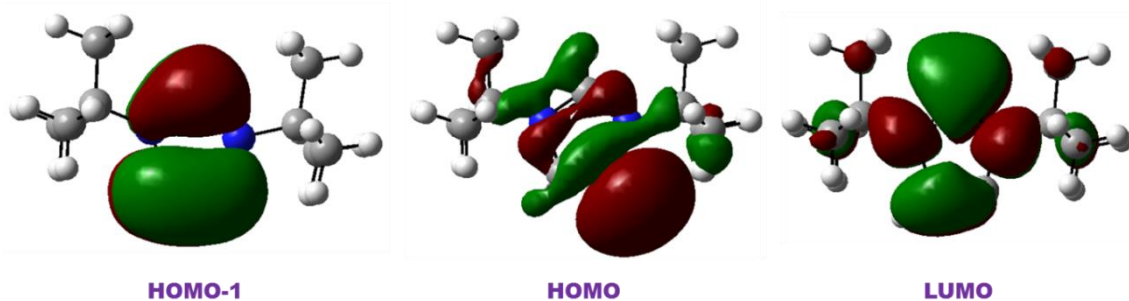


Figure S33 Representation of molecular orbitals HOMO-1, HOMO and LUMO of \mathbf{II}_{tBu} .

14. Optimized geometry of normal $\text{IBu}\cdot\text{GaR}_3$ complex ($\mathbf{III}_{\text{tBu}}$)

Several models of normal $\text{IBu}\cdot\text{GaR}_3$ were constructed and their geometries were optimized. The resulting structures had a long C1-Ga bond and an energy value which showed no stabilisation over that of the separate species. One of the models is shown next.

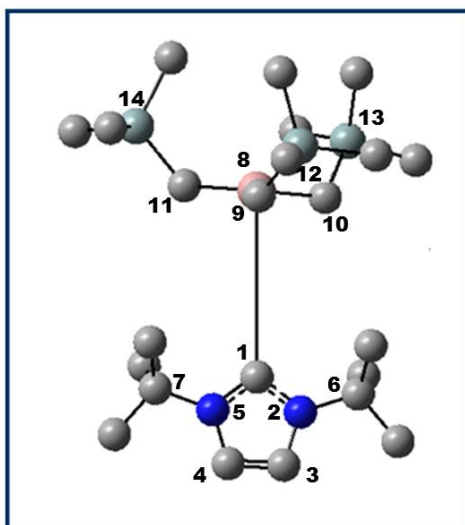
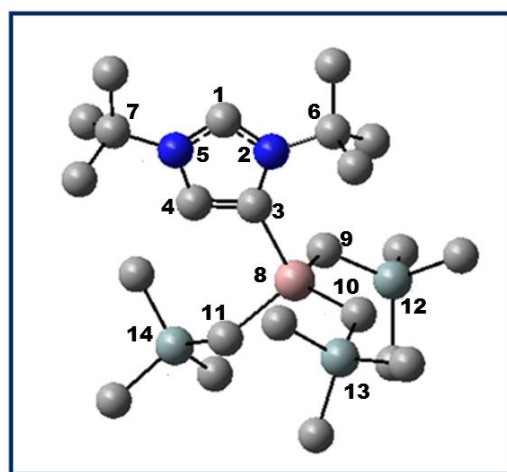


Table S18 Optimized geometry of normal $\text{IBu}\cdot\text{GaR}_3$ complex ($\mathbf{III}_{\text{tBu}}$).

Principal bond lengths (Å)		Principal bond angles(°)	
$\text{C}_1\text{-N}_2$	1.365	$\text{C}_1\text{-N}_2\text{-C}_3$	112.0
$\text{N}_2\text{-C}_3$	1.392	$\text{N}_2\text{-C}_3\text{-C}_4$	106.4
$\text{C}_3\text{-C}_4$	1.353	$\text{C}_3\text{-C}_4\text{-N}_5$	106.4
$\text{C}_4\text{-N}_5$	1.392	$\text{C}_4\text{-N}_5\text{-C}_1$	112.0
$\text{N}_5\text{-C}_1$	1.365	$\text{N}_5\text{-C}_1\text{-N}_2$	103.2
$\text{N}_2\text{-C}_6$	1.495	$\text{C}_1\text{-N}_2\text{-C}_6$	122.0
$\text{N}_5\text{-C}_7$	1.494	$\text{C}_1\text{-N}_5\text{-C}_7$	122.0
$\text{Si}_{12}\text{-C}_{\text{Me}}$	1.895; 1.894; 1.893	$\text{C}_3\text{-N}_2\text{-C}_6$	125.9
$\text{Si}_{13}\text{-C}_{\text{Me}}$	1.894; 1.895; 1.892	$\text{C}_4\text{-N}_5\text{-C}_7$	126.0

$\text{Si}_{14}\text{-C}_{\text{Me}}$	1.893; 1.895; 1.894	$\text{N}_2\text{-C}_1\text{-Ga}_8$	129.2
$\text{C}_1\text{-Ga}_8$	4.546	$\text{N}_5\text{-C}_1\text{-Ga}_8$	126.5
$\text{Ga}_8\text{-C}_9$	1.996	$\text{C}_1\text{-Ga}_8\text{-C}_9$	81.9
$\text{Ga}_8\text{-C}_{10}$	1.996	$\text{C}_1\text{-Ga}_8\text{-C}_{10}$	87.8
$\text{Ga}_8\text{-C}_{11}$	1.998	$\text{C}_1\text{-Ga}_8\text{-C}_{11}$	95.8
$\text{C}_9\text{-Si}_{12}$	1.884	$\text{Ga}_8\text{-C}_9\text{-Si}_{12}$	121.5
$\text{C}_{10}\text{-Si}_{13}$	1.885	$\text{Ga}_8\text{-C}_{10}\text{-Si}_{13}$	121.6
$\text{C}_{11}\text{-Si}_{14}$	1.885	$\text{Ga}_8\text{-C}_{11}\text{-Si}_{14}$	121.1
		$\text{C}_9\text{-Si}_{12}\text{-C}_{\text{Me}}$	109.7; 110.3; 111.3
		$\text{C}_{10}\text{-Si}_{13}\text{-C}_{\text{Me}}$	110.6; 111.2; 109.6
		$\text{C}_{11}\text{-Si}_{14}\text{-C}_{\text{Me}}$	111.3; 109.7; 110.5

15. Optimized geometry of abnormal IBu·GaR₃ complex (**IV_{IBu}**)**Table S19** Optimized geometry of **IV_{IBu}**.

Principal bond lengths (Å)		Principal bond angles(°)		Principal Bond Indices	
$\text{C}_1\text{-N}_2$	1.342	$\text{C}_1\text{-N}_2\text{-C}_3$	110.3	$\text{C}_1\text{-N}_2$	1.342
$\text{N}_2\text{-C}_3$	1.412	$\text{N}_2\text{-C}_3\text{-C}_4$	103.0	$\text{N}_2\text{-C}_3$	1.414
$\text{C}_3\text{-C}_4$	1.33	$\text{C}_3\text{-C}_4\text{-N}_5$	110.7	$\text{C}_3\text{-C}_4$	1.372
$\text{C}_4\text{-N}_5$	1.388	$\text{C}_4\text{-N}_5\text{-C}_1$	106.9	$\text{C}_4\text{-N}_5$	1.389
$\text{N}_5\text{-C}_1$	1.335	$\text{N}_5\text{-C}_1\text{-N}_2$	109.2	$\text{N}_5\text{-C}_1$	1.334
$\text{N}_2\text{-C}_6$	1.506	$\text{C}_1\text{-N}_2\text{-C}_6$	122.3	$\text{N}_2\text{-C}_6$	1.508
$\text{N}_5\text{-C}_7$	1.498	$\text{C}_1\text{-N}_5\text{-C}_7$	127.4	$\text{N}_5\text{-C}_7$	1.498
$\text{Si}_{12}\text{-C}_{\text{Me}}$	1.900; 1.902; 1.895	$\text{C}_3\text{-N}_2\text{-C}_6$	127.1	$\text{Si}_{12}\text{-C}_{\text{Me}}$	1.903; 1.899; 1.894
$\text{Si}_{13}\text{-C}_{\text{Me}}$	1.903; 1.898; 1.901	$\text{C}_4\text{-N}_5\text{-C}_7$	125.7	$\text{Si}_{13}\text{-C}_{\text{Me}}$	1.895; 1.902; 1.897
$\text{Si}_{14}\text{-C}_{\text{Me}}$	1.903; 1.896; 1.896	$\text{N}_2\text{-C}_3\text{-Ga}_8$	139.2	$\text{Si}_{14}\text{-C}_{\text{Me}}$	1.905; 1.903; 1.893

$C_3\text{-Ga}_8$	2.164	$C_4\text{-C}_3\text{-Ga}_8$	117.5	$C_3\text{-Ga}_8$	2.170
$Ga_8\text{-C}_9$	2.056	$C_3\text{-Ga}_8\text{-C}_9$	109.4	$Ga_8\text{-C}_9$	2.055
$Ga_8\text{-C}_{10}$	2.049	$C_3\text{-Ga}_8\text{-C}_{10}$	107.6	$Ga_8\text{-C}_{10}$	2.056
$Ga_8\text{-C}_{11}$	2.052	$C_3\text{-Ga}_8\text{-C}_{11}$	98.5	$Ga_8\text{-C}_{11}$	2.059
$C_9\text{-Si}_{12}$	1.877	$Ga_8\text{-C}_9\text{-Si}_{12}$	123.6	$C_9\text{-Si}_{12}$	1.876
$C_{10}\text{-Si}_{13}$	1.871	$Ga_8\text{-C}_{10}\text{-Si}_{13}$	124.2	$C_{10}\text{-Si}_{13}$	1.878
$C_{11}\text{-Si}_{14}$	1.875	$Ga_8\text{-C}_{11}\text{-Si}_{14}$	123.1	$C_{11}\text{-Si}_{14}$	1.873
		$C_9\text{-Si}_{12}\text{-C}_{\text{Me}}$	111.7; 110.2; 113.2		
		$C_{10}\text{-Si}_{13}\text{-C}_{\text{Me}}$	112.0; 110.7; 112.9		
		$C_{11}\text{-Si}_{14}\text{-C}_{\text{Me}}$	110.0; 112.3; 111.7		

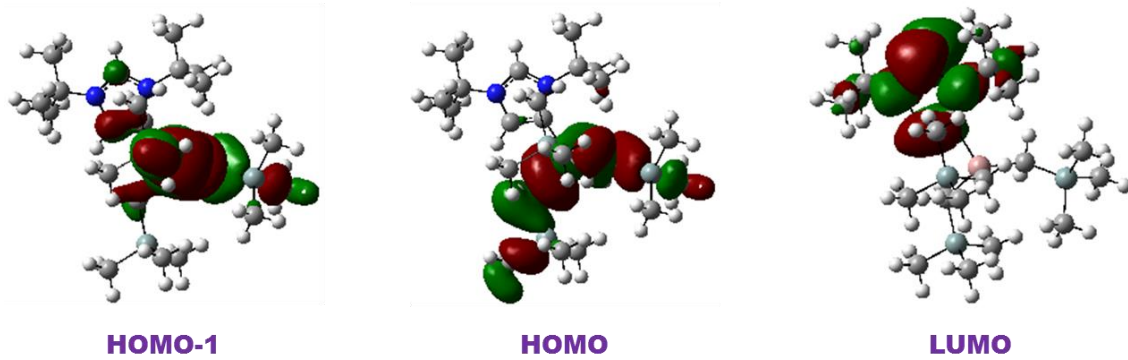


Figure S34 Representation of molecular orbitals HOMO-1, HOMO and LUMO of **IV_{Bu}**.

16. Energy of formation for the proposed intermediate

If the intermediate is formed from 2 molecules of free IPr (each having energy -1160.324211 a.u.) and a molecule of GaR₃ (-3270.872410 a.u.) the formed intermediate (**A**) has the energy of -5591.502154 a.u. which makes it + 11.7 kcal mol⁻¹ higher in energy than the starting material. Several models of the analogous intermediate, which would be formed from free carbenes and has no GaR₃ coordinated, were attempted but they their geometries were not possible to optimize.

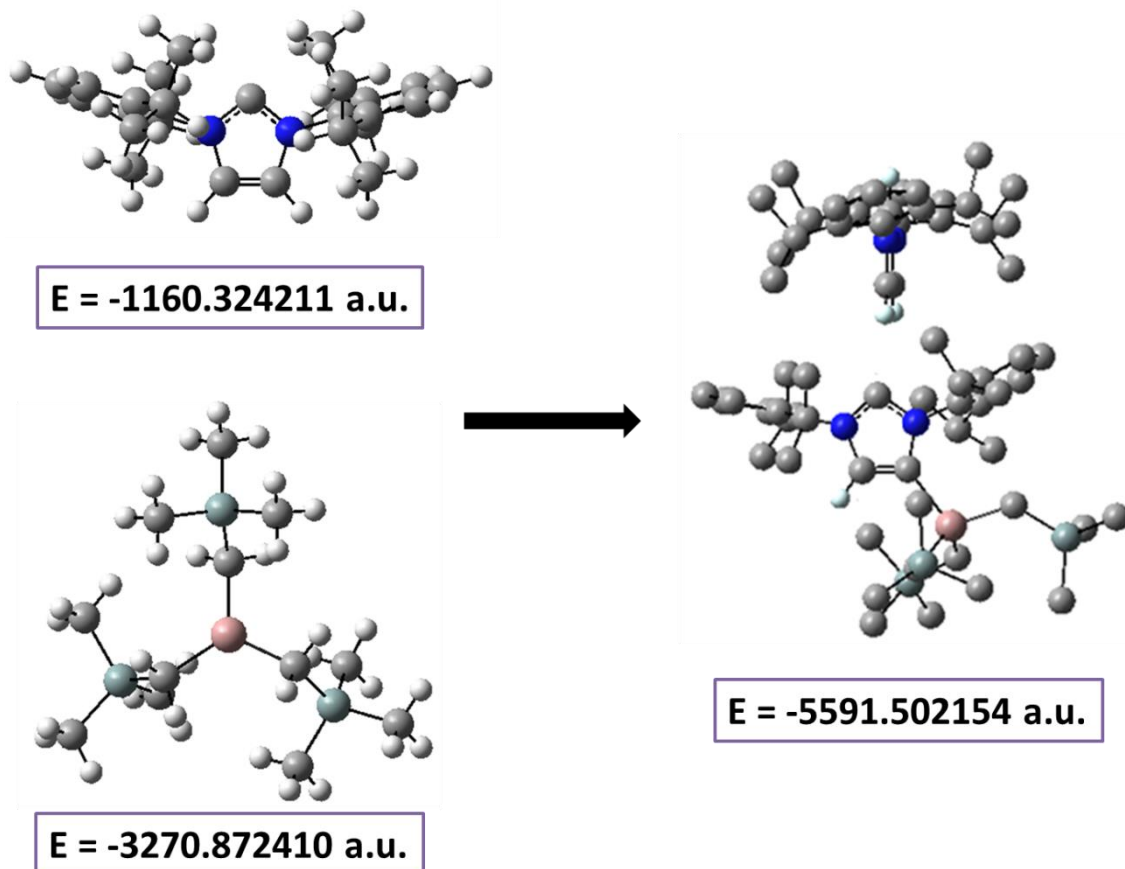


Figure S35 DFT study on the reaction of model systems **IPr** and **GaR₃** to afford intermediate **A**.

NMR spectra of products

Table S20 Chemical shifts for related organometallic species.

compound	<i>d</i> ₆ -benzene		<i>d</i> ₈ -THF	
	$\delta^{1\text{H}}$ (CH ₃)	$\delta^{1\text{H}}$ (CH ₂)	$\delta^{1\text{H}}$ (CH ₃)	$\delta^{1\text{H}}$ (CH ₂)
Li(CH ₂ SiMe ₃)	0.16	-2.03	-0.20	-2.20
Ga(CH ₂ SiMe ₃) ₃	0.13	0.13	-0.01	-0.55
LiGa(CH ₂ SiMe ₃) ₄	0.24	-1.13	-0.11	-1.03
Zn(CH ₂ SiMe ₃) ₂	0.05	-0.63	-0.03	-0.85
Mg(CH ₂ SiMe ₃) ₂	n/a	n/a	-0.11	-1.77

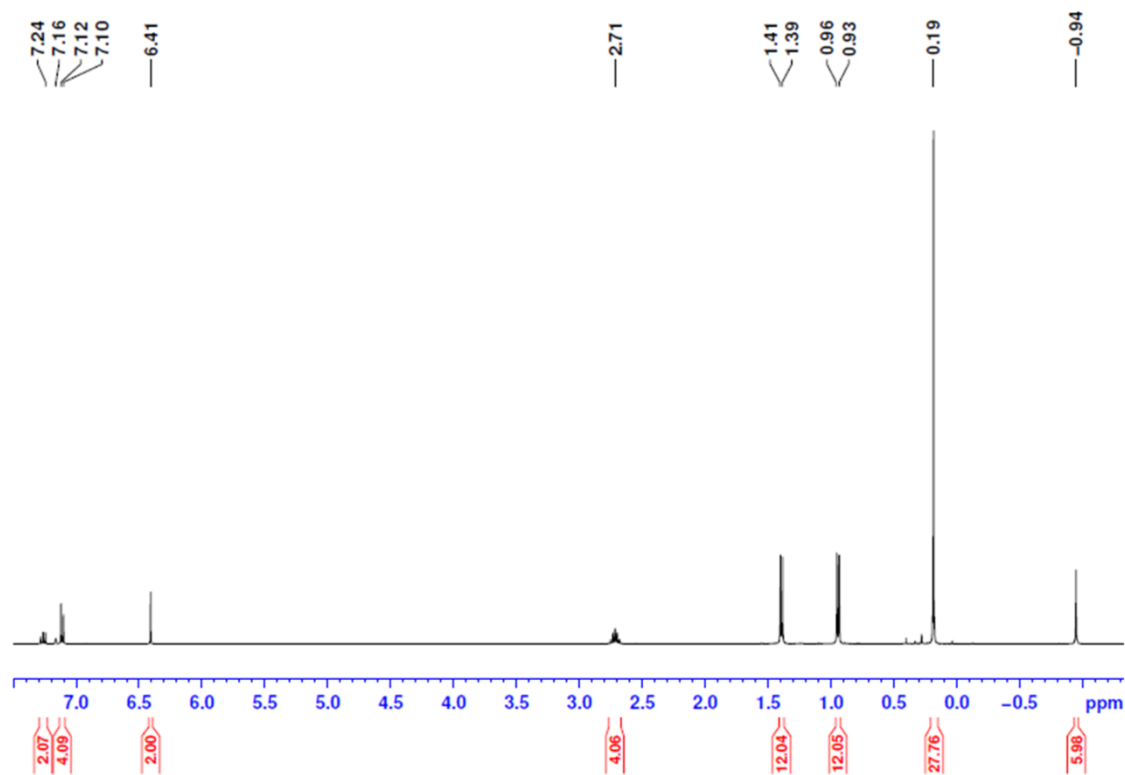


Figure S36: ^1H NMR of **1** in C_6D_6 solution.

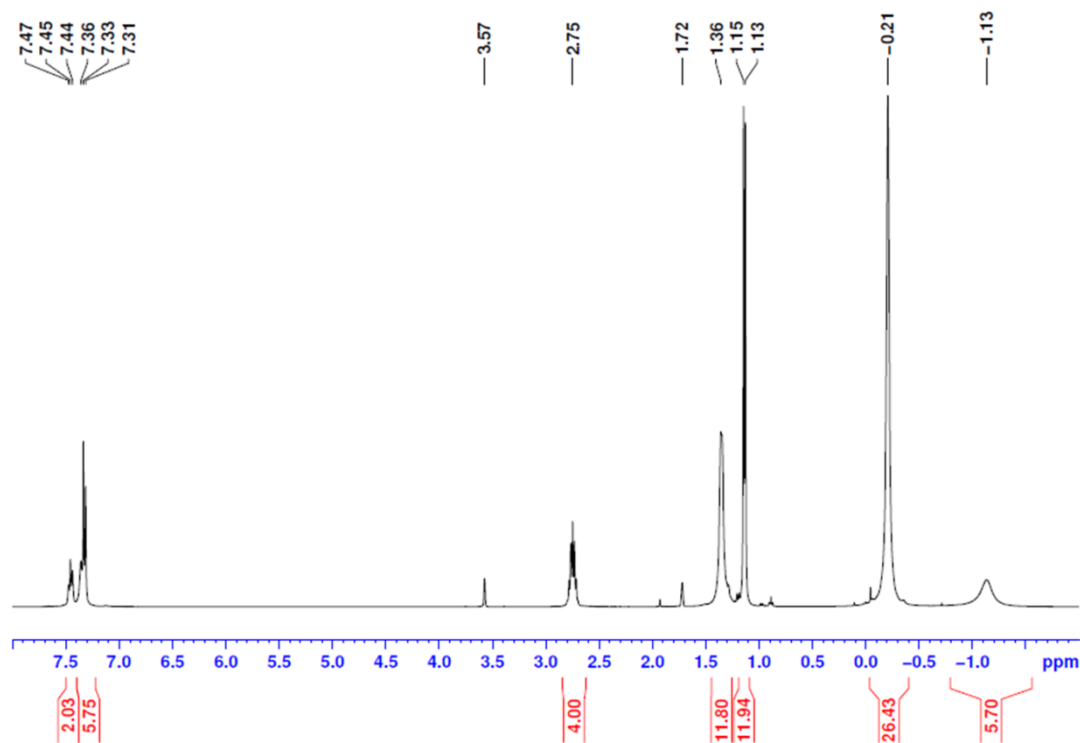


Figure S37 ^1H NMR of **1** in $d_8\text{-THF}$ solution.

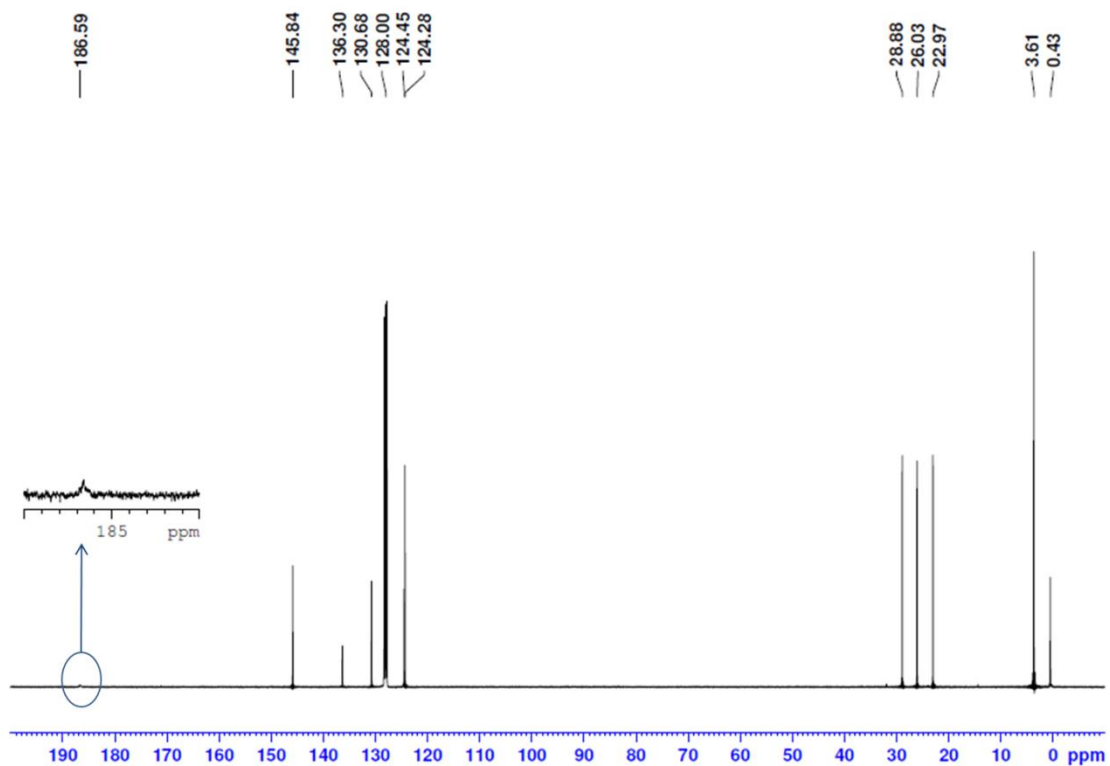


Figure S38 $^{13}\text{C}\{\text{H}\}$ NMR of **1** in C_6D_6 solution.

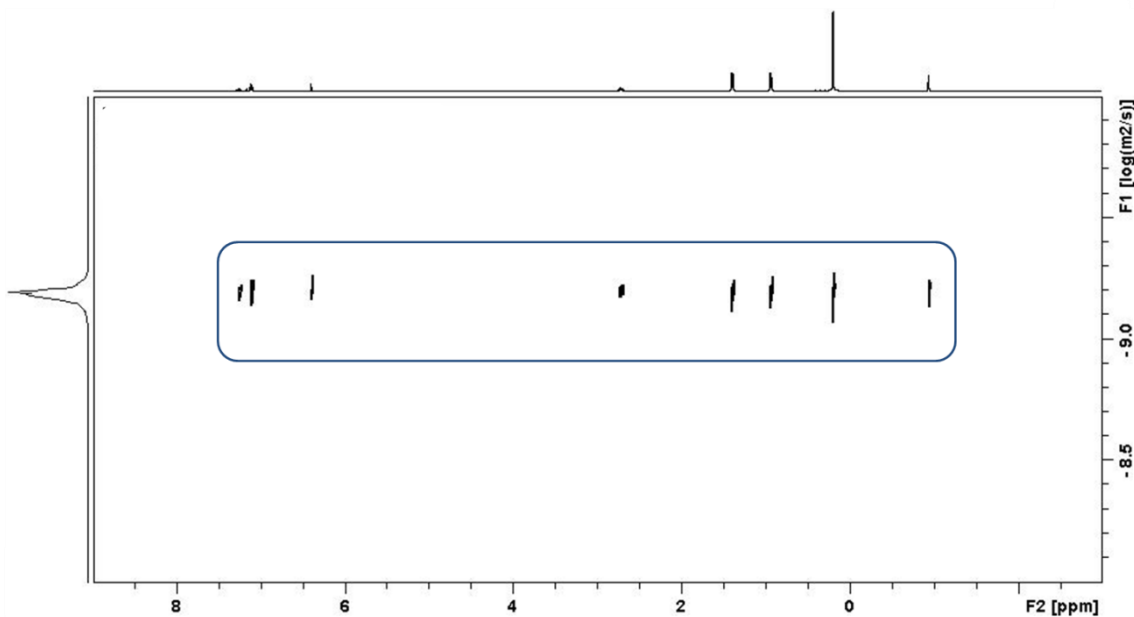


Figure S39 ^1H DOSY of **1** in C_6D_6 solution.

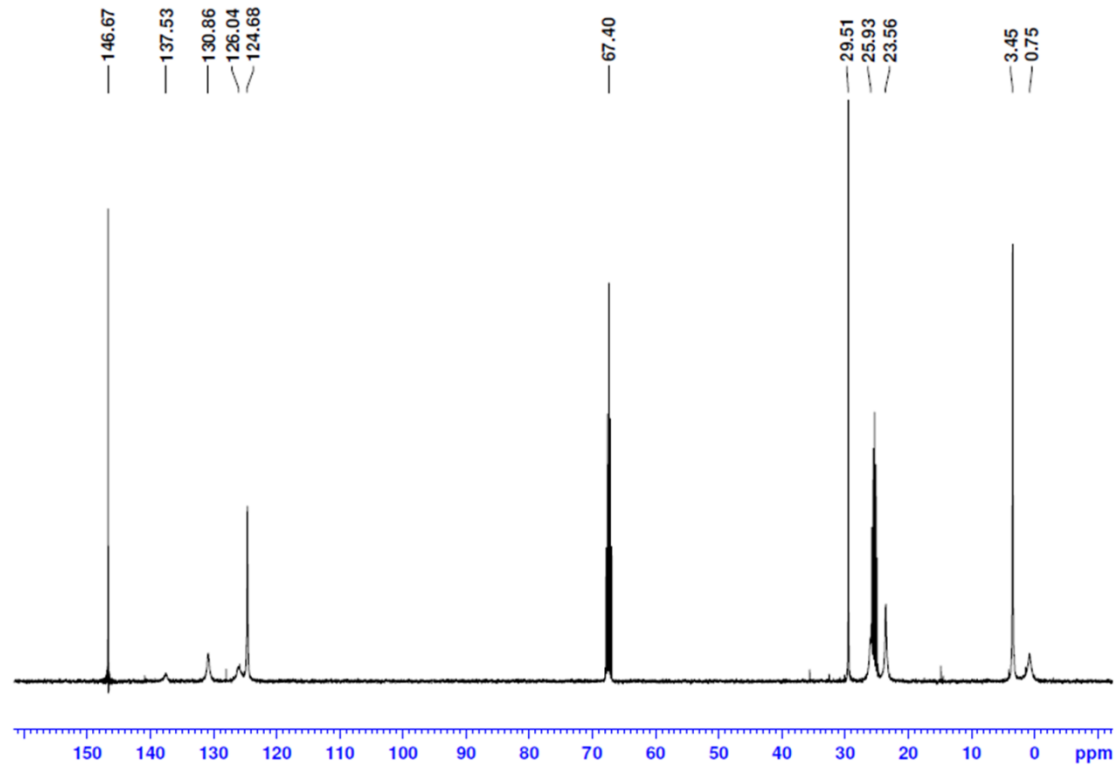


Figure S40 $^{13}\text{C}\{^1\text{H}\}$ NMR of **1** in $d_8\text{-THF}$ solution.

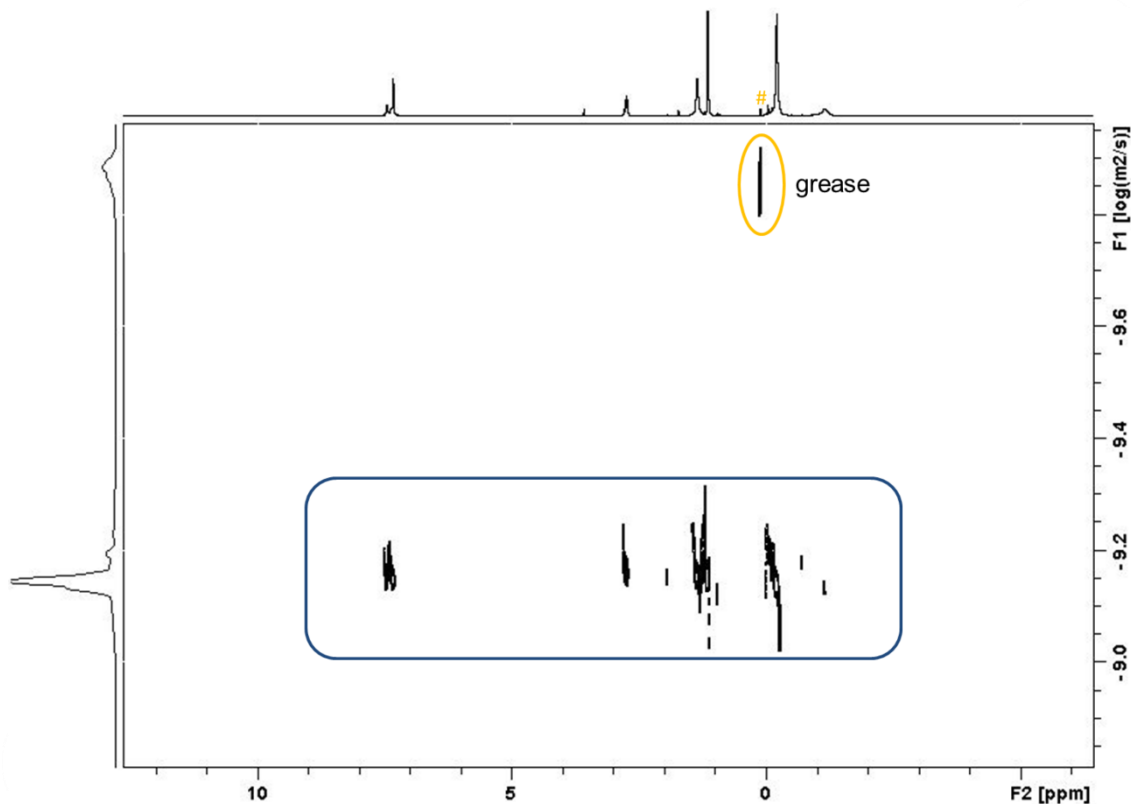


Figure S41 ^1H DOSY of **1** in $d_8\text{-THF}$ solution.

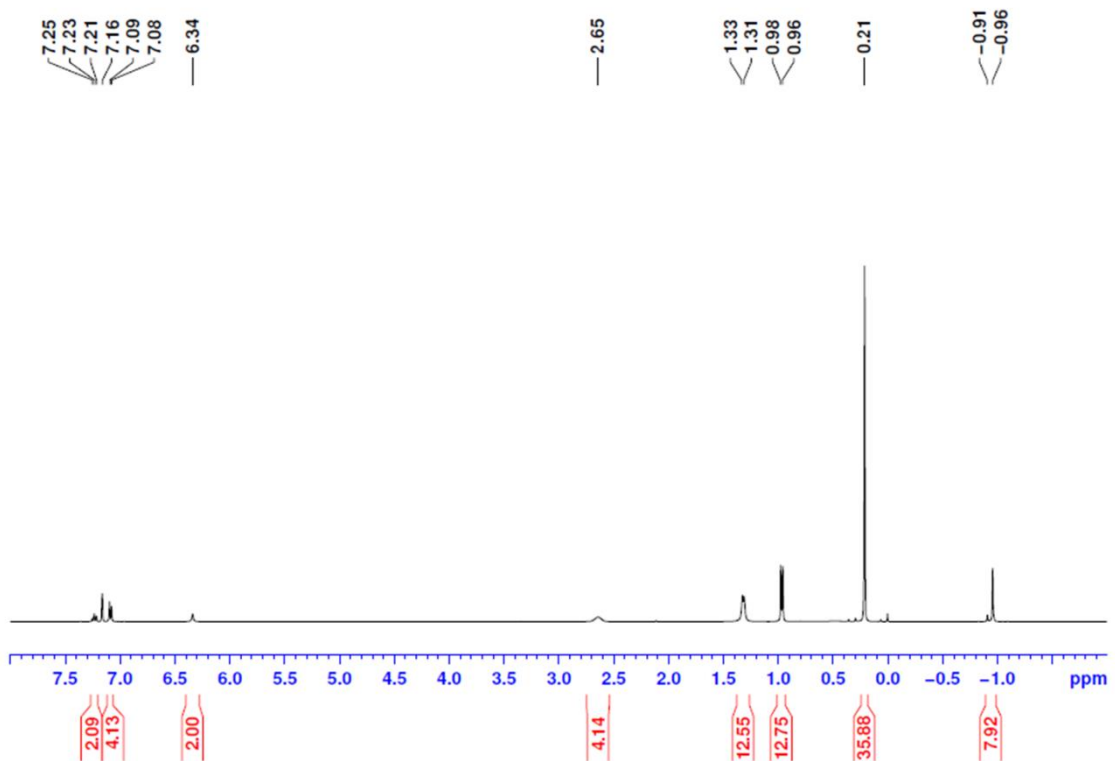


Figure S42 ¹H of **2** in C_6D_6 solution.

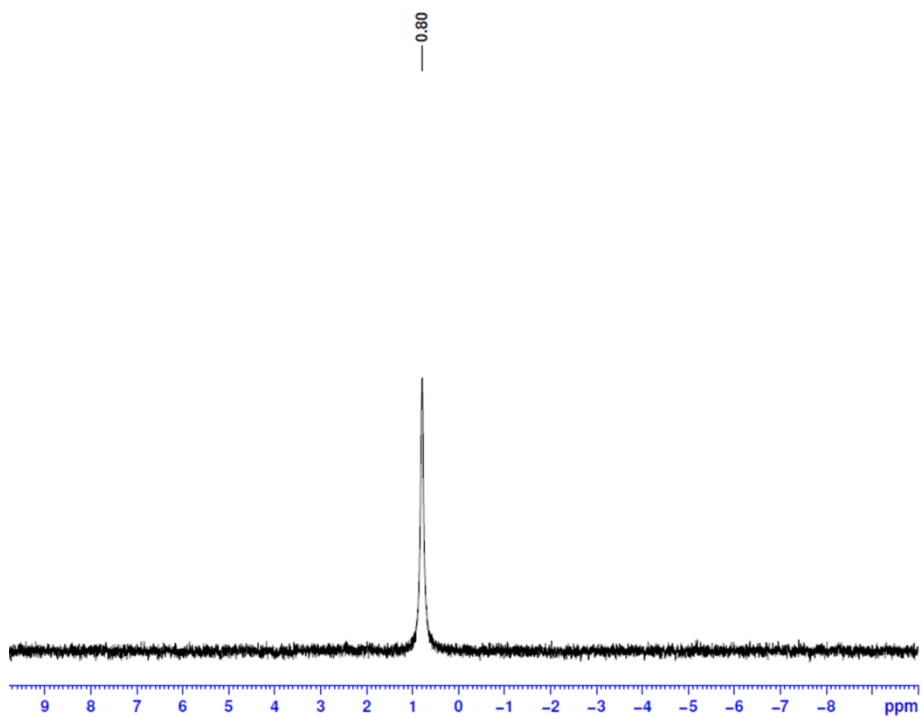


Figure S43 ⁷Li of **2** in C_6D_6 solution.

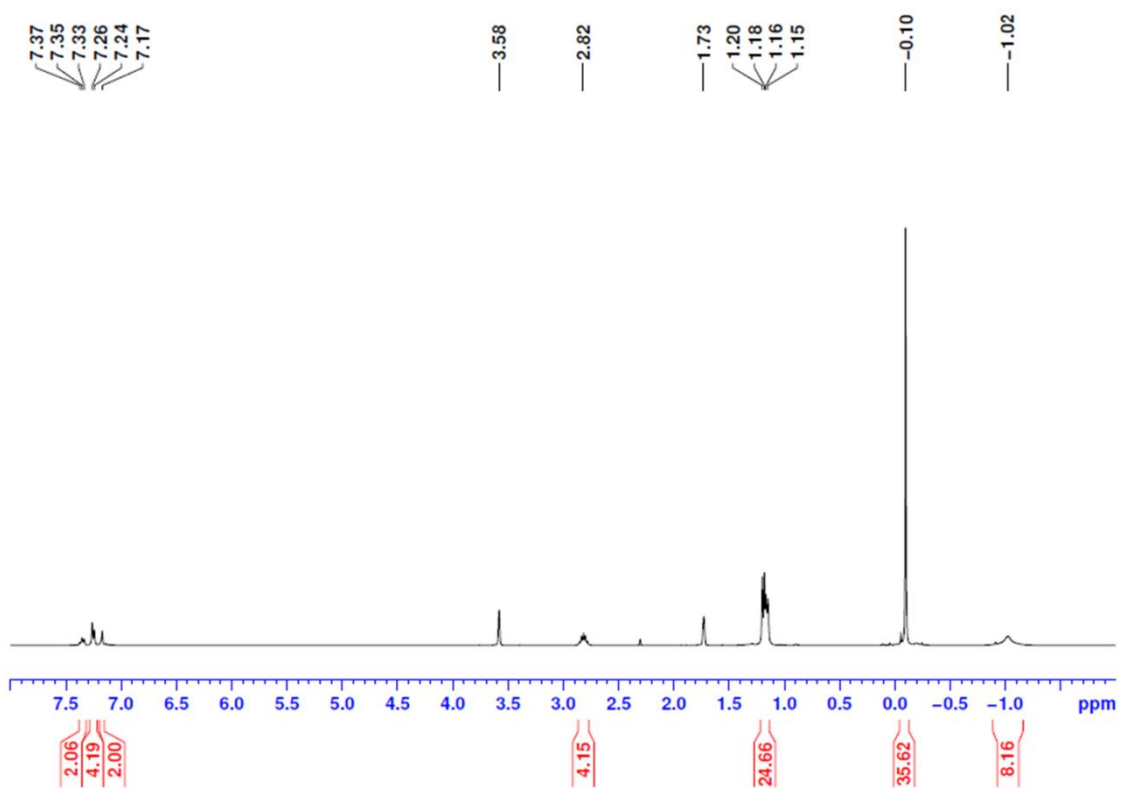


Figure S44 ¹H of **2** in ^d₈-THF solution.

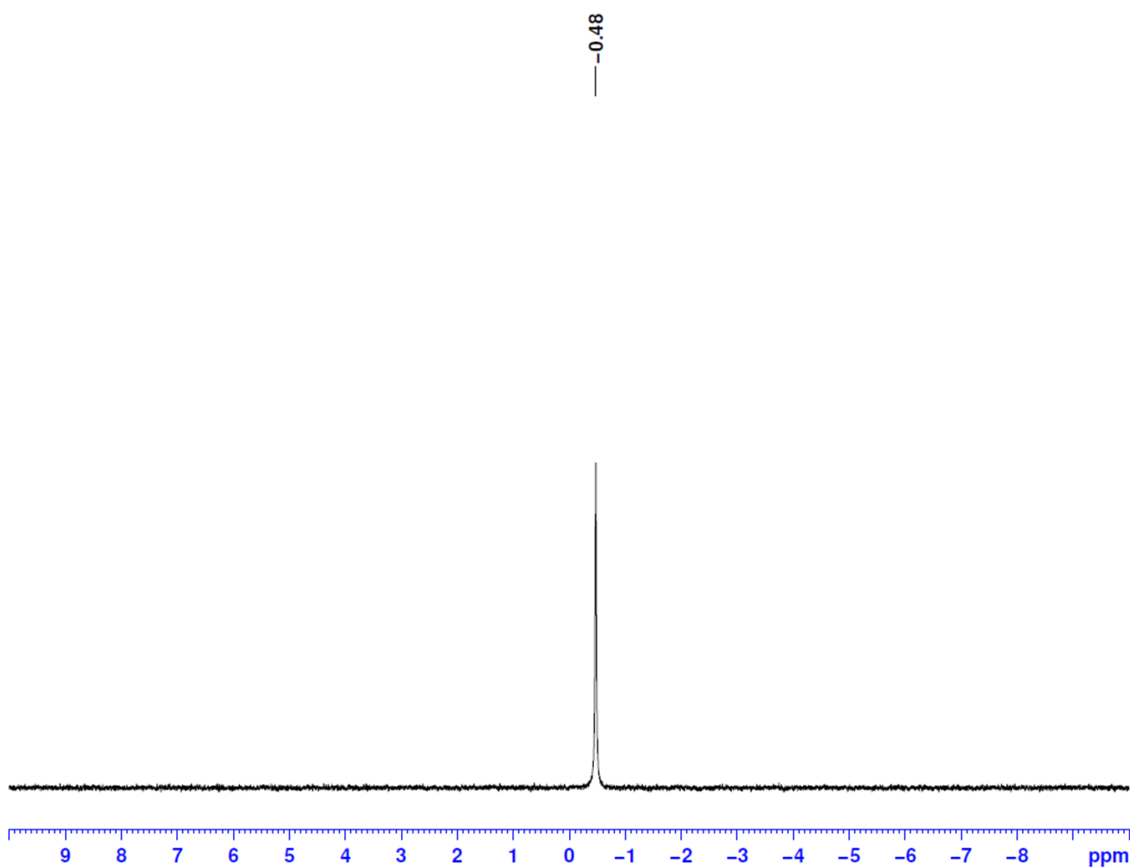


Figure S45 ⁷Li of **2** in ^d₈-THF solution.

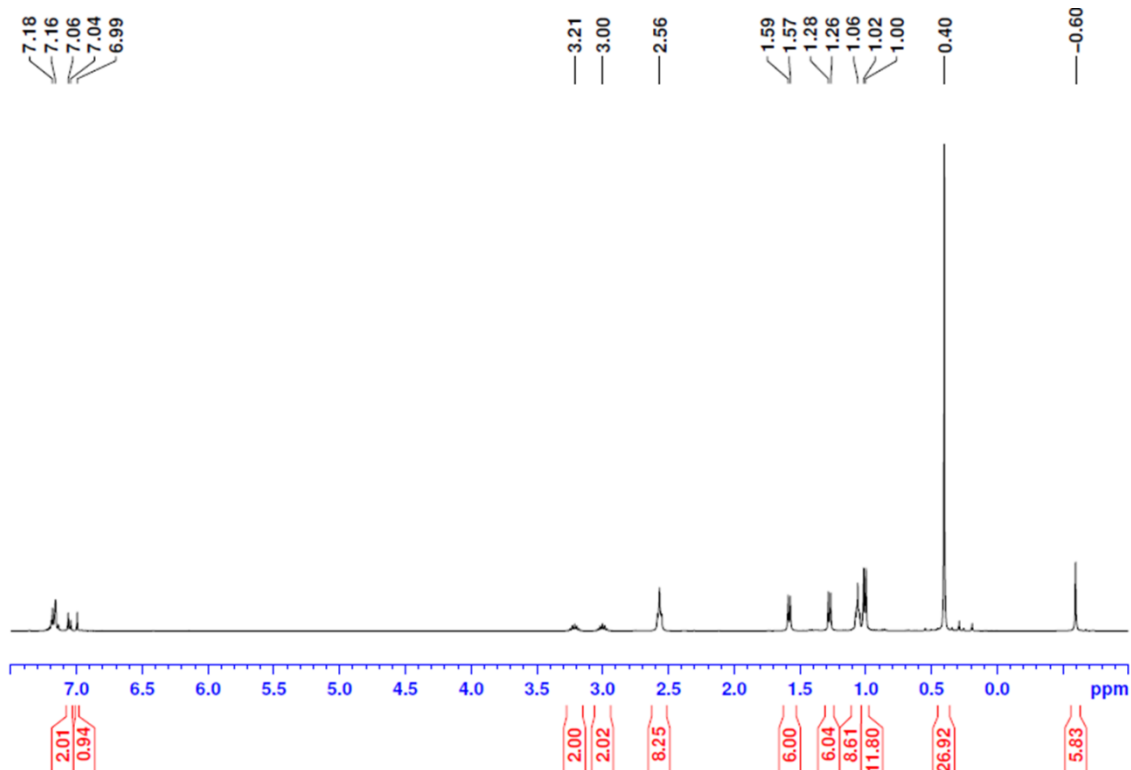


Figure S46 ^1H NMR of **3** in C_6D_6 solution.

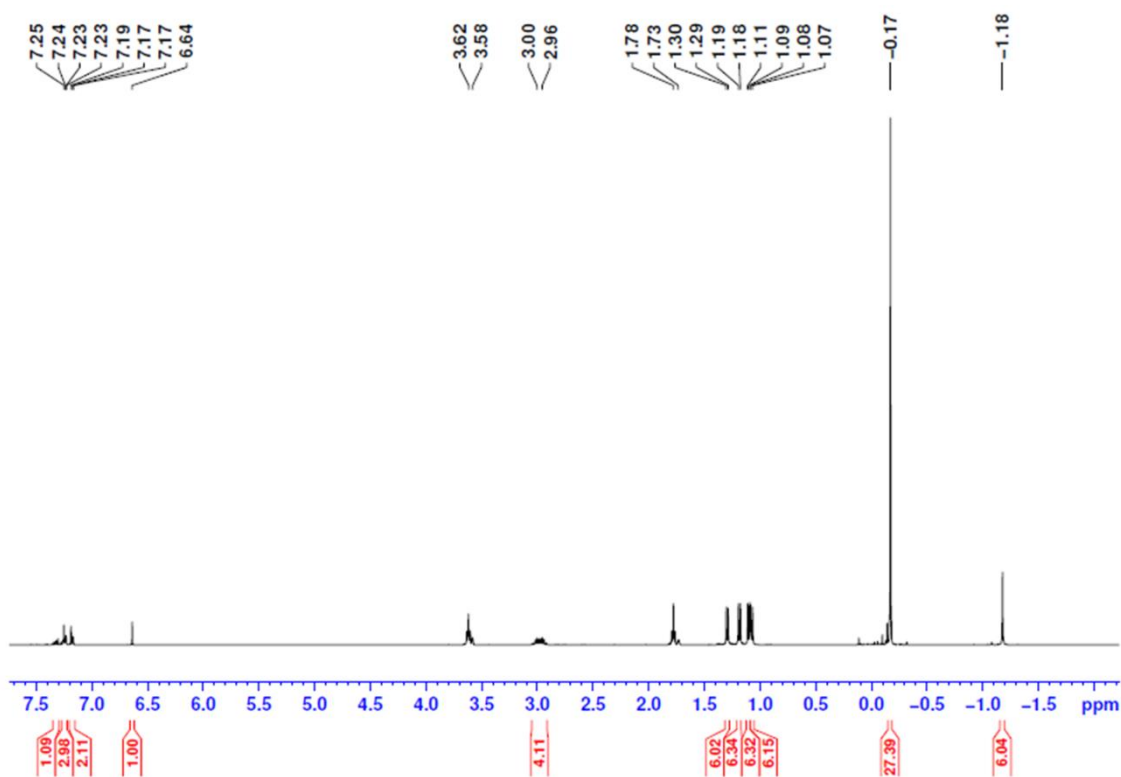


Figure S47 ^1H NMR of **3** in $\text{d}_8\text{-THF}$ solution.

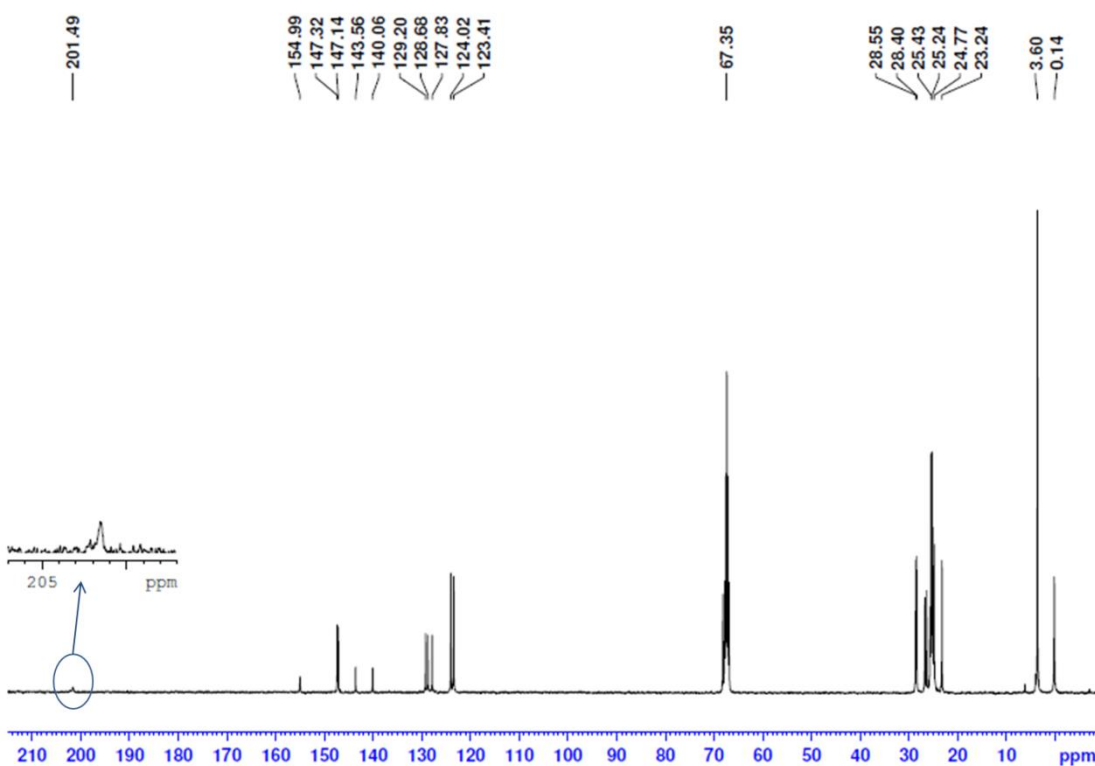


Figure S48 $^{13}\text{C}\{^1\text{H}\}$ NMR of **3** in $\text{d}_8\text{-THF}$ solution.

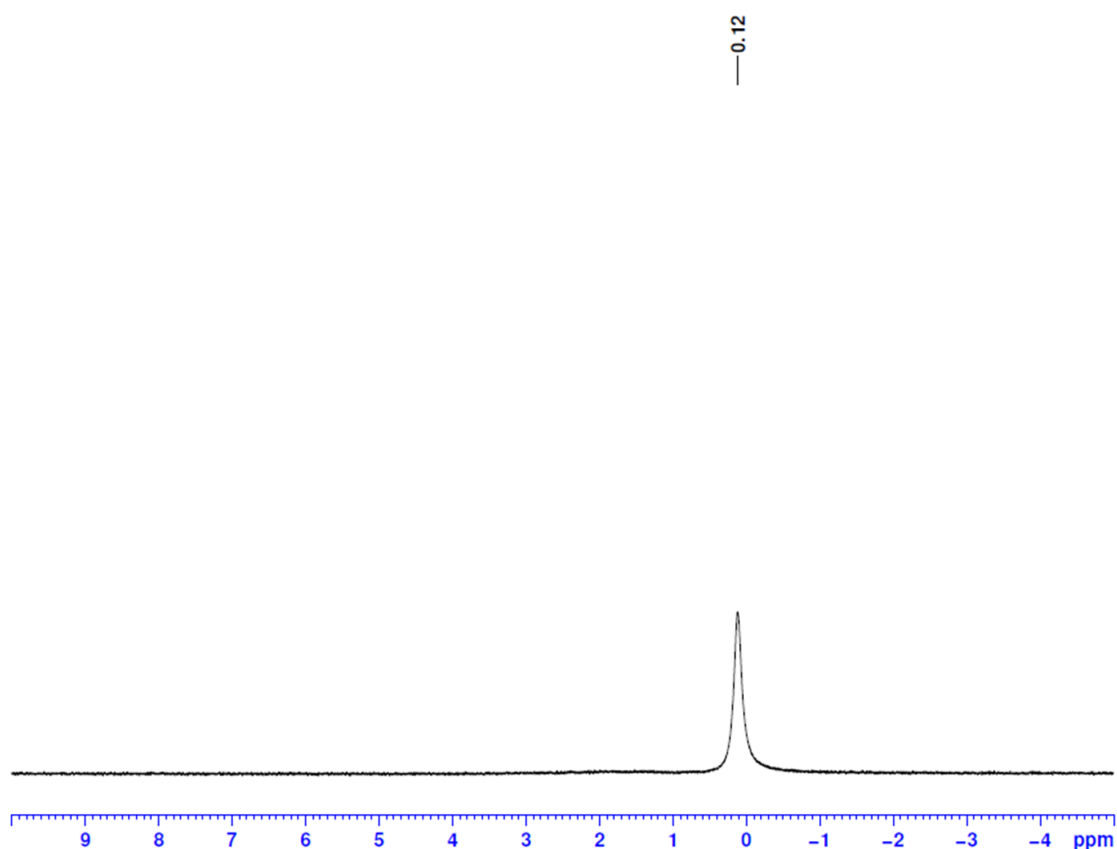


Figure S49 ^7Li NMR of **3** in $\text{d}_8\text{-THF}$ solution.

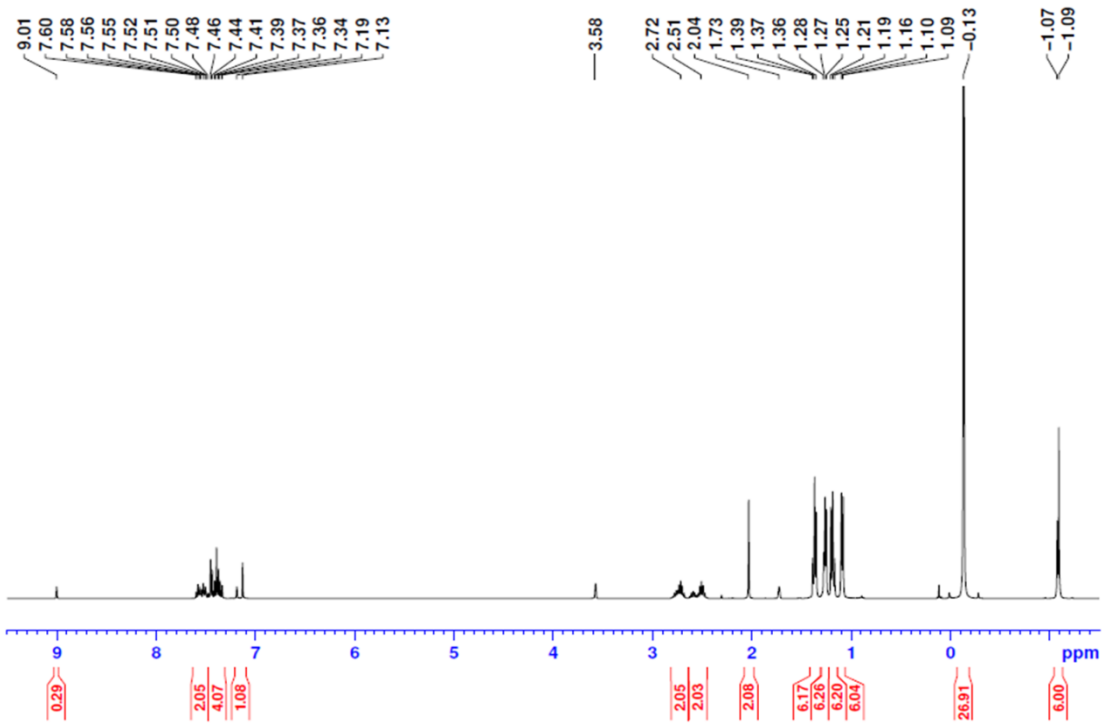


Figure S50 ^1H NMR of **4** in $\text{d}_8\text{-THF}$ solution.

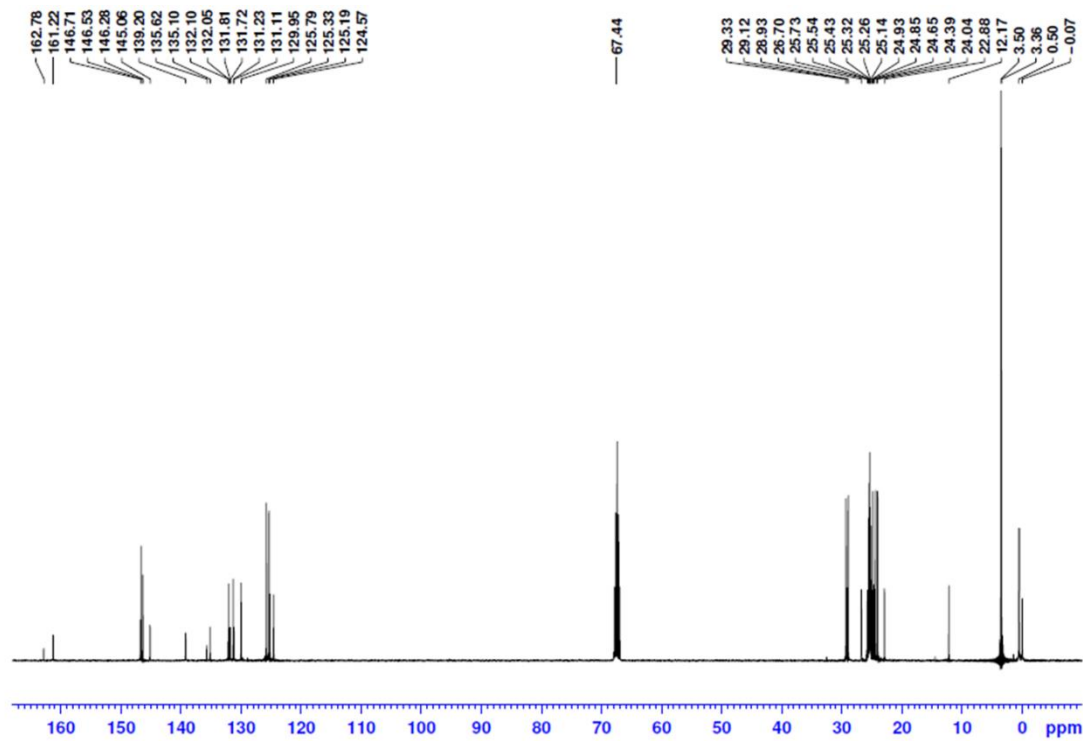


Figure S51 $^{13}\text{C}\{^1\text{H}\}$ NMR of **4** in $\text{d}_8\text{-THF}$ solution.

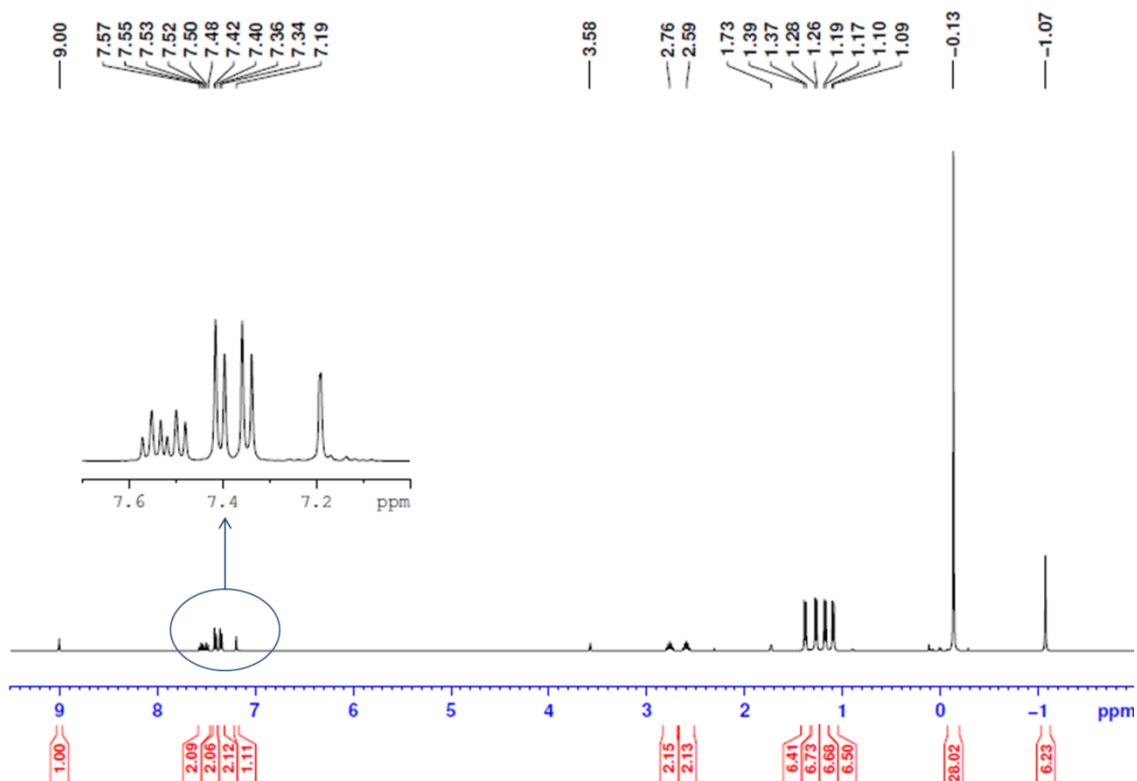


Figure S52 ¹H NMR of **5** in ^d₈-THF solution.

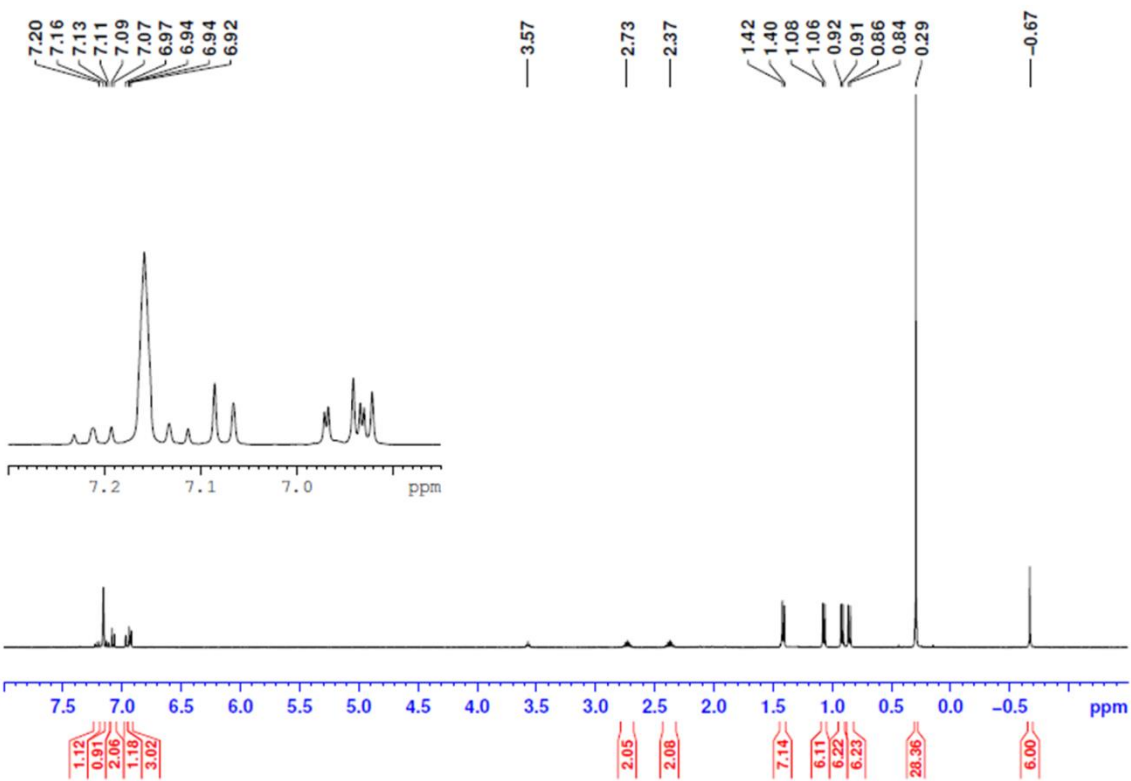


Figure S53 ¹H NMR of **5** in ⁶C₆D₆ solution.

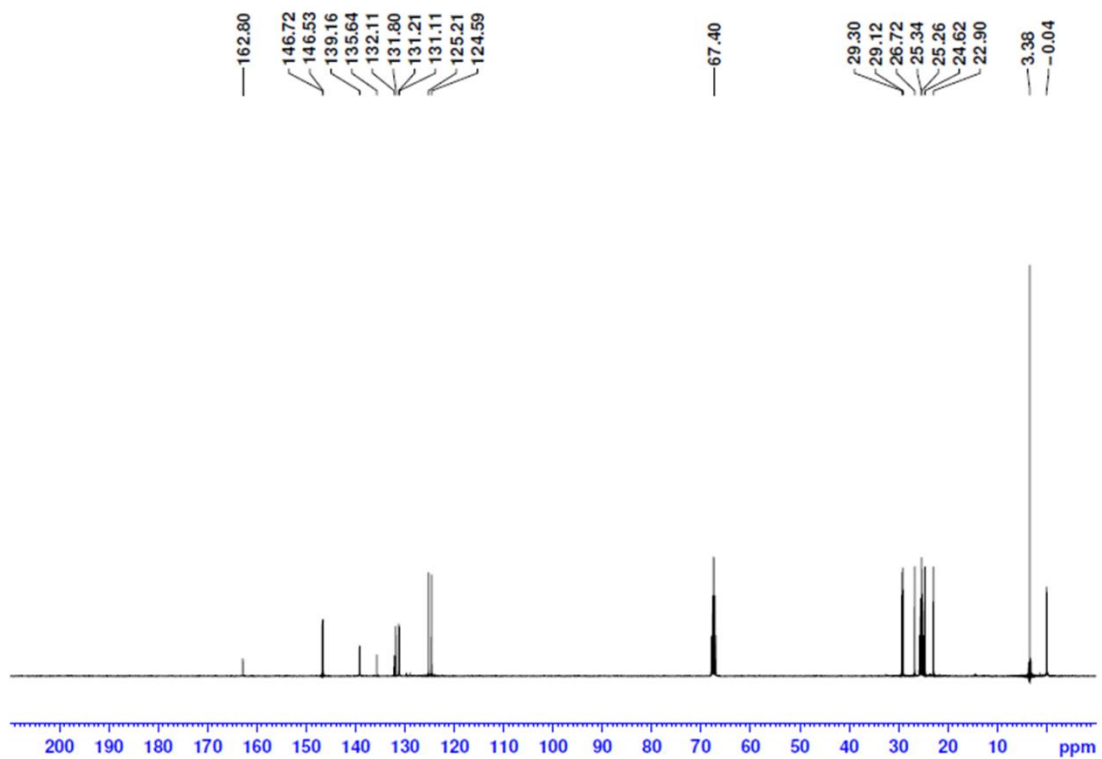


Figure S54 ^{13}C NMR of **5** in d_8 -THF solution.

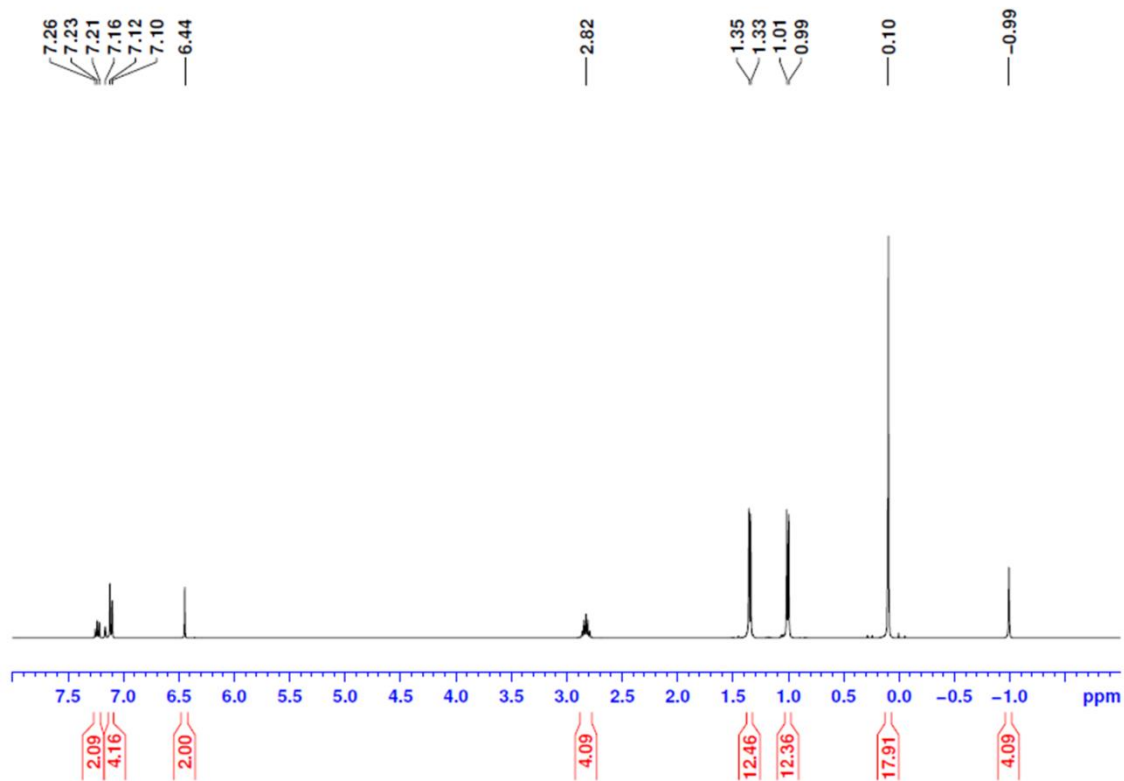


Figure S55 ^1H NMR of **6** in C_6D_6 solution.

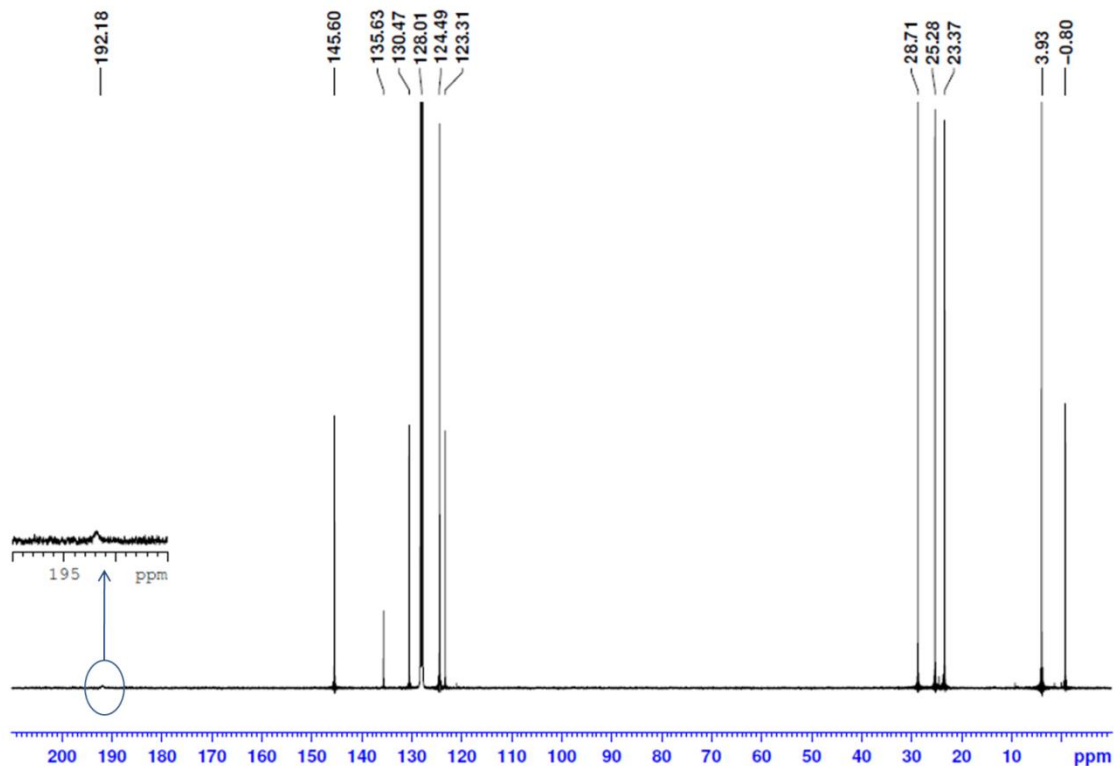


Figure S56 $^{13}\text{C}\{\text{H}\}$ NMR of **6** in C_6D_6 solution.

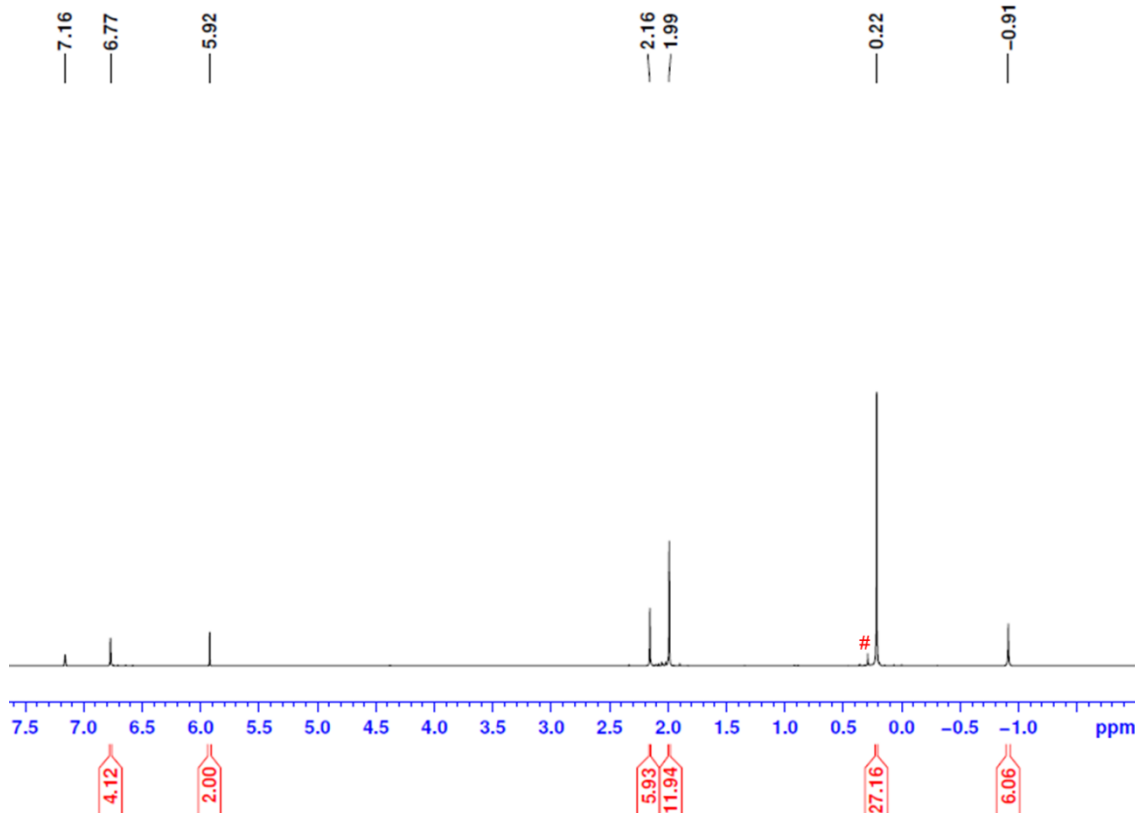


Figure S57 ^1H NMR of **7** in C_6D_6 solution. # traces of grease.

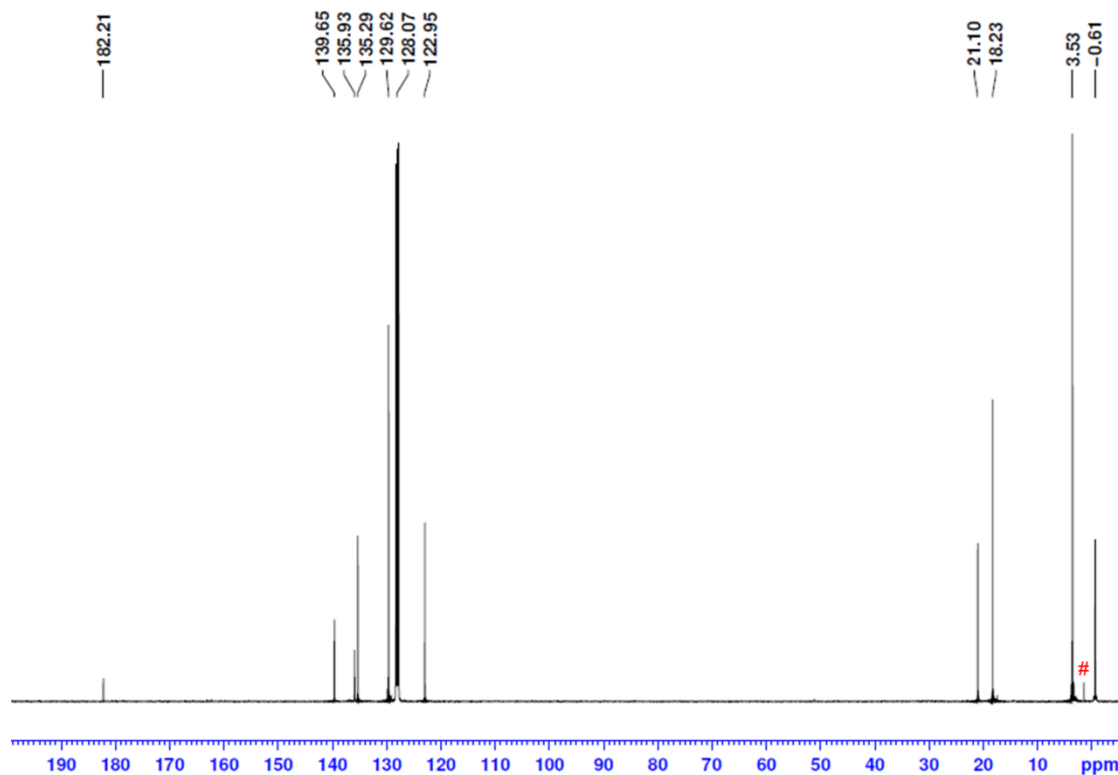


Figure S58 $^{13}\text{C}\{\text{H}\}$ NMR of **7** in C_6D_6 solution. # traces of grease.

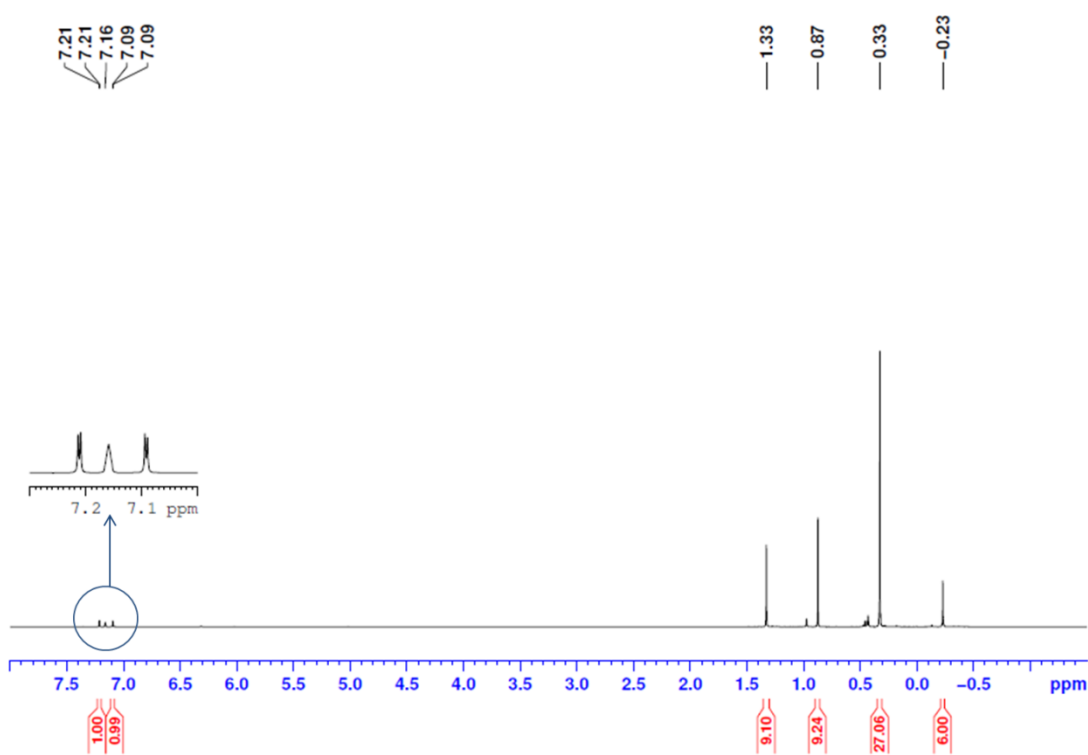


Figure S59 ^1H NMR of **8** in C_6D_6 solution.

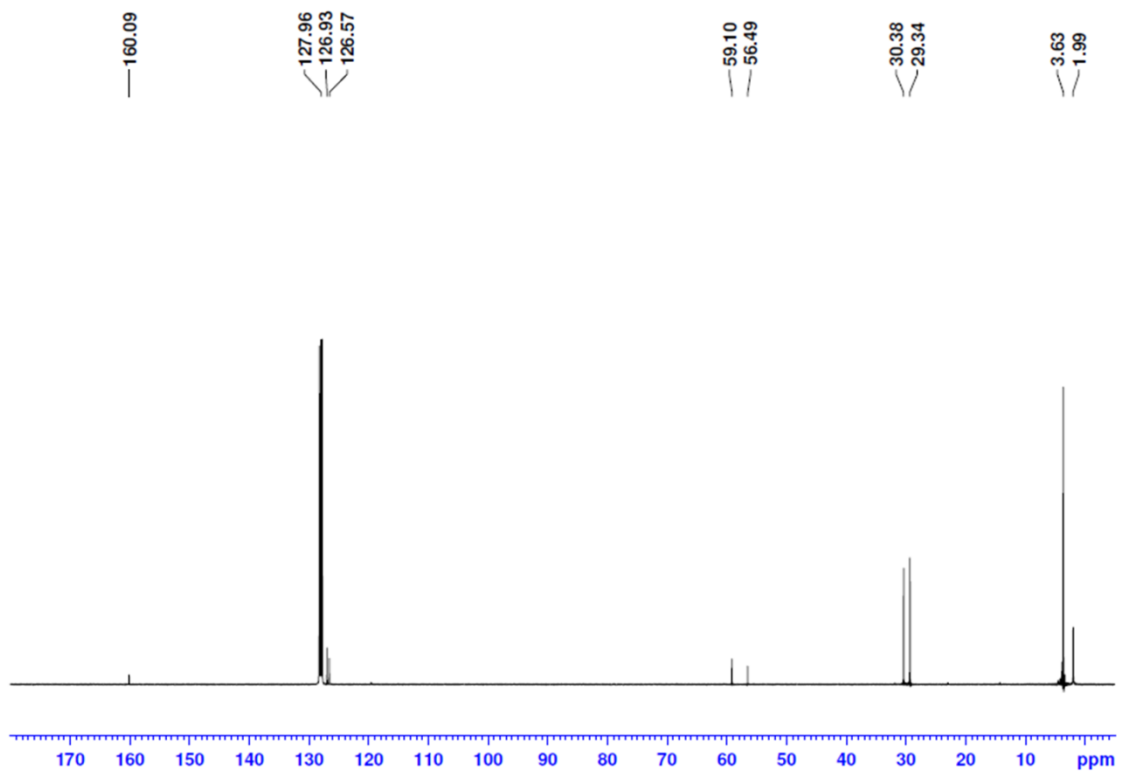


Figure S60 $^{13}\text{C}\{\text{H}\}$ NMR of **8** in C_6D_6 solution.